Conversion of methyl ethyl ketone (MEK) to valuable chemicals over multifunctional supported catalysts

by

Zahraa Fadhil Zuhwar Al-Auda

B.S., the University of Technology, Iraq, 2004
M.S., the University of Technology, Iraq, 2008

AN ABSTRACT OF A DISSERTATION
submitted in partial fulfillment of the requirements for the degree

DOCTOR OF PHILOSOPHY

Department of Chemical Engineering
College of Engineering

KANSAS STATE UNIVERSITY
Manhattan, Kansas

2018

Abstract

The present work describes the conversion of bio-derived methyl ethyl ketone (MEK) into different useful chemicals.

The first part discusses the direct conversion of MEK to butene over supported copper catalysts (Cu-Al_2O_3, Cu-zeolite Y sodium (Cu-ZYNa) and Cu-zeolite Y hydrogen (Cu-ZYH)) in a fixed bed reactor. In this reaction, MEK is hydrogenated to 2-butanol over metal sites, and further dehydrated on acid sites to produce butene. Experimental results showed that the selectivity of butene was the highest over Cu-ZYNa, and it was improved by finding the optimum reaction temperature, hydrogen pressure and the percentage of copper loaded on ZYNa. The highest selectivity of butene (97.9%) was obtained at 270 °C and 20 wt% Cu-ZYNa. Over Cu-Al_2O_3, the selectivity of butenes was less than Cu-ZYNa since subsequent hydrogenation of butene occurred to produce butane. It was also observed that with increasing H_2/MEK molar ratio, butane selectivity increased. However, when this ratio was decreased, hydrogenation of butene was reduced, but dimerization to C_8 alkenes and alkane began to be favored. The main products over 20% Cu-Al_2O_3 were butene and butane, and the maximum selectivity of butene (87%) was achieved at an H_2/MEK molar ratio of five. The lowest selectivity of butene was obtained using Cu-ZYH, reaching ~40%. It was found that the amount of acidity in Cu-ZYH is much higher than in Cu-ZYNa (from (NH_3-TPD) measurements). This could have caused the selectivity of butene to decrease as a result of dimerization, oligomerization and cracking reactions.

The second part describes the conversion of MEK to higher ketones in one step using a multifunctional catalyst having both aldol condensation (aldolization and dehydration) and hydrogenation properties. 15% Cu supported zirconia (ZrO_2) was investigated in the catalytic gas phase reaction of MEK in a fixed bed reactor. The results showed that the main product was 5-methyl-3-heptanone in addition to 5-methyl-3-heptanol and 2-butanol with side products including other heavy products (C_{12} and up). The effects of temperature and the molar ratio of reactants (H_2/MEK) on overall product selectivity were studied. It was found that with increasing temperature, the selectivity to C_8 ketone increased, while selectivity to 2-butanol decreased. The hydrogen pressure plays significant role on the selectivity of products. It was observed that with increasing the H_2/MEK molar ratio, 2-butanol selectivity increased due to hydrogenation reaction while decreasing this ratio leads to increasing aldol condensation products. In addition, it was noted that both conversion and selectivity to the main product increased using a low loading percentage of copper, 1% Cu-ZrO_2. The highest selectivity of 5-methyl-3-heptanone (~63%) was obtained at temperatures around 180 °C and a molar ratio of H_2/MEK of 2. Other metals (Ni, Pd and Pt) supported on ZrO_2 also produced 5-methyl 3-heptanone as the main product with slight differences in selectivity, suggesting that a hydrogenation catalyst is important for making the C_8 ketone, but the exact identity of the metal is less important.

The third part discusses the conversion of C_8 ketones to C_8 alkenes and C_8 alkane over a catalyst consisting of a transition metal (Cu or Pt) loaded on alumina (Al_2O_3). These bifunctional catalysts provide both hydrogenation and dehydration functionalities. The

main products over 20% Cu-Al_2O_3 were a mixture of 5-methyl-3-heptene, 5-methyl-2-heptene and 3-methyl heptane. However, using 1% Pt-Al_2O_3 the major product was 3-methyl heptane with a selectivity reaching over 97% and a conversion of 99.9 %. Both temperature and the hydrogen pressure play an important role on the conversion of C_8 ketone as well as the selectivity of products (C_8 alkenes and C_8 alkane). Over 20% Cu-Al_2O_3, it was observed that increasing the reaction temperature led to an increase in the selectivity to C_8 alkane as a result of hydrogenation of the C_8 alkene. Also, it was observed that with an increase in H_2/C_8 ketone molar ratio, C_8 alkane selectivity increased. However, when this ratio was decreased, the further hydrogenation of C_8 alkene to C_8 alkane was reduced. The highest selectivity of C_8 alkene (81.7%) was obtained at 220 °C and a H_2/C_8 ketone molar ratio of 2. In addition, an experiment was carried out using a low loading percentage of copper, and it was noted that both conversion and selectivity to the main products decreased over 1% Cu-Al_2O_3. Over 1% Pt-Al_2O_3, C_8 alkane was the major product with different temperatures indicating that further hydrogenation of C_8 alkene was promoted on 1% Pt-Al_2O_3. At low temperature, for both Cu-Al_2O_3 and Pt-Al_2O_3, significant amounts of C_8 alcohols are formed because subsequent reactions do not proceed at a fast enough rate. Also using 1% Pt-Al_2O_3, the main product selectivity is still C_8 alkane with all H_2/C_8 ketone ratios.

Conversion of methyl ethyl ketone (MEK) to valuable chemicals over multifunctional supported catalysts

by

Zahraa Fadhil Zuhwar Al-Auda

B.S., the University of Technology, Iraq, 2004

M.S., the University of Technology, Iraq, 2008

A DISSERTATION

submitted in partial fulfillment of the requirements for the degree

DOCTOR OF PHILOSOPHY

Department of Chemical Engineering
College of Engineering

KANSAS STATE UNIVERSITY
Manhattan, Kansas

2018

Approved by:

Major Professor

Keith L. Hohn

Copyright

Abstract

The present work describes the conversion of bio-derived methyl ethyl ketone (MEK) into different useful chemicals.

The first part discusses the direct conversion of MEK to butene over supported copper catalysts (Cu-Al_2O_3, Cu-zeolite Y sodium (Cu-ZYNa) and Cu-zeolite Y hydrogen (Cu-ZYH)) in a fixed bed reactor. In this reaction, MEK is hydrogenated to 2-butanol over metal sites, and further dehydrated on acid sites to produce butene. Experimental results showed that the selectivity of butene was the highest over Cu-ZYNa, and it was improved by finding the optimum reaction temperature, hydrogen pressure and the percentage of copper loaded on ZYNa. The highest selectivity of butene (97.9%) was obtained at 270 °C and 20 wt% Cu-ZYNa. Over Cu-Al_2O_3, the selectivity of butenes was less than Cu-ZYNa since subsequent hydrogenation of butene occurred to produce butane. It was also observed that with increasing H_2/MEK molar ratio, butane selectivity increased. However, when this ratio was decreased, hydrogenation of butene was reduced, but dimerization to C_8 alkenes and alkane began to be favored. The main products over 20% Cu-Al_2O_3 were butene and butane, and the maximum selectivity of butene (87%) was achieved at an H_2/MEK molar ratio of five. The lowest selectivity of butene was obtained using Cu-ZYH, reaching ~40%. It was found that the amount of acidity in Cu-ZYH is much higher than in Cu-ZYNa (from (NH_3-TPD) measurements). This could have caused the selectivity of butene to decrease as a result of dimerization, oligomerization and cracking reactions.

The second part describes the conversion of MEK to higher ketones in one step using a multifunctional catalyst having both aldol condensation (aldolization and dehydration) and hydrogenation properties. 15% Cu supported zirconia (ZrO_2) was investigated in the catalytic gas phase reaction of MEK in a fixed bed reactor. The results showed that the main product was 5-methyl-3-heptanone in addition to 5-methyl-3-heptanol and 2-butanol with side products including other heavy products (C_{12} and up). The effects of temperature and the molar ratio of reactants (H_2/MEK) on overall product selectivity were studied. It was found that with increasing temperature, the selectivity to C_8 ketone increased, while selectivity to 2-butanol decreased. The hydrogen pressure plays significant role on the selectivity of products. It was observed that with increasing the H_2/MEK molar ratio, 2-butanol selectivity increased due to hydrogenation reaction while decreasing this ratio leads to increasing aldol condensation products. In addition, it was noted that both conversion and selectivity to the main product increased using a low loading percentage of copper, 1% Cu-ZrO_2. The highest selectivity of 5-methyl-3-heptanone (~63%) was obtained at temperatures around 180 °C and a molar ratio of H_2/MEK of 2. Other metals (Ni, Pd and Pt) supported on ZrO_2 also produced 5-methyl 3-heptanone as the main product with slight differences in selectivity, suggesting that a hydrogenation catalyst is important for making the C_8 ketone, but the exact identity of the metal is less important.

The third part discusses the conversion of C_8 ketones to C_8 alkenes and C_8 alkane over a catalyst consisting of a transition metal (Cu or Pt) loaded on alumina (Al_2O_3). These bifunctional catalysts provide both hydrogenation and dehydration functionalities. The

main products over 20% Cu-Al_2O_3 were a mixture of 5-methyl-3-heptene, 5-methyl-2-heptene and 3-methyl heptane. However, using 1% Pt-Al_2O_3 the major product was 3-methyl heptane with a selectivity reaching over 97% and a conversion of 99.9 %. Both temperature and the hydrogen pressure play an important role on the conversion of C_8 ketone as well as the selectivity of products (C_8 alkenes and C_8 alkane). Over 20% Cu-Al_2O_3, it was observed that increasing the reaction temperature led to an increase in the selectivity to C_8 alkane as a result of hydrogenation of the C_8 alkene. Also, it was observed that with an increase in H_2/C_8 ketone molar ratio, C_8 alkane selectivity increased. However, when this ratio was decreased, the further hydrogenation of C_8 alkene to C_8 alkane was reduced. The highest selectivity of C_8 alkene (81.7%) was obtained at 220 °C and a H_2/C_8 ketone molar ratio of 2. In addition, an experiment was carried out using a low loading percentage of copper, and it was noted that both conversion and selectivity to the main products decreased over 1% Cu-Al_2O_3. Over 1% Pt-Al_2O_3, C_8 alkane was the major product with different temperatures indicating that further hydrogenation of C_8 alkene was promoted on 1% Pt-Al_2O_3. At low temperature, for both Cu-Al_2O_3 and Pt-Al_2O_3, significant amounts of C_8 alcohols are formed because subsequent reactions do not proceed at a fast enough rate. Also using 1% Pt-Al_2O_3, the main product selectivity is still C_8 alkane with all H_2/C_8 ketone ratios.

Table of Contents

List of Figures

List of Tables

Acknowledgements

I would like to thank my advisor Dr. Keith Hohn for the continuous support of my PhD study and research at Kansas State University. His patience, encouragement, and motivation to solve the problems I faced in my research helped me to finish my PhD degree.

I would also like to express my gratefulness to my committee members, Dr. Placidus Amama, Dr. Bin Liu, Dr. Peter Sues, and Outside Chair Dr. Donghai Wang for their comments and contributions on my PhD thesis.

Also, Higher Committee for Education Development in Iraq (HCED) is gratefully acknowledged especially Mr. Zeyad T. Flayyeh, the director of student academic affairs department, and Mr. Firas Rafid Saleem.

My sincerest appreciation and thanks are to the former Iraqi Cultural Attaché, Professor Tahani Alsandook, for her efforts during my study.

I am grateful to the awesome guy, Hayder Al-Atabi, for designing, modifying, repairing equipment, and his help in the lab during all my research. I would like also to thank Quanxing Zheng for training and helping me in the lab. My thanks are extended to Jingyi Xie for training me on the XPS device. I wish also to thank Xu Li for helping me with Brunauer–Emmett–Teller (BET) measurements. I am also grateful to Yixiao Li for helping me with GC-MS.

In addition, I am thankful to the staff in the Department of Chemical Engineering: Danita Deters, Karen Strathman, Cynthia Fowler, and David Threewit for their assistance and cooperation in events related to my research.

Dedication

To all of my family

To my parents, the kindest people to me

Fadhil Al-Auda and Ensaf Al-Bzweni

To my one and only brother

Mustafa Al-Auda

To my husband, my life partner and best friend

Hayder Al-Atabi

To my children, a part of my heart

Ghasaq and Ali

Chapter 1- Introduction

Since the last century, oil has been the main source of chemicals and energy, and the demand for it is forecasted to increase significantly in the next years. However, petroleum is a finite resource. For this reason, it is imperative to develop new sustainable sources for fuels and bulk chemicals [1–5]. Biomass is the most attractive alternative feedstock since it is widely available as a sustainable carbon source. It is composed of several compounds such as carbohydrates, lignin, fatty acids, lipids and proteins. Practically, carbohydrates show promise since they form a considerable natural source of carbon. The main disadvantage of carbohydrates as a feedstock is the excess of oxygen inside their molecular structures. This oxygen content of carbohydrates can be reduced by three main ways. The first method includes the removal of small, highly oxidized carbon molecules like CO_2, formaldehyde (CH_2O), and formic acid (CH_2O_2). The second way is hydrogenolysis, which includes removing oxygen from the molecule at the expense of one molecule of hydrogen for each oxygen atom, producing water. The third method involves the removal of water via the dehydration of carbohydrates into a wide variety of interesting compounds such as furans and levulinic acid [4]. Overall, the aim of biomass conversion processes is to remove oxygen as a combination of CO, CO_2, and water to produce hydrocarbon products with enriched hydrogen and minimized oxygen content [3].

2,3 butanediol (2,3 BDO), which is a main product resulting from fermentation of sugars (carbohydrates) from renewable resources [6–11], has recently been studied for conversion to a number of important chemicals such as 1,3 butadiene (BD) [12–14], methyl ethyl ketone (MEK) [15–17] and butene isomers [18]. MEK, which can be produced from 2,3 BDO easily with high selectivity, can be converted to several useful products via subsequent chemical reactions like hydrogenation, dehydration, and aldol condensation reactions. However, there are few studies to convert MEK to chemicals like butene, C_8 ketones and C_8 alkenes.

MEK, also known as 2-butanone, is a colorless organic compound that is described by satisfactory boiling point (79.6 °C), good solubility, easy volatilization, and stability. It is commonly used as a solvent in paint, dye, pharmaceutical, and refining industries [19]. Commercially, MEK is mainly produced via dehydrogenation of 2-butanol (roughly 92% of MEK worldwide is produced using this processing technique). 2-butanol can be produced easily via hydration of n-butenes, which can be obtained from petrochemically-produced C_4-raffinate. This is achieved either with a two-step process which uses liquid sulfuric acid as a catalyst or in a single step by adding water directly on a stabilized acidic ion exchange resin. The last 8% of MEK is produced by Fisher-Tropsh [20] or by oxidizing n-butane to produce acetic acid with MEK as byproduct [21].

The aim of the present work is to focus on producing different valuable chemicals (butene, C_8 ketone, C_8 alkene and C_8 alkane) from bio-derived MEK. This can be achieved by finding suitable bifunctional or multifunctional catalysts that combine key catalytic

functionalities in a single material. Also, investigation of the effect of operating conditions, such as reaction temperature and H_2/reactant molar ratio, plays a significant role in reaching optimum catalyst activity and selectivity towards the formation of desired products. Specifically, the present work includes three projects:

1. Developing bifunctional catalysts for selectively converting MEK to butene via hydrogenation-dehydration reactions.
2. Synthesizing catalysts to convert MEK to C_8 ketones and/or C_8 alcohols through subsequent reactions including aldol condensation (aldolization-dehydration) reactions followed hydrogenation reaction in a single step using one reactor and one bed of multifunctional catalyst.
3. Studying catalysts that convert C_8 ketones to C_8 branched alkenes and/or C_8 alkane, which can be used as gasoline blended components to increase the octane number in gasoline by means of hydrogenation dehydration reactions.

For each of the three projects, the goal is to develop an active and selective catalyst for the desired chemical reactions. In addition, this research probes the reaction mechanisms responsible for the formation of the observed products and elucidates the catalyst properties that are important in each project. Scheme 1.1 summarizes the different aspects of the proposed research.

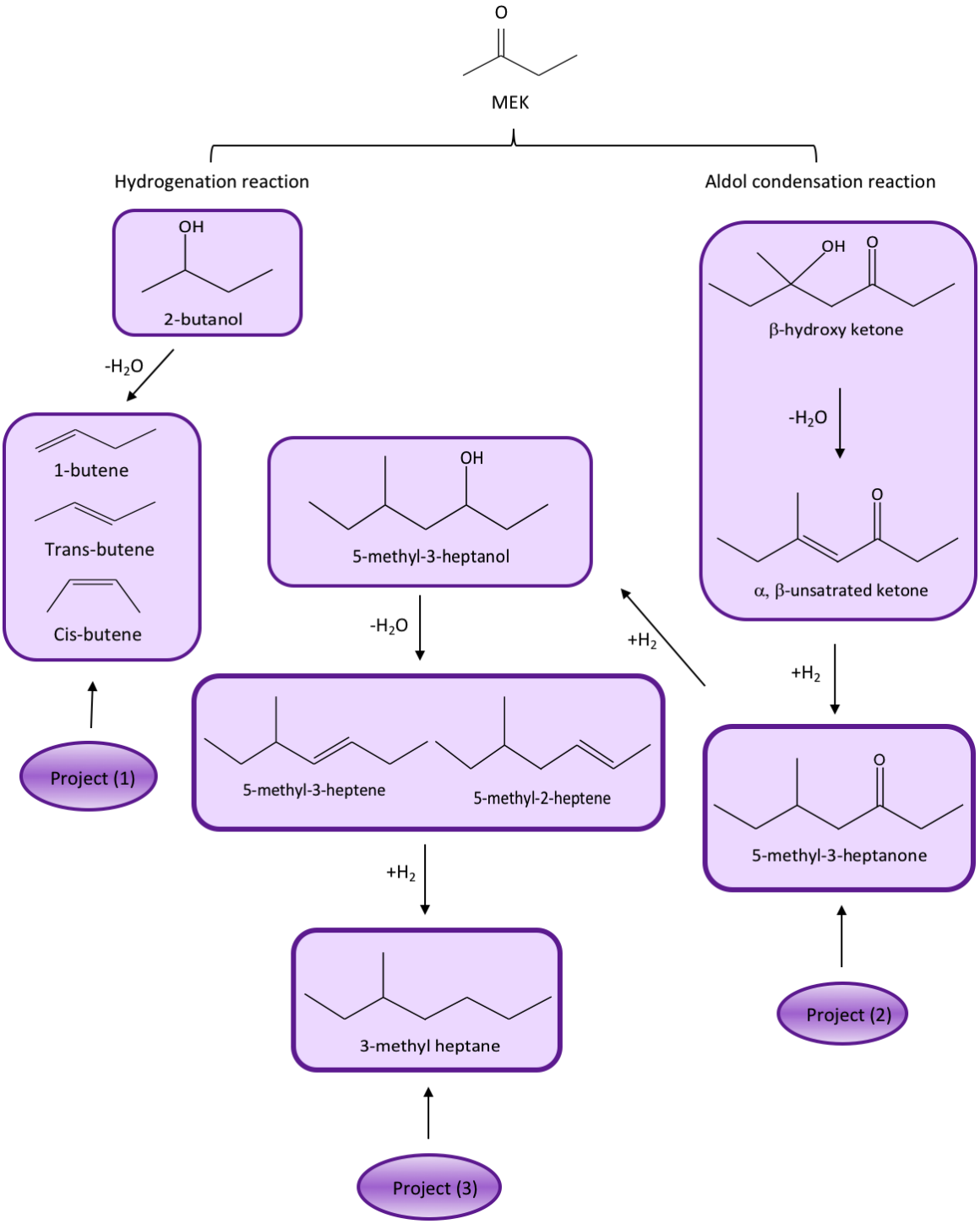

Scheme 1.1. The proposed pathways to obtain different chemicals from MEK.

1.1 Fermentation to Produce 2,3 BDO

In recent years, 2,3 BDO has attracted considerable attention since it can be produced in large amounts and high concentrations via fermentation of sugars. Several microorganisms can be used including *Klebsiella pneumoniae* [22], *Entaerobacter aerogenes* [10,23], *Bacillus polymyxa* [24], *Aeromonas hydrophilia* and several species of *Serratia* [25]. *Klebsiella pneumoniae*, *Klebsiella oxytoca* and *Bacillus polymyxa* are more efficient than other microorganisms at the production of 2,3 BDO. Jansen *et al.* [26] studied the fermentation of xylose using *K. oxytoca* ATCC 8724. They reported that the concentration of 2,3 BDO obtained was 12.63 g/L by fermentation of media containing 50 g/L of xylose in a 7 L batch fermentor. Using different xylose concentrations ranging from 5-150 g/L, a maximum 2,3 BDO productivity of 1.35 g/L/h was obtained with an initial xylose concentration of 100 g/L. Qureshi and Cheryan [27] obtained a maximum 2,3 BDO concentration of 84.2 g/L with yield of 0.5 g/g of glucose using *K. oxytoca* ATCC 8724. Ji *et al*. [8] reported the fermentation of glucose using *Klebsiella oxytoca*. The maximum 2,3 BDO concentration obtained was 95.5 g/L with a yield and productivity of 0.48 g/g of glucose and 1.71 g/L/h, respectively, by fermentation of media containing 200 g/L of glucose in a 3 L batch fermentor. Saha and Bothast [28] investigated the fermentation of arabinose using *Enterobacter cloacae*. They reported that the yield of 2,3 BDO was 0.4 g/g arabinose with a productivity of 0.63 g/L/h by fermentation of media with an initial arabinose concentration of 50 g/L.

The optimum fermentation conditions for production of 2,3 BDO have been intensively studied. The oxygen level, pH, temperature, substrate concentration, and agitation are critical to trigger 2,3 BDO production and reduce other byproducts formation like ethanol and lactate [29,30]. With *K. oxytoca* for instance, the optimum pH for 2,3 BDO production is in the range pH *5.0-6.0* [31,32] and the optimum temperature is 37 °C [31]. Also, the yield of 2,3 BDO is affected greatly by the availability of oxygen. By minimizing the oxygen availability, the 2,3 BDO yield can be increased since this limits respiration. However, a small oxygen supply makes the rates of conversion slow and produces little cell mass. By increasing the oxygen availability, the 2,3 BDO production rate can be increased since this leads to a higher cell density [32]. In the absence of oxygen, both 2,3 BDO and ethanol are produced with approximately equimolar amounts [33], while the ratio of acetoin to 2,3 BDO rises by increasing the oxygen supply rate [31].

1.2 Conversion of 2,3 BDO to Different Chemicals

When 2,3 BDO is produced from fermentation reactions, it can be converted to other chemicals and hydrocarbons via different chemical processes. The attention given to 2,3 BDO in recent years has increased because 2,3 BDO has a considerable number of potential industrial applications such as in the manufacture of printing inks, pharmaceuticals, perfumes, plasticizers, fumigants and food [34,35].

2,3 BDO is considered an important feedstock for several interesting chemical reactions like dehydration, dehydrogenation, ketalization and esterification as explained in scheme 1.2 [7]. It can be dehydrated to MEK (industrial solvent for resin and lacquer

production) [36] and to BD which is an organic intermediate for the manufacture of synthetic rubber [13]. Also, it can be dehydrogenated into acetoin and diacetyl where acetoin is used as an aroma carrier in flavors, and diacetyl is significant for the organoleptic quality of dairy products like cheese, butter, and fermented cream [37]. Ketalization of 2,3 BDO with acetone yields a tetramethyl dioxolane, which is a potential gasoline blending agent similar to the commonly-used methyl tert-butyl ether (MTBE). By esterification of 2,3 BDO with monobasic acids or their functional equivalents, diesters of 2,3 BDO can be produced which could be used as a precursor for drugs and cosmetics in addition to their use as effective plasticizers for thermoplastic polymers like cellulose nitrate, cellulose acetate butyrate, cellulose triacetate, polyvinyl esters, polyvinyl chloride, polyacrylates, and polymethylacrylates [38].

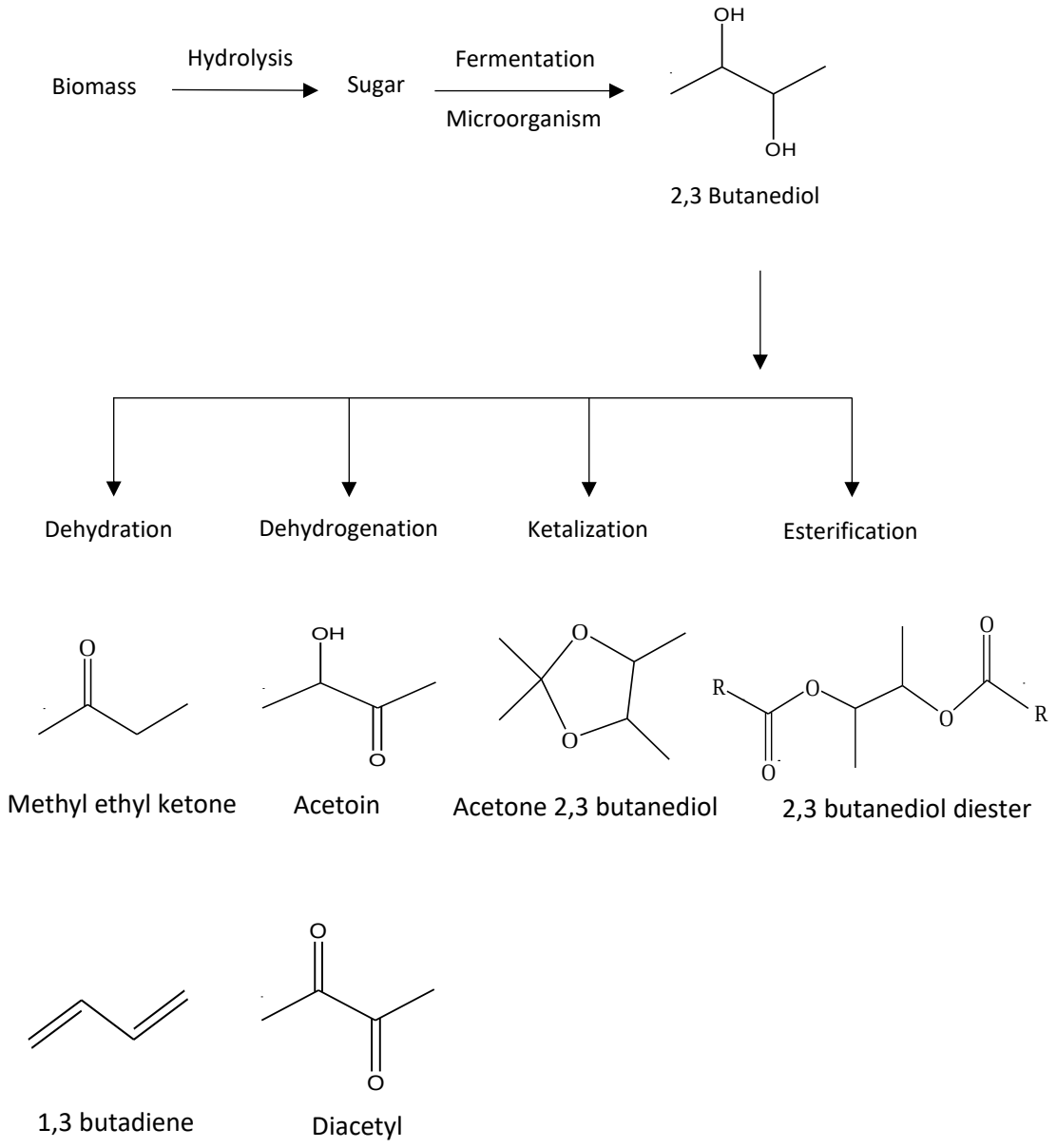

Scheme 1.2. Derivatives of 2,3-butanediol produced biologically, modified from [7].

1.3 Dehydration of 2,3 BDO

1.3.1 Dehydration of 2,3 BDO to BD

Dehydration of 2,3 BDO to BD has been studied using many kinds of catalysts. Winfield [12] reported that in the dehydration of 2,3 BDO over ThO_2, 3-buten-2-ol (3B2OL) was mostly obtained with a selectivity of 70% at 350 °C while BD was mainly produced with a selectivity of about 62% together with 3B2OL selectivity of only 8% at 500 °C. Duan *et al*. [13] studied the dehydration of 2,3 BDO over Sc_2O_3 at high temperatures around 425 °C, and they found that Sc_2O_3 showed excellent selectivity to produce 88.3% BD at 411°C. In addition, they tested the effect of using double bed catalysts consisting of Sc_2O_3 and Al_2O_3, and the results showed that the 2,3 BDO can be converted directly to BD with a selectivity of 94% at 318 °C and with the conversion of 100% for 2,3 BDO. Kim *et al.* [14] investigated the effect of using silica-supported sodium phosphates for a wide range of Na/P ratios (Na/P = 0–3) for the dehydration of 2,3 BDO. The major products were BD and MEK for long contact times. 3B2OL and MEK are the main products for short contact times. The achieved yields of elimination products BD and 3B2OL were over 60% at Na/P = 1.8–1.9 which was found to be the optimum combination of acidic and basic components for the production of BD or 3B2OL from 2,3 BDO. The pathway to produce BD goes through sequential 1,2-eliminations of water. 3B2OL is obtained from the first dehydration and BD is produced from the second dehydration. Both 3B2OL and BD should be formed through E1cB eliminations [39].

1.3.2 Dehydration of 2,3 BDO to MEK

MEK, used mainly as a solvent, can be produced easily via dehydration of 2,3 BDO using acidic catalysts such as zeolite and alumina which catalyze rearrangement mechanisms. MEK can be obtained via a 1,2-hydride shift while 2-methylpropanal is produced by a 1,2-methyl shift. MEK dominates over 2-methylpropanal in the products because hydride shifts are faster than methyl shifts [14]. Depending on the assumed mechanism of elimination [39], MEK and 2-methylpropanal may be produced via the acid catalyzed E2 elimination. Scheme 1.3 shows the mechanism of 2,3 BDO dehydration.

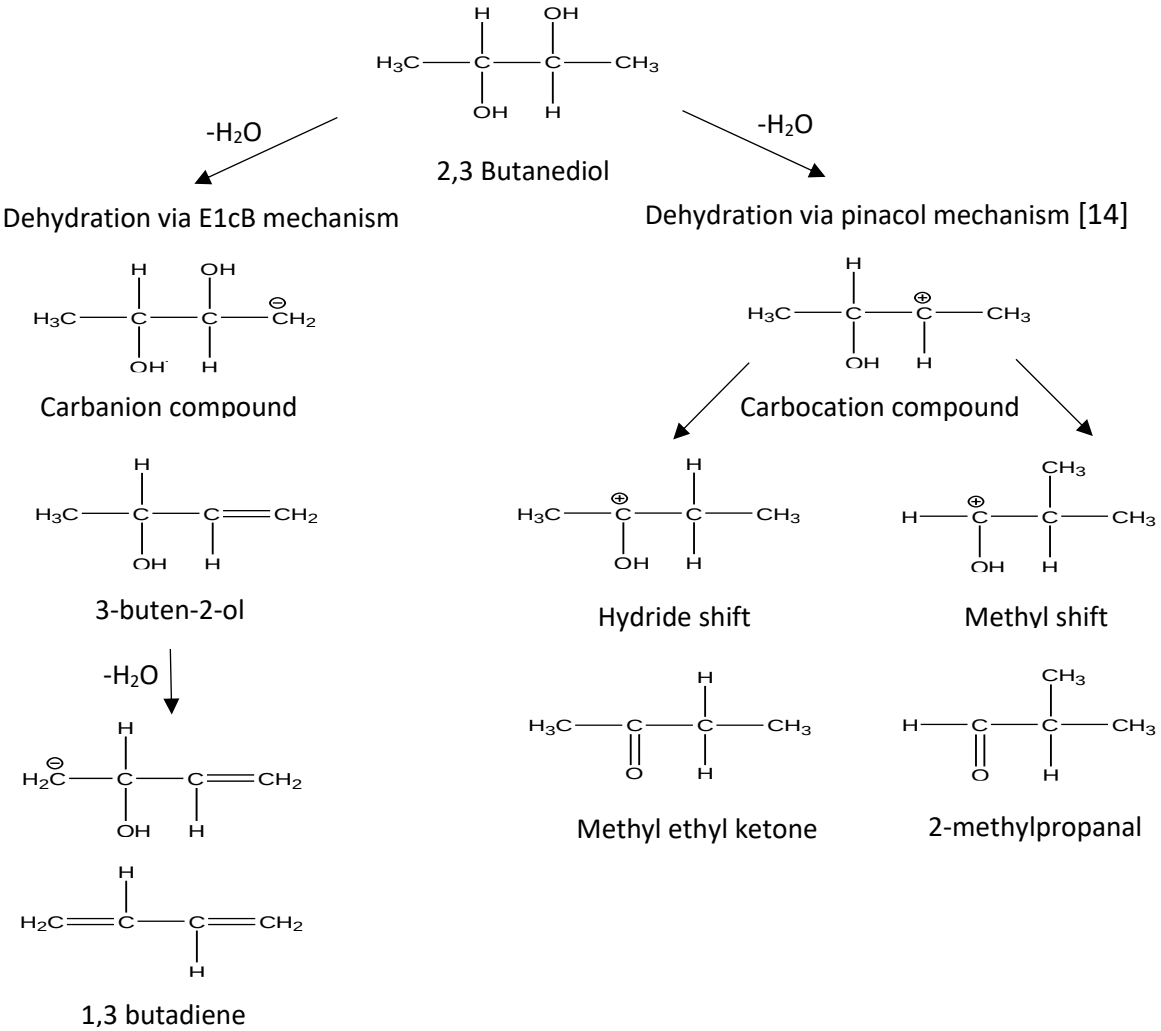

Scheme 1.3. The mechanism of dehydration of 2,3 BDO.

Molnar *et al.* [40] studied the dehydration of 2,3 BDO to MEK over zeolite NaX, NaY, NaHX and NaHY. They reported that the Y-zeolite gave the highest selectivity (80%) for pinacol rearrangement under suitable operating conditions (250 °C). This was attributed to the differences in acid/base and electrostatic properties between X and Y zeolite [40]. Zhang *et al.* [41] investigated the dehydration of 2,3 BDO to MEK on HZSM-5 for different Si/Al ratios (Si/Al=28-360). They found that HZSM-5(360) showed the highest yield of MEK (62.1%) and highest selectivity for 2-methylpropanal (18.9%) at 200 °C. Also, they reported that the performance of HZSM-5 (360) was enhanced by modifying it with boric acid (B_2O_3 < 1.0 %) with 2,3 BDO conversions of 97.2% and a selectivity for MEK above 68.4% at 180 °C. Multer *et al.* [16] reported a combined fermentation/catalysis process to form 2,3 BDO. First, glucose was fermented with bacteria *Klebsiella oxytoca* to produce 2,3 BDO. Then, 2,3 BDO was dehydrated on HZSM-5 to obtain MEK. The yield of 2,3 BDO from total glucose consumed was about 0.63 g/g of glucose with a concentration of 0.03 mol/L and the selectivity to MEK was over 90% with 2-methylpropanal as the only other product detected. This selectivity was in accordance with results reported by Bucsi *et al.*, [42] using supported heteropoly acids. Török *et al.* [43] also studied dehydration of 2,3 BDO to MEK on Nafion and NaHX zeolite. They pointed out that high selectivity to MEK (less than 80%) was obtained with dioxolanes as an important side product. Emerson *et al.* [44] reported MEK yield was over 90% using sulfuric acid suggesting that aldol condensation limited MEK selectivity. Nikitina *et al.*, [45] studied dehydration of 2,3 BDO on several catalysts such as boron (BP), aluminum (AlP), titanium (TiP), zirconium (ZrP), and niobium (NbP) phosphates. They

reported that the reactivity of phosphates increased in the order: BP< TiP< ZrP= NbP< AlP, and AlP showed the best catalytic performance with an MEK selectivity of 78% at a 2,3 BDO conversion of 100%. Lee *et al.* [17] studied dehydration of 2,3 BDO over ZSM-5, mordenite, β and Y-zeolites. They reported that by increasing the pore size in the order ZSM-5 < mordenite < β < Y, the products shifted from MEK exclusively to MEK with both ketal and acetal and then to only ketal and acetal because larger pores allowed condensation reactions.

Although there are considerable studies to obtain chemicals from 2,3 BDO, there are few attempts to obtain light olefins such as butene using bifunctional catalysts. These olefins are widely obtained from Fluid Catalytic Cracking (FCC) effluent and can be converted into heavier hydrocarbons (C_5-C_{10}) for use as sulfur-free fuels [46,47]. Zheng *et al.* [18] studied the potential to obtain butene from 2,3 BDO directly using a bifunctional catalyst consisting of copper loaded on ZSM-5 with different SiO_2/Al_2O_3 ratios (23, 50 and 280). They reported that enhanced butene yields were obtained with a high SiO_2/Al_2O_3 ratio (280), and they ascribed that to the lower acidity of the high SiO_2/Al_2O_3 ratio catalyst. Also, they investigated the effect of copper loading percentage on producing butene. They found that increasing copper loading had a relatively slight effect on the catalytic results, although butene yield increased with copper loading. In addition, the impact of the reaction temperature was studied, and the results showed that the optimal temperature was around 250 °C. Lower temperatures (~230 °C) were favorable for dehydrogenation of 2,3 BDO. Higher temperatures (270 °C and 300 °C) were beneficial for oligomerization and cracking reactions, resulting in increasing the selectivities of C_3 and

C_5^+ olefins significantly. The optimum selectivity of the mixture of butene (1-butene, trans-butene and cis-butene) was obtained with a total selectivity of 71% over the bifunctional catalyst 19.2% CuO-ZSM-5 (280) at temperature of 250 °C. The same researchers investigated 20% CuO supported on three different types of mesoporous materials (Al-MCM-48, Al-SBA-15 and meso-ZSM-5 (where mesoporosity was introduced into ZSM-5 through sodium hydroxide treatment) to convert 2,3 BDO to butenes. They reported that the introduction of mesopores on the Al-MCM-48 and Al-SBA-15 catalysts could reduce the cracking products (C_3 and C_5–C_7 alkene) while the selectivity of C_8 alkene resulting from oligomerization of butenes was found to increase with increasing pore size of the catalysts. Cu/meso-ZSM-5 catalyst displayed high activity for both cracking and oligomerization reactions since it has both micropores (diameter of 0.55 nm) and mesopores (pore size of 23 nm) [48].

This step is considered a first stage in converting 2,3 BDO to fuel-range hydrocarbons. Dimerization/oligomerization of butene over acid sites [49] would be the next step to obtain fuel. Conversion of light olefins such as propene and butene to dimers and oligomers was one of the earliest commercial processes in the petroleum industry [50].

BD obtained from 2,3 BDO via dehydration reactions can be converted to butene by a selective hydrogenation reaction. Many studies about hydrogenation of BD to butene have been done over different catalysts. Naito *et al.* [51] showed that hydrogenation of BD over ZnO can produce 79% 1-butene and some cis-2-butene. Yan *et al.* [52] studied

hydrogenation of BD over a Pd/ graphene catalyst and found that the selectivity of 1-butene was 71% and a total yield of butenes (1-butene and 2-butene) was 99.5% with conversions of 95%. Hou *et al.* [53] investigated hydrogenation of BD on Pd-Ni-Al_2O_3, and they reported that Pd-Ni/γ-Al_2O_3 gave the highest 1-butene selectivity.

1.4 Conversion of MEK to Butene

In the petroleum industry, the conversion of propene and butylenes to dimers and oligomers was one of the first commercial processes [50]. Butene is considered a useful intermediate in the production of fuels as well as many chemicals. It can be converted into a variety of oligomers such as dimers, trimers, tetramers, etc. [54,55], which can be hydrogenated to saturated hydrocarbons (high-grade liquid fuel) [55].

One of the more valuable isomers of butene is 1-butene because having a double bond at the primary or alpha position enhances its reactivity, making 1-butene easily dimerized and oligomerized to produce fuel. In addition to 1-butene, 2-butene is important in increasing the octane number of gasoline when it is alkylated with isobutane. Alkylation reactions can be achieved by chemical combination of isobutane with any one of propylene, butylenes, or amylenes to produce a mixture of highly branched paraffins which have high antiknock features with a good stability [56,57]. In the United States, typically butylenes and propylene are used. Among the butylenes, 2-butene is preferable to 1-butene. The dominant paraffin produced from this reaction is isooctane in addition to mixture of iso-paraffins which range from pentanes to decanes and higher [58]. Besides these uses, butylenes can be blended with liquefied petroleum gas (LPG) for bottle gas

because their heating values are similar to LPG [56]. In Europe, it is common to use butylenes as fuel because LPG is unavailable. In the United States however, butylenes have a higher value as an alkylate feed, and LPG is used as a fuel instead of butylene since it is readily available [58].

It is reasonable to consider whether there is potential to obtain butenes with high selectivity from bio-derived MEK directly. The easiest route to produce butene is likely to hydrogenate MEK to 2-butanol and then dehydrate this secondary alcohol to obtain butene as demonstrated in scheme 1.4.

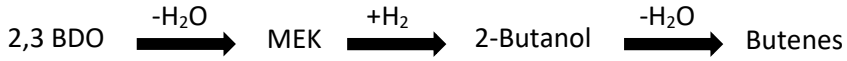

Scheme 1.4. The route for conversion of 2,3 BDO to Butenes.

MEK can be hydrogenated to 2-butanol using hydrogenation catalysts such as Ni, Cu, Ru, Pt and Pd. Copper catalysts can selectively hydrogenate C=O bonds and are relatively inactive for hydrogenolysis of C–C bonds, which is attractive for this project [59]. Sato *et al.* [60] mentioned that reduced Cu catalyst could catalyze the dehydration of glycerol to hydroxyacetone and the hydrogenation of hydroxyacetone followed by hydrogenolysis in H_2 to produce ethylene glycol, acetaldehyde and ethanol. Vasiliadou *et al.* [61] studied the hydrogenolysis of glycerol to propylene glycol over highly dispersed Cu/SiO_2 catalyst. They reported that Cu selectively produced propylene glycol from glycerol by sequential dehydration/ hydrogenation reactions with selectivity around 92–

97%. Lilga *et al.* [62] tested hydrogenation of MEK to 2-butanol on several hydrogenation catalysts supported on carbon, such as Ru/C, Pt/C, Re/Ni/C and Pd/C. They found that the temperature of the reaction and the kind of metal used affected the selectivity of 2-butanol. Using Ru/C, the selectivity of 2-butanol was 97.5% and the optimum temperature was 120 °C, while using Pt/C, the selectivity was 68.5% at an optimum temperature of 180 °C. For Re/Ni/C and Pd/C, the selectivity was 81.7% and 34.8% and the optimum temperatures were 160 and 260 °C, respectively. The same researchers studied the conversion of 2-butanol to hydrocarbons over HZSM-5 (30) at different reaction temperatures. They pointed out that at low temperatures (250 °C), the majority of the products are hydrocarbons consisting of normal and branched olefins (C_5-C_{12}) with almost no aromatic products. However, at high temperatures, (400 °C), aromatics are formed, while at moderate temperatures (300 °C) a mixture of aromatics and normal and branched olefins were produced.

Generally, alcohols can be dehydrated to olefins and ethers over acidic catalysts and dehydrogenated to aldehydes or ketones over basic catalysts. However, sometimes, heterogeneous basic catalysts promote dehydration of 2-alcohols to obtain 1-olefins by mechanisms different from those for acid catalyzed dehydration [63]. For example, ZrO_2 [64], ThO_2 [65] and rare earth metal oxides [66] are dehydration catalysts capable of converting 2-butanol to 1-butene with high selectivity via activating the methyl group of alcohols and abstracting both OH^- and H^+ of the terminal methyl group from 2-butanol to form 1-butene. Those catalysts are considered as potential acid-base bifunctional catalysts because they have moderate strength acidic and basic sites. In contrast, strongly

acidic catalysts like Al_2O_3 and SiO_2-Al_2O_3 do not activate the methyl groups of alcohols, and the major products in the dehydration of 2-butanol over these catalysts is 2-butene [64]. Strongly basic catalysts as CaO lead to dehydrogenation of the alcohol to a ketone [67]. This mechanism is explained in scheme 1.5.

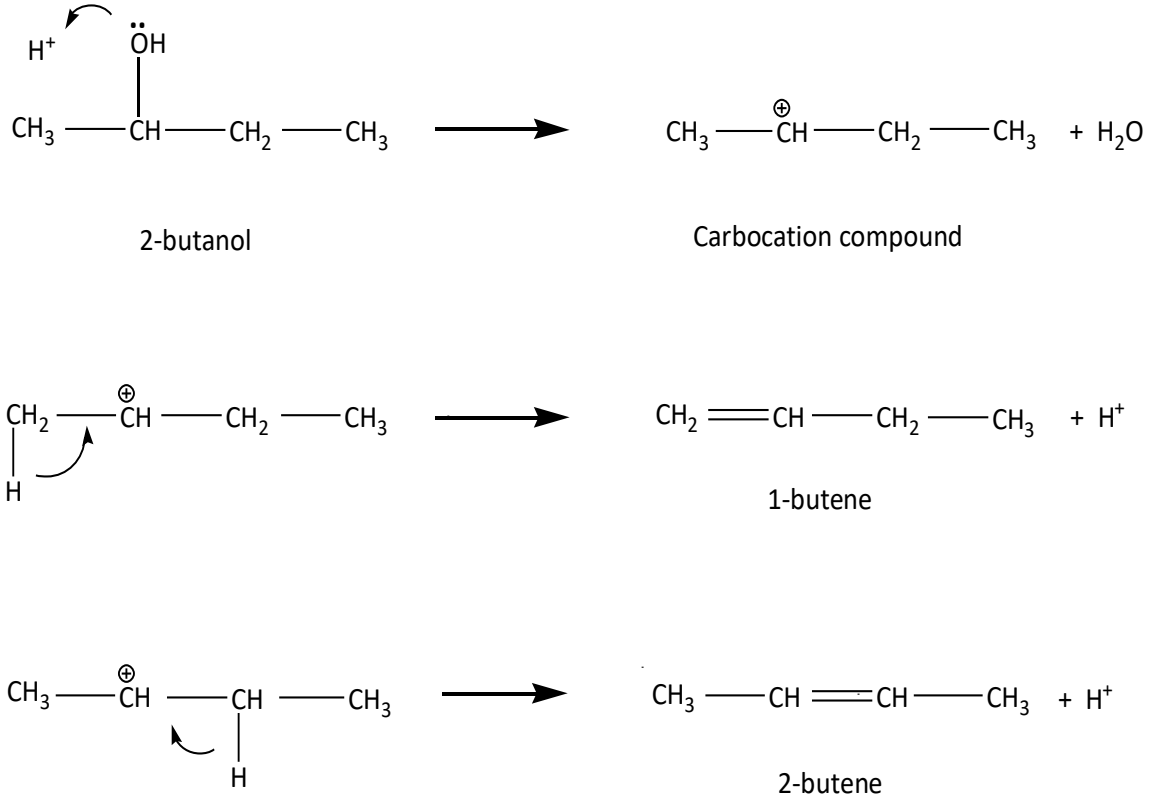

Scheme 1.5. Mechanism of dehydration of 2-butanol.

Yashima *et al.* [68] studied the decomposition of 2-propanol over alkali cation-exchanged X and Y zeolites. They reported that for zeolites X and Y exchanged with Li^+ and Na^+, dehydration became appreciable, whereas for zeolites exchanged with K^+, Rb^+ and

Cs^+ the dehydrogenation reaction became dominant although the selectivity to dehydration surpassed that to dehydrogenation at 425 °C.

1.5 Conversion MEK to C_8 Ketones and Guerbet Alcohols

MEK can be converted to C_8 ketones and/or C_8 alcohols via aldol condensation reactions followed by hydrogenation reaction. C_8 ketones can be used as a solvent as well as a useful intermediate to produce branched C_8 alcohols, C_8 alkenes, and C_8 alkanes.

The aldol condensation reaction is considered to be one of the most powerful carbon-carbon bond-forming reactions [69]. The aldol condensation reactions of aldehydes and ketones are widely used in organic synthesis to form products containing a double bond conjugated with a carbonyl group. The C-C bond formation proceeds via condensation between a molecule containing a carbonyl group and another molecule with an activated methylene group by choosing suitable operating conditions [70]. The aldol condensation involves reactions forming β-hydroxy aldehydes (β-aldol) or β-hydroxy ketones (β-ketol) either via self-condensations or mixed condensations of aldehydes and ketones. Then, by dehydration of intermediate β-aldol or β-ketol, α-β unsaturated aldehydes or α-β unsaturated ketones are formed [71]. In the fine chemical industry, base-catalyzed aldol condensation is a common method of coupling organic molecules via C–C bond formation [72]. Finally, these unsaturated aldehydes or ketones can be hydrogenated to aldehydes and ketones. Several of the aldehydes and ketones synthesized from the application of aldol condensation processes are attractive for use as

solvents because of the noteworthy polarity they exhibit such as methyl isobutyl ketone (MIBK) [73].

The largest volume aldol reaction product of acetone is MIBK which is an excellent solvent for cellulose, vinyl, epoxy and acrylic resins in addition to resin based coating systems [74]. Traditionally, it is manufactured by three steps[75] :

1. The base catalyzed aldol reaction of acetone in the liquid phase to produce diacetone alcohol.
2. The second step includes the acid catalyzed dehydration of diacetone alcohol to mesityl oxide.
3. The final step is the hydrogenation of mesityl oxide to MIBK and further to methyl isobutyl carbinol.

These processes are intricate and require high operating costs, so recently a one-step process to convert acetone to MIBK has become commercially possible. Reichle [76] described the condensation of aldehydes and ketones in the gas phase, especially acetone over catalysts consisting of lithium ions supported on a complex of mixture magnesium-aluminum hydroxides and oxides. The reactions formed *iso*-phorone and mesityl oxide with *iso*-phorone/mesityl oxide ratios>1. Kelly [74] studied aldol condensation reaction of acetone over two beds of catalysts consisting of 3 mL of the K-SiO_2 catalyst followed by a 3 mL bed of a hydrogenation catalyst consisting of 1% palladium supported on carbon. The highest selectivity of MIBK was 68.1 % at conversions of 15%. Other products included mesityl oxide with selectivity of 19.3% and *iso*-phorone with selectivity of 12.6%. Kelly

also investigated aldol condensation of MEK over different catalysts. He reported that using Na-SiO_2 and Cs-SiO_2, the major product was an α-β unsaturated ketone (5-methyl-4-hepten-3-one), with both isomers (*cis* and *trans*) being formed at temperatures between 325 and 400 °C. When an aldol condensation of MEK was conducted over two beds comprising Na-SiO_2 and Cu-Zn, the main products were 5-methyl-3-heptanone and 5-methyl-3-heptanol. Over just one bed consisting of Cu-Zn alone, however, the main products were believed to be bicyclo-[3,3,0]-octane-3,7-dione resulting from a dehydrogenation reaction of two molecules of MEK with little evidence of aldol condensation compounds.

Higher ketones, produced from the aldol condensation of small ketones, can be hydrogenated to large alcohols, known as Guerbet alcohols. Alternatively, alcohols produced in biomass conversion can be converted to larger alcohols via the Guerbet reaction. This reaction includes a condensation of two alcohols (either primary or secondary alcohols with a methylene group adjacent to the hydroxylated carbon atom) to produce a Guerbet alcohol with the elimination of one molecule of water. This kind of condensation occurs with the same alcohol (self-condensation) or another alcohol (cross-condensation) to produce a heavier and usually branched alcohol having the sum of the carbon atoms of the reactants. Besides this reaction, side reactions can occur, resulting in the formation of undesirable products like esters, carboxylic acids or salts. These byproducts frequently poison the catalytic system, so it is useful to minimize the formation of these by-products [77].

Two different reaction pathways have been proposed to explain the formation of Guerbet alcohols. The direct condensation pathway was proposed by Yang and Meng [78], and Ndou *et al.* [79]. This pathway includes a direct surface coupling reaction resulting in dehydration from the hydroxyl of one alcohol and the hydrogen attached to the α-carbon of a second molecule. The directed condensation router to Guerbet alcohols is shown in scheme 1.6 [80].

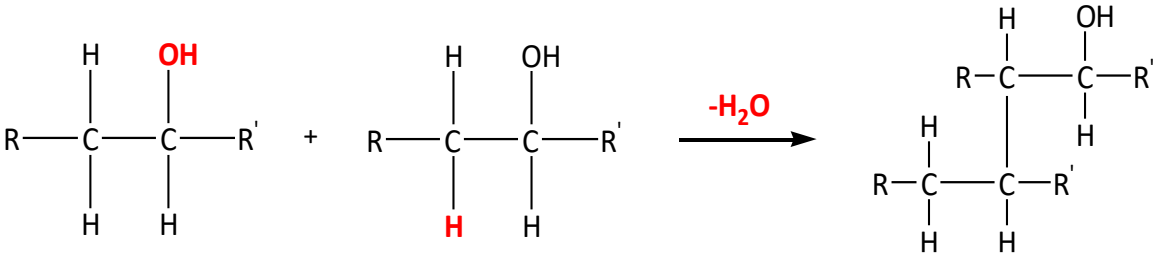

Scheme 1.6. Direct condensation of second alcohol, modified from [80].

The second route to obtain Guerbet alcohols from smaller alcohols includes a complex sequence of several different reactions: dehydrogenation of an alcohol to a ketone, aldolization of the ketone to obtain a β-hydroxy ketone, dehydration of the β-hydroxy ketone to give an α,β-unsaturated ketone and finally a hydrogenation reaction to produce a saturated ketone and further to produce the Guerbet alcohol. This path predicts how ketones can be converted to Gurebet alcohols. First, two ketones are coupled via aldol condensation, followed by dehydration and hydrogenation steps. This route skips the first dehydrogenation step of the Guerbet reaction. These reactions facilitate the direct upgrading of mixed feedstocks like acetone, n-butanol and ethanol fermentation (ABE fermentation) mixtures [81–83]. Ketones may be either condensed

with the same molecule (self-condensation) or condensed with another activated reagent, depending on the nature of the hydrocarbon groups attached to the carbonyl, using base catalysts [84].

Both pathways to condense alcohols to heavy alcohols via the Guerbet reaction can be described briefly in scheme 1.7 as illustrated below [77].

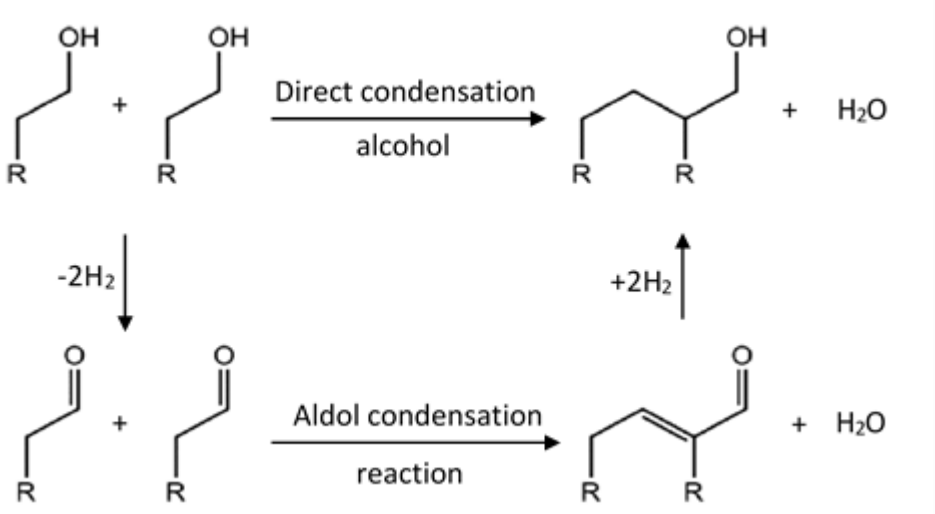

Scheme 1.7. Pathways of the Guerbet reaction for primary alcohols, modified from [77].

Branched Guerbet alcohols are less viscous than their linear equivalents, which is desirable for surfactants in a number of detergent formulations where a low temperature is necessary [77]. The importance of this reaction in biomass conversion is growing because it allows smaller alcohols to be upgraded to heavier branched chain alcohols [85,86].

From the above literature review, many routes to convert MEK to valuable chemicals are possible. One of them is direct subsequent hydrogenation-dehydration

reactions to convert MEK to light olefins (butenes). Another route is the direct condensation of MEK (aldol reaction), dehydration of the aldol products and hydrogenation of the resulting α-β unsaturated ketones to obtain heavy ketones, which can be further hydrogenated to produce Guerbet alcohols. Then, C_8 alkenes can be obtained via dehydration of the Guerbet alcohols.

1.6 Conversion of C_8 Ketone and/or C_8 Alcohol to C_8 Alkenes and C_8 Alkane

Significant effort has been devoted to developing alternative pathways to produce biofuel and chemicals from a sustainable source such as biomass because of declining petroleum resources and rising oil prices. One approach is to convert biomass-derived chemicals to hydrocarbons that can directly replace petroleum-based hydrocarbons.

Biomass-derived C_8 ketone (5-methyl-3-heptanone) can be produced by dehydrating biomass-derived 2,3 BDO to MEK followed by aldol condensation and hydrogenation reactions. This is considered as a valuable intermediate to produce C_8 alcohol (5-methyl-3-heptanol). This heavy alcohol can be further converted to C_8 alkenes (5-methyl-3-heptene and 5-methyl-2-heptene) by dehydration, and to branched C_8 alkane (3-methyl heptane) via subsequent dehydration-hydrogenation reactions, which can be used as fuels. Branching alkanes possess higher octane numbers than linear alkanes and can be used as octane boosters [87]. Increasing branching reduces the effective surface area obtainable for intermolecular interactions, meaning that branched molecules of the same carbon number as a linear molecule will have lower boiling and flash points [88].

The whole pathway to obtain C_8 alkenes and alkanes from biomass is shown in scheme 1.8.

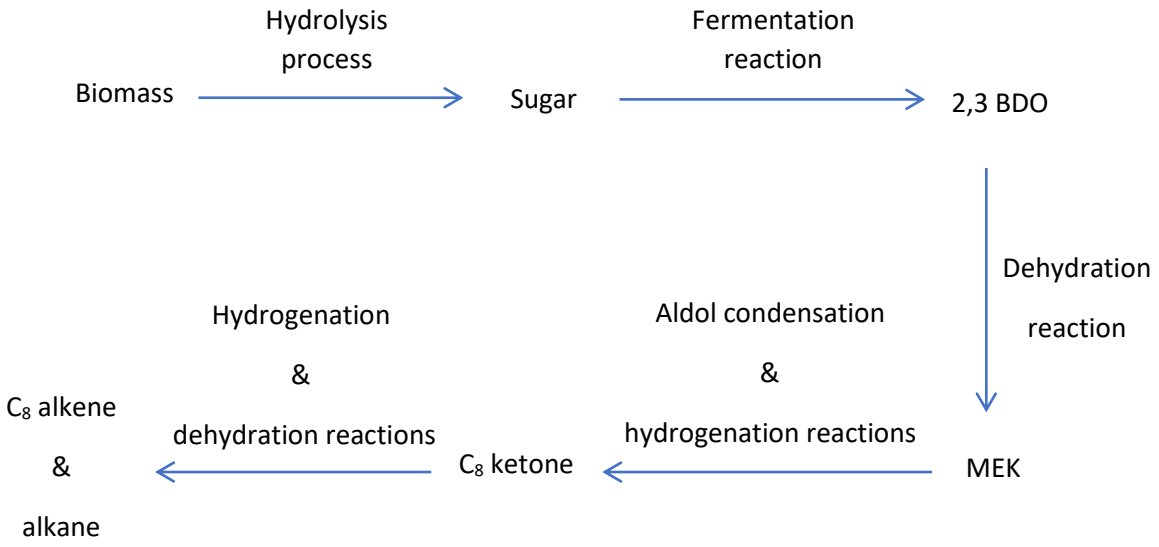

Scheme 1.8. The route of conversion of biomass to biofuel (C_8 alkene & alkane).

Generally, some metals, such as Pt, Ru, Rh, Ni, and Cu, catalyze the hydrogenation of carbonyl groups [89]. In combination with an acid catalyst, oxygen atoms can be removed through hydrogenation of C=O bond on metal sites followed by subsequent dehydration of the produced alcohols to alkenes over acid sites. Carbonyl hydrogenation catalysts also have a high hydrogenation activity for C=C bonds, except for Cu which is known to be relatively inactive for the hydrogenolysis of C–C bonds [59], so the product C=C bonds (alkene) can be further hydrogenated by the metal catalysts to produce alkane. This is the most typical approach for total hydrodeoxygenation. Cu [89–92] and Pt [93–

95] based catalysts were recorded to display good catalytic activity for the hydrogenation of carbonyl groups.

Sitthisa and Resasco [96] studied the hydrodeoxygenation of furfural over Cu, Pd and Ni supported on SiO_2. The result showed that the Cu catalyst mainly produced furfuryl alcohol by hydrogenation of the carbonyl group because of the weak interaction of Cu with alkene. Nagaraja *et al.* [91] reported the hydrogenation of furfural to furfuryl alcohol over a Cu-MgO catalyst made using different methods (coprecipitation, impregnated and solid–solid wetting) at atmospheric pressure. The results showed that high conversion of furfural (98%) and high selectivity of furfuryl alcohol (98%) could be obtained over Cu-MgO prepared by a coprecipitation method. The catalyst's high activity was attributed to the larger number of surface Cu sites measured using N_2O pulse chemisorption technique in addition to the defective sites at Cu and MgO interfacial region. Fan *et al*. [89] investigated Cu-γAl_2O_3 and Ni-γAl_2O_3 to hydrogenate 2,2,6,6-tetramethylpiperidin-4-one to 2,2,6,6 tetramethylpiperidin-4-ol at 140 °C. The results demonstrated that Cu-γAl_2O_3 gave much better activity and selectivity than Ni-γAl_2O_3. Also, they studied the effect of introducing Cr into Cu-γAl_2O_3 and found that Cu-Cr/γAl_2O_3 displayed better catalytic performance over Cu-γAl_2O_3. Poondi and Vannice [93] studied the hydrogenation of phenylacetaldehyde over Pt loaded on different supports (TiO_2, SiO_2 and Al_2O_3). The selectivity for 2-phenylethanol increased remarkably over Pt-TiO_2, giving 70% selectivity at 60% conversions. Also, Vannice and Poondi [95] investigated Pt on various supports (TiO_2, SiO_2 and Al_2O_3) for the hydrogenation of benzaldehyde to benzyl alcohol. The most

active catalyst among all Pt catalysts was Pt-TiO_2, selectively giving 100% benzyl alcohol at conversions up to at least 80%.

Dehydration of alcohols over alumina has been known for centuries [97], and it is considered as a traditional choice for alcohol dehydration [98–100]. Kostestkyy *et al.* [101] investigated the catalyzed dehydration of simple alcohols (1-propanol, 2-propanol and 2-methyl-2-propanol) on TiO_2, ZrO_2 and γAl_2O_3 oxide catalysts. The results showed that γAl_2O_3 was more active in catalyzing the dehydration reactions than either TiO_2 or ZrO_2.

It is well known that hydrodeoxygenation of ketones to alkanes is a significant reaction in the production of biofuels [102]. However, hydrodeoxygenation reactions are seldom used in industrial chemistry, and the development of successful catalytic systems has only been explored in recent years.

Ma *et al.* [103] studied the hydrodeoxygenation of hypnone to phenylethane over different catalysts (Ni-γAl_2O_3, Cu-γAl_2O_3 and Cu-Cr/γAl_2O_3) at 200 °C. The results demonstrated that the catalytic performance of Cu-γAl_2O_3 was better than Ni-γAl_2O_3 and its activity can be improved by adding Cr to it. Kong *et al.* [104] investigated the hydrodeoxygenation of cyclohexanone to cyclohexane over Ni supported on (γAl_2O_3, parent HZSM-5 (HZSM-5-P) and alkali-treated HZSM-5 (HZSM-5-At) at a reaction temperature 160 °C and under a H_2 pressure of 2 MPa. They reported that the highest selectivity was obtained over Ni-HZSM-5-At (above 99 %) while the lowest selectivity was 7.3% over Ni-γAl_2O_3. On Ni-γAl_2O_3, the main product was cyclohexanol, produced with a

selectivity that reached 83.7%. Yang *et al.* [105] performed the total hydrodeoxygenation of 2-cyclopentylidene cyclopentanone in a flow system at 230 °C to bi-cyclopentane (bicyclopentyl) over different supported metals. The reactant of this reaction (2-cyclopentylidene cyclopentanone) was obtained by the self-condensation of cyclopentanone, produced from C_5 carbohydrates via dehydration and selective catalytic reduction [106–110]. The whole mechanism is shown in the scheme 1.9 [105].

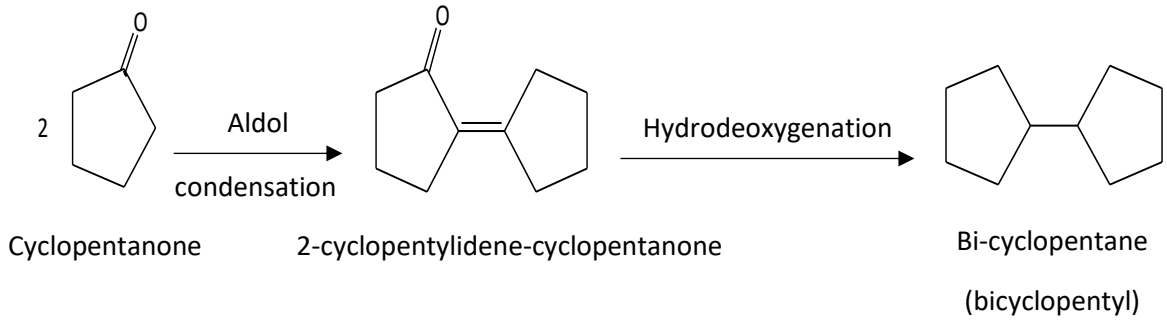

Scheme 1.9. Route to produce bi-cyclopentane from cyclopentanone derived from lignocellulose, modified from [105].

They reported that ≥90% yields of bicyclopentyl were obtained over Pd/SiO_2 and Ni/SiO_2, while yields were lower (~80%) over Pd catalysts with more acidic supports like SiO_2-Al_2O_3, H-zeolites (H-beta, H-ZSM-5), and zirconium phosphate. Yang *et al.* [111] reported the hydrodeoxygenation of 2-cyclopentylidene cyclopentanone over Ru/H-ZSM-5 at a lower temperature of 180 °C. The yield of bicyclopentyl was 91 %. Alotaibi *et al.* [112] investigated a number of supported metal catalysts consisting of Pt, Pd, Ru and Cu supported on silica and activated carbon for the hydrogenation of methyl isobutyl ketone (MIBK) in a continuous flow fixed bed reactor in the temperature range between 100 to

400 °C. The results displayed that these catalysts were active for the hydrogenation of MIBK to 4-methyl-2-pentanol (MPol) at 100–200 °C. The best results were obtained using 10% Pt-C, 10% Pd-C, 5% Ru-C and copper chromite, with selectivities for MPol ranging for 93-100% and conversions of MIBK of 92-96% at 100 °C. The selectivity to MPol reduced with increasing temperature because of the formation of 2-methyl pentane (MP) in addition to hydrogenolysis of C–C bonds, giving C_1–C_5 hydrocarbons. The highest selectivities of MP were 87% and 94% over 10% Pt-C and 10% Pd-C catalysts, respectively, with 52% and 84% conversions at a temperature as high as 300 °C. Also, they studied the hydrodeoxygenation of MIBK over metal catalysts (Pt, Pd, Ru, or Cu) loaded on $Cs_{2.5}H_{0.5}PW_{12}O_{40}$ (CsPW) at 100 °C under a H_2 flow. They stated that amongst the bifunctional catalysts studied, 0.5% Pt-CsPW was the best, yielding 99% MP at 100 °C with 100% MP selectivity and 99% MIBK conversion. 0.5% Ru-CsPW gave the same selectivity of MP as the Pt catalyst but showed much lower conversions of MIBK (5%). With higher loadings of Ru (5% Ru-CsPW), the conversion of MIBK increased to 99%. Over 0.5% Pd-CsPW, both conversion of MIBK (7%) and MP selectivity (34%) were lower than over the 0.5% Pt-CsPW and 5% Ru-CsPW catalysts. 0.5% Pd-CsPW produced a large amount of heavy condensation products. 5% Cu-CsPW did not show catalytic activity at 100 °C.

This dissertation comprises 6 chapters. Chapter 1 provides an introduction of background information and the aims of this dissertation and a literature review dealing with different projects described in this study. Chapter 2 includes a brief description of the experimental procedures. Chapter 3 discusses the conversion of MEK to butene, an intermediate to produce biofuel. In chapter 4, aldol condensations of MEK to higher

ketones, an intermediate to produce further important products like alcohols, alkenes and alkanes, is described. Chapter 5 presents the conversion of higher ketones (C_8 ketone) to C_8 alkenes and alkane, which can be used as gasoline blended components to increase the gasoline octane number. Chapter 6 consists of summarizing conclusions in addition to some potential work for the future, drawing from the conclusions and achievements described in this work.

References

1. Huber, G. W.; Iborra, S.; Corma, A. Synthesis of transportation fuels from biomass: chemistry, catalysts, and engineering. *Chem. Rev.* **2006**, *106*, 4044–4098.

2. Klass, D. L. *Biomass for renewable energy, fuels, and chemicals*; Elsevier, **1998**.

3. Cheng, Y. T.; Huber, G. W. Chemistry of furan conversion into aromatics and olefins over HZSM-5: a model biomass conversion reaction. *ACS Catal.* **2011**, *1*, 611–628.

4. van Putten, R.J.; Van Der Waal, J. C.; De Jong, E. D.; Rasrendra, C. B.; Heeres, H. J.; de Vries, J. G. Hydroxymethylfurfural, a versatile platform chemical made from renewable resources. *Chem. Rev.* **2013**, *113*, 1499–1597.

5. Alonso, D. M.; Wettstein, S. G.; Dumesic, J. A. Gamma-valerolactone, a sustainable platform molecule derived from lignocellulosic biomass. *Green Chem.* **2013**, *15*, 584–595.

6. Magee, R. J.; Kosaric, N. The microbial production of 2,3-butanediol. *Adv. Appl. Microbiol.* **1987**, *32*, 89–161.

7. Ji, X. J.; Huang, H.; Ouyang, P. K. Microbial 2,3-butanediol production: a state-of-the-art review. *Biotechnol. Adv.* **2011**, *29*, 351–364.

8. Ji, X. J.; Huang, H.; Du, J.; Zhu, J. G.; Ren, L. J.; Hu, N.; Li, S. Enhanced 2,3-butanediol production by Klebsiella oxytoca using a two-stage agitation speed control strategy. *Bioresour. Technol.* **2009**, *100*, 3410–3414.

9. Ji, X. J.; Huang, H.; Du, J.; Zhu, J. G.; Ren, L. J.; Li, S.; Nie, Z. K. Development of an industrial medium for economical 2,3-butanediol production through co-fermentation of glucose and xylose by Klebsiella oxytoca. *Bioresour. Technol.* **2009**, *100*, 5214–5218.

10. Perego, P.; Converti, A.; Del Borghi, A.; Canepa, P. 2,3-Butanediol production by Enterobacter aerogenes: selection of the optimal conditions and application to food industry residues. *Bioprocess Eng.* **2000**, *23*, 613–620.

11. Perego, P.; Converti, A.; Del Borghi, M. Effects of temperature, inoculum size and starch hydrolyzate concentration on butanediol production by Bacillus licheniformis. *Bioresour. Technol.* **2003**, *89*, 125–131.

12. Winfield, M. E. The catalytic dehydration of 2,3-butanediol to butadiene. *Aust. J. Sci. Res. A* **1945**, *3*, 290–305.

13. Duan, H.; Yamada, Y.; Sato, S. Efficient production of 1,3-butadiene in the catalytic dehydration of 2,3-butanediol. *Appl. Catal. A Gen.* **2015**, *491*, 163–169.

14. Kim, W.; Shin, W.; Lee, K. J.; Song, H.; Kim, H. S.; Seung, D.; Filimonov, I. N. 2,3-Butanediol dehydration catalyzed by silica-supported sodium phosphates. *Appl. Catal. A Gen.* **2016**, *511*, 156–167.

15. Tran, A. V; Chambers, R. P. The dehydration of fermentative 2,3-butanediol into methyl ethyl ketone. *Biotechnol. Bioeng.* **1987**, *29*, 343–351.

16. Multer, A.; McGraw, N.; Hohn, K.; Vadlani, P. Production of methyl ethyl ketone from biomass using a hybrid biochemical/catalytic approach. *Ind. Eng. Chem. Res.* **2012**, *52*, 56–60.

17. Lee, J.; Grutzner, J. B.; Walters, W. E.; Delgass, W. N. The conversion of 2,3-butanediol to methyl ethyl ketone over zeolites. *Stud. Surf. Sci. Catal.* **2000**, *130*, 2603–2608.

18. Zheng, Q.; Wales, M. D.; Heidlage, M. G.; Rezac, M.; Wang, H.; Bossmann, S. H.; Hohn, K. L. Conversion of 2,3-butanediol to butenes over bifunctional catalysts in a single reactor. *J. Catal.* **2015**, *330*, 222–237.

19. Zhenhua, L. I. U.; Wenzhou, H. U. O.; Hao, M. A.; Kai, Q. Development and commercial application of methyl-ethyl-ketone production technology. *Chinese J. Chem. Eng.* **2006**, *14*, 676–684.

20. Hoell, D.; Mensing, T.; Roggenbuck, R.; Sakuth, M.; Sperlich, E.; Urban, T.; Neier, W.; Strehlke, G. 2-Butanone. *Ullmann's Encycl. Ind. Chem.* **2000**, 6, 431–444.

21. Cox, N. R. Oxidation of hydrocarbons. U.S. Patent No. 3,196,182. **1965**.

22. Yu, E. K.; Saddler, J. N. Fed-batch approach to production of 2,3 butanediol by Klebsiella pneumoniae grown on high substrate concentrations. *Appl. Environ. Microbiol.* **1983**, *46*, 630–635.

23. Zeng, A. P.; Biebl, H.; Deckwer, W. D. Effect of pH and acetic acid on growth and 2, 3-butanediol production of Enterobacter aerogenes in continuous culture. *Appl. Microbiol. Biotechnol.* **1990**, *33*, 485–489.

24. Mas, C. De; Jansen, N. B.; Tsao, G. T. Production of optically active 2,3-butanediol by Bacillus polymyxa. *Biotechnol. Bioeng.* **1988**, *31*, 366–377.

25. Ledingham, G. A.; Neish, A. C. Fermentative Production of 2,3 Butanediol Industrial Fermentations, LA Underkofler and RJ Hickey, Eds. **1954**,2, 27–93.

26. Jansen, N. B.; Flickinger, M. C.; Tsao, G. T. Production of 2,3-butanediol from D-xylose by Klebsiella oxytoca ATCC 8724. *Biotechnol. Bioeng.* **1984**, *26*, 362–369.

27. Qureshi, N.; Cheryan, M. Effects of aeration on 2,3-butanediol production from glucose by Klebsiella oxytoca. *J. Ferment. Bioeng.* **1989**, *67*, 415–418.

28. Saha, B. C.; Bothast, R. J. Production of 2,3-butanediol by newly isolated Enterobacter cloacae. *Appl. Microbiol. Biotechnol.* **1999**, *52*, 321–326.

29. Celińska, E.; Grajek, W. Biotechnological production of 2,3-butanediol—current state and prospects. *Biotechnol. Adv.* **2009**, *27*, 715–725.

30. Petrov, K.; Petrova, P. Enhanced production of 2,3-butanediol from glycerol by forced pH fluctuations. *Appl. Microbiol. Biotechnol.* **2010**, *87*, 943–949.

31. Pirt, S. J.; Callow, D. S. Exocellular product formation by microorganisms in continuous culture. I. Production of 2,3 butanediol by aerobacter aerogenes in a single stage process. *J. Appl. Bacteriol.* **1958**, *21*, 188–205.

32. Jansen, N. B.; Flickinger, M. C.; Tsao, G. T. Application of bioenergetics to modeling the batch fermentation of D-xylose to 2,3-butanediol by Klebsiella oxytoca. *Biotechnol.Bioeng* **1984**, *26*, 362–368.

33. Neish, A. C.; Ledingham, G. A. Production and properties of 2,3 butanediol: XXXII. 2,3 butanediol fermentations at poised hydrogen ion concentrations. *Can. J. Res.* **1949**, *27*, 694–704.

34. Garg, S. K.; Jain, A. Fermentative production of 2,3-butanediol: a review. *Bioresour. Technol.* **1995**, *51*, 103–109.

35. Syu, M. J. Biological production of 2, 3-butanediol. *Appl. Microbiol. Biotechnol.* **2001**, *55*, 10–18.

36. Van Haveren, J.; Scott, E. L.; Sanders, J. Bulk chemicals from biomass. *Biofuels, Bioprod. Biorefining* **2008**, *2*, 41–57.

37. Xiao, Z.; Xu, P. Acetoin metabolism in bacteria. *Crit. Rev. Microbiol.* **2007**, *33*, 127–140.

38. Voloch, M.; Jansen, N. B.; Ladisch, M. R.; Tsao, G. T.; Narayan, R.; Rodwell, Vw. 2, 3 Butanediol. *Industrial Chemicals, Biochemicals and Fuels.* **1985**, 933–947.

39. Biggs, R. A.; Ogilvie, W. W. *6.18 Eliminations to Form Alkenes, Allenes, and Alkynes and Related Reactions*; Elsevier Ltd, **2014**, 6, 802-841.

40. Molnár, Á.; Bucsi, I.; Bartók, M. Pinacol Rearrangement on Zeolites. *Stud. Surf. Sci. Catal.* **1988**, *41*, 203–210.

41. Zhang, W.; Yu, D.; Ji, X.; Huang, H. Efficient dehydration of bio-based 2,3-butanediol to butanone over boric acid modified HZSM-5 zeolites. *Green Chem.* **2012**, *14*, 3441–3450.

42. Bucsi, I.; Molnár, Á.; Bartók, M.; Olah, G. A. Transformation of 1,2-diols over perfluorinated resinsulfonic acids (Nafion-H). *Tetrahedron* **1994**, *50*, 8195–8202.

43. Török, B.; Bucsi, I.; Beregszászi, T.; Kapocsi, I.; Molnár, Á. Transformation of diols in the presence of heteropoly acids under homogeneous and heterogeneous conditions. *J. Mol. Catal. A Chem.* **1996**, *107*, 305–311.

44. Emerson, R. R.; Flickinger, M. C.; Tsao, G. T. Kinetics of dehydration of aqueous 2,3-butanediol to methyl ethyl ketone. *Ind. Eng. Chem. Prod. Res. Dev.* **1982**, *21*, 473–477.

45. Nikitina, M. A.; Ivanova, I. I. Conversion of 2,3-Butanediol over Phosphate Catalysts. *ChemCatChem* **2016**, *8*, 1346–1353.

46. Peratello, S.; Molinari, M.; Bellussi, G.; Perego, C. Olefins oligomerization: thermodynamics and kinetics over a mesoporous silica–alumina. *Catal. today.* **1999**, *52*, 271–277.

47. Grieken, R. Van; Escola, J. M.; Moreno, J.; Rodriguez, R. Direct synthesis of mesoporous M-SBA-15 (M= Al, Fe, B, Cr) and application to 1-hexene oligomerization. *Chem. Eng. J.* **2009**, *155*, 442–450.

48. Zheng, Q.; Grossardt, J.; Almkhelfe, H.; Xu, J.; Grady, B. P.; Douglas, J. T.; Amama, P. B.; Hohn, K. L. Study of mesoporous catalysts for conversion of 2,3-butanediol to butenes. *J. Catal.* **2017**, *354*, 182–196.

49. Villegas, J.; Kumar, N.; Heikkilä, T.; Lehto, V. P.; Salmi, T.; Murzin, D. A study on the dimerization of 1-butene over Beta zeolite. *Top. Catal.* **2007**, *45*, 187–190.

50. Schmerling, L.; Ipatieff, V. N. The mechanism of the polymerization of alkenes. *Adv. Catal.* **1950**, *2*, 21–80.

51. Naito, S.; Sakurai, Y.; Shimizu, H.; Onishi, T.; Tamaru, K. Reaction mechanism of unsaturated hydrocarbons with deuterium over zinc oxide. *Trans. Faraday Soc.* **1971**, *67*, 1529–1537.

52. Yan, H.; Cheng, H.; Yi, H.; Lin, Y.; Yao, T.; Wang, C.; Li, J.; Wei, S.; Lu, J. Single-atom Pd1/graphene catalyst achieved by atomic layer deposition: remarkable performance in selective hydrogenation of 1,3-butadiene. *J. Am. Chem. Soc.* **2015**, *137*, 10484–10487.

53. Hou, R.; Yu, W.; Porosoff, M. D.; Chen, J. G.; Wang, T. Selective hydrogenation of 1, 3-butadiene on Pd Ni bimetallic catalyst: From model surfaces to supported catalysts. *J. Catal.* **2014**, *316*, 1–10.

54. Coelho, A.; Caeiro, G.; Lemos, M.; Lemos, F.; Ribeiro, F. R. 1-Butene oligomerization over ZSM-5 zeolite: Part 1–Effect of reaction conditions. *Fuel* **2013**, *111*, 449–460.

55. Wright, M. E.; Harvey, B. G.; Quintana, R. L. Highly efficient zirconium-catalyzed batch conversion of 1-butene: a new route to jet fuels. *Energy & Fuels* **2008**, *22*, 3299–3302.

56. Gary, J. H.; Handwerk, G. E. *Petroleum refining. Technology and economics.* Marcel Dekker, Inc., New York, **1975**; *Volume 5*.

57. Considine, D. M. *Chemical and process technology encyclopedia*; McGraw-Hill, **1974,** pp. 492.

58. Calamur, N.; Carrera, M. E.; Wilsak, R. A. Butylenes. *Kirk-othmer Encycl. Chem. Technol.* **2000**, *4*, 402-433.

59. Brands, D. S.; Poels, E. K.; Bliek, A. Ester hydrogenolysis over promoted Cu/SiO_2 catalysts. *Appl. Catal. A Gen.* **1999**, *184*, 279–289.

60. Sato, S.; Akiyama, M.; Takahashi, R.; Hara, T.; Inui, K.; Yokota, M. Vapor-phase reaction of polyols over copper catalysts. *Appl. Catal. A Gen.* **2008**, *347*, 186–191.

61. Vasiliadou, E. S.; Eggenhuisen, T. M.; Munnik, P.; Jongh, P. E. De; Jong, K. P. De; Lemonidou, A. A. Synthesis and performance of highly dispersed Cu/SiO_2 catalysts for the hydrogenolysis of glycerol. *Appl. Catal. B Environ.* **2014**, *145*, 108–119.

62. Lilga, M. A.; Lee, G. S.; Lee, S. J. Conversion of 2,3-butanediol to 2-butanol, olefins and fuels. U.S. Patent No. 9,517,984. **2016**.

63. Hattori, H. Heterogeneous basic catalysis. *Chem. Rev.* **1995**, *95*, 537–558.

64. Yamaguchi, T.; Nakano, Y.; Iizuka, T.; Tanabe, K. Catalytic activity of ZrO_2 and ThO_2 for HD exchange reaction between methyl group of adsorbed isopropyl alcohol-d8 and surface OH group. *Chem. Lett.* **1976**, 677–678.

65. Tomatsu, T.; Yoneda, N.; Ohtsuka, H. Some Catalytic Behavoirs of Thoria in the Dehydration of Alcohols. *J. Japan Oil Chem. Soc.* **1968**, *17*, 236–245.

66. Lundeen, A. J.; VanHoozer, R. Selective catalytic dehydration. Thoria-catalyzed dehydration of alcohols. *J. Org. Chem.* **1967**, *32*, 3386–3389.

67. Szabó, Z. G.; Jover, B.; Ohmacht, R. The joint application of flow-system and micropulse techniques for a comparative study of 2-propanol decomposition over MgO, CaO and SrO. *J. Catal.* **1975**, *39*, 225–233.

68. Yashima, T.; Suzuki, H.; Hara, N. Decomposition of 2-propanol over alkali cation exchanged zeolites. *J. Catal.* **1974**, *33*, 486–492.

69. Yoshikawa, N.; Yamada, Y. M. A.; Das, J.; Sasai, H.; Shibasaki, M. Direct catalytic asymmetric aldol reaction. *J. Am. Chem. Soc.* **1999**, *121*, 4168–4178.

70. Cosimo, J. I. Di; Diez, V. K.; Apesteguía, C. R. Base catalysis for the synthesis of α,β-unsaturated ketones from the vapor-phase aldol condensation of acetone. *Appl. Catal. A Gen.* **1996**, *137*, 149-166.

71. Nielsen, A. T.; Houlihan, W. J. The aldol condensation. *Org. React.* **1968**, 16, pp 2–3.

72. Roelofs, J.; van Dillen, A. J.; Jong, K. P. De Base-catalyzed condensation of citral and acetone at low temperature using modified hydrotalcite catalysts. *Catal. Today.* **2000**, *60*, 297–303.

73. Muthusamy, D.; Wang, C. C.; Swain, R. D.; Litzen, D. B.; Pledger, W. R. Process of making ketones. U.S. Patent 5,583,263. **1996**.

74. Kelly, G. J. Aldol condensation reaction and catalyst therefor. U.S. Patent 6,706,928. **2004**.

75. Weissermel, K. *Industrial organic chemistry*; Weinheim: VCH ; New York: VCH, **1997**, pp. 280.

76. Reichle, W. T. Catalytic aldol condensations. U.S. Patent No. 4,165,339. **1979**.

77. Gabriëls, D.; Hernández, W. Y.; Sels, B.; Voort, P. Van Der; Verberckmoes, A. Review of catalytic systems and thermodynamics for the Guerbet condensation reaction and challenges for biomass valorization. *Catal. Sci. Technol.* **2015**, *5*, 3876–3902.

78. Yang, C.; Meng, Z. Y. Bimolecular condensation of ethanol to 1-butanol catalyzed by alkali cation zeolites. *J. Catal.* **1993**, *142*, 37–44.

79. Ndou, A. S.; Plint, N.; Coville, N. J. Dimerisation of ethanol to butanol over solid-base catalysts. *Appl. Catal. A Gen.* **2003**, *251*, 337–345.

80. Burk, P. L.; Pruett, R. L.; Campo, K. S. The rhodium-promoted guerbet reaction: Part II. Secondary alcohols and methanol as substrates. *J. Mol. Catal.* **1985**, *33*, 15–21.

81. Breitkreuz, K.; Menne, A.; Kraft, A. New process for sustainable fuels and chemicals from bio-based alcohols and acetone. *Biofuels, Bioprod. Biorefining* **2014**, *8*, 504–515.

82. Anbarasan, P.; Baer, Z. C.; Sreekumar, S.; Gross, E.; Binder, J. B.; Blanch, H. W.; Clark, D. S.; Toste, F. D. Integration of chemical catalysis with extractive fermentation to produce fuels. *Nature* **2012**, *491*, 235–239.

83. Sreekumar, S.; Baer, Z. C.; Gross, E.; Padmanaban, S.; Goulas, K.; Gunbas, G.; Alayoglu, S.; Blanch, H. W.; Clark, D. S.; Toste, F. D. Chemocatalytic upgrading of tailored fermentation products toward biodiesel. *ChemSusChem* **2014**, *7*, 2445–2448.

84. Hwang, Y. L.; Bedard, T. C. Ketones. *Kirk-Othmer Encyclopedia of Chemical Technology.* **2000**.

85. O'Lenick, A. J. Guerbet chemistry. *J. Surfactants Deterg.* **2001**, *4*, 311–315.

86. Kozlowski, J. T.; Davis, R. J. Heterogeneous catalysts for the Guerbet coupling of alcohols. *ACS Catal.* **2013**, *3*, 1588–1600.

87. Roldán, R.; Romero, F. J.; Jiménez-Sanchidrián, C.; Marinas, J. M.; Gómez, J. P. Influence of acidity and pore geometry on the product distribution in the hydroisomerization of light paraffins on zeolites. *Appl. Catal. A Gen.* **2005**, *288*, 104–115.

88. Jenkins, R. W.; Moore, C. M.; Semelsberger, T. A.; Chuck, C. J.; Gordon, J. C.; Sutton, A. D. The Effect of Functional Groups in Bio-Derived Fuel Candidates. *ChemSusChem* **2016**, *9*, 922–931.

89. Fan, X.; Liu, S.; Yan, X.; Du, X.; Chen, L. A continuous process for the production of 2, 2, 6, 6-tetramethylpiperidin-4-ol catalyzed by Cu–Cr/γ-Al_2O_3. *Catal. Commun.* **2010**, *11*, 960–963.

90. Saadi, A.; Rassoul, Z.; Bettahar, M. M. Gas phase hydrogenation of benzaldehyde over supported copper catalysts. *J. Mol. Catal. A Chem.* **2000**, *164*, 205–216.

91. Nagaraja, B. M.; Kumar, V. S.; Shasikala, V.; Padmasri, A. H.; Sreedhar, B.; Raju, B. D.; Rao, K. S. R. A highly efficient Cu/MgO catalyst for vapour phase hydrogenation of furfural to furfuryl alcohol. *Catal. Commun.* **2003**, *4*, 287–293.

92. Chambers, A.; Jackson, S. D.; Stirling, D.; Webb, G. Selective hydrogenation of cinnamaldehyde over supported copper catalysts. *J. Catal.* **1997**, *168*, 301–314.

93. Poondi, D.; Vannice, M. A. The influence of MSI (metal-support interactions) on phenylacetaldehyde hydrogenation over Pt catalysts. *J. Mol. Catal. A Chem.* **1997**, *124*, 79–89.

94. Vannice, M. A.; Sen, B. Metal-support effects on the intramolecular selectivity of crotonaldehyde hydrogenation over platinum. *J. Catal.* **1989**, *115*, 65–78.

95. Vannice, M. A.; Poondi, D. The effect of metal-support interactions on the hydrogenation of benzaldehyde and benzyl alcohol. *J. Catal.* **1997**, *169*, 166–175.

96. Sitthisa, S.; Resasco, D. E. Hydrodeoxygenation of furfural over supported metal catalysts: a comparative study of Cu, Pd and Ni. *Catal. Letters* **2011**, *141*, 784–791.

97. Bondt, N.; Deiman, J. R.; van Troostwyk, P.; Lauwerenburg, A. *Ann, chem. phys* **1797**, *21*, 48.

98. Knözinger, H.; Köhne, R. The dehydration of alcohols over alumina: I. The reaction scheme. *J. Catal.* **1966**, *5*, 264–270.

99. Knözinger, H.; Scheglila, A. The dehydration of alcohols on alumina: XII. Kinetic isotope effects in the olefin formation from butanols. *J. Catal.* **1970**, *17*, 252–263.

100. Knözinger, H.; Bühl, H.; Kochloefl, K. The dehydration of alcohols on alumina: XIV. Reactivity and mechanism. *J. Catal.* **1972**, *24*, 57–68.

101. Kostestkyy, P.; Yu, J.; Gorte, R. J.; Mpourmpakis, G. Structure–activity relationships on metal-oxides: alcohol dehydration. *Catal. Sci. Technol.* **2014**, *4*, 3861–3869.

102. Nakagawa, Y.; Liu, S.; Tamura, M.; Tomishige, K. Catalytic total hydrodeoxygenation of biomass-derived polyfunctionalized substrates to alkanes. *ChemSusChem* **2015**, *8*, 1114–1132.

103. Ma, J.; Liu, S.; Kong, X.; Fan, X.; Yan, X.; Chen, L. A continuous process for the reductive deoxygenation of aromatic ketones over $Cu_{30}Cr_{10}/\gamma Al_2O_3$. *Res. Chem. Intermed.* **2012**, *38*, 1341–1349.

104. Kong, X.; Lai, W.; Tian, J.; Li, Y.; Yan, X.; Chen, L. Efficient Hydrodeoxygenation of Aliphatic Ketones over an Alkali-Treated Ni/HZSM-5 Catalyst. *ChemCatChem* **2013**, *5*, 2009–2014.

105. Yang, J.; Li, N.; Li, G.; Wang, W.; Wang, A.; Wang, X.; Cong, Y.; Zhang, T. Synthesis of renewable high-density fuels using cyclopentanone derived from lignocellulose. *Chem. Commun.* **2014**, *50*, 2572–2574.

106. Hronec, M.; Fulajtarová, K. Selective transformation of furfural to cyclopentanone. *Catal. Commun.* **2012**, *24*, 100–104.

107. Hronec, M.; Fulajtarová, K.; Liptaj, T. Effect of catalyst and solvent on the furan ring rearrangement to cyclopentanone. *Appl. Catal. A Gen.* **2012**, *437*, 104–111.

108. Zhou, M.; Zhu, H.; Niu, L.; Xiao, G.; Xiao, R. Catalytic hydroprocessing of furfural to cyclopentanol over Ni/CNTs catalysts: model reaction for upgrading of bio-oil. *Catal. Letters* **2014**, *144*, 235–241.

109. Li, X. L.; Deng, J.; Shi, J.; Pan, T.; Yu, C. G.; Xu, H. J.; Fu, Y. Selective conversion of furfural to cyclopentanone or cyclopentanol using different preparation methods of Cu–Co catalysts. *Green Chem.* **2015**, *17*, 1038–1046.

110. Guo, J.; Xu, G.; Han, Z.; Zhang, Y.; Fu, Y.; Guo, Q. Selective conversion of furfural to cyclopentanone with CuZnAl catalysts. *ACS Sustain. Chem. Eng.* **2014**, *2*, 2259–2266.

111. Yang, Y.; Du, Z.; Huang, Y.; Lu, F.; Wang, F.; Gao, J.; Xu, J. Conversion of furfural into cyclopentanone over Ni–Cu bimetallic catalysts. *Green Chem.* **2013**, *15*, 1932–1940.

112. Alotaibi, M. A.; Kozhevnikova, E. F.; Kozhevnikov, I. V Efficient hydrodeoxygenation of biomass-derived ketones over bifunctional Pt-polyoxometalate catalyst. *Chem. Commun.* **2012**, *48*, 7194–7196.

Chapter 2 - Research Plan

For the three projects described in this thesis, the research followed a similar sequence of steps, including choosing a suitable catalyst, synthesizing the catalyst, characterizing its chemical and physical properties, testing its catalytic activity and studying the roles of operating conditions on catalytic performance.

2.1 Choosing a Suitable Catalyst

This step is significant for obtaining a specific desired product. Seeking and finding a suitable catalyst is a big challenge since there are hundreds of catalysts which can be used, and screening and testing catalysts takes extensive time. Therefore, this step requires choosing an appropriate catalyst via extensive research and knowledge of the properties of catalysts and their functions for different chemical reactions.

Regarding the first project that focused on converting MEK to butene, copper metal was chosen as the hydrogenation catalyst since copper is well known to selectively hydrogenate C=O bonds while leaving C-C bonds alone. In addition, its price is much less than other hydrogenation catalysts like palladium (Pd), platinum (Pt), and ruthenium (Ru) metals. The support was chosen to catalyze dehydration reactions with high selectivity. As mentioned in the literature, alumina and zeolites are suitable dehydration reactions. Among many kinds of zeolites, zeolite Y sodium was chosen as a support because it showed the ability of dehydrating 2-propanol to propene [1]. Then by loading copper on

the support, the hydrogenation-dehydration properties can be combined into one catalyst.

For the second project, converting MEK to C_8 ketone requires sequential reactions including aldol condensation (aldol-dehydration) and hydrogenation reactions as explained previously. Our aim in this work was to seek a catalyst that works as a multifunctional catalyst. ZrO_2 was chosen as a support since it has both acidic and basic properties [2]. It is hypothesized that the basic sites on ZrO_2 facilitate the aldol reaction. However, the acidic sites are appropriate for dehydration reactions [3], as mentioned in the literature. Also, supported metals like copper help to hydrogenate aldol condensation products (α,β-unsaturated ketones) to saturated ketones. We hypothesized that Cu-ZrO_2 would be capable of catalyzing the different steps involving aldol condensation and hydrogenation reactions to produce C_8 ketones.

In regards to the third project, conversion of C_8 ketone to C_8 alkenes and alkane was studied using bifunctional catalysts having hydrogenation-dehydration properties in one bed. C_8 alkenes and alkane can be obtained from a C_8 ketone by hydrogenating the ketone to a C_8 alcohol, followed by dehydration of the C_8 alcohol to obtain branched C_8 alkenes and further hydrogenation to give a C_8 alkane. For this project, we chose Al_2O_3 as a support since it is well known for the dehydration of alcohols. Cu and Pt were loaded on the support to facilitate hydrogenation reactions (hydrogenation of C=O for the ketone and C=C for the alkene), and the comparison between these two different metals is reported. Hydrogenation of C_8 ketone to C_8 alcohol occurred on metal sites while

dehydration of the alcohol occurred on the acid sites generating C_8 alkenes. These can be further hydrogenated on metal sites to produce C_8 alkane.

The question that could be raised is whether bi-functional and multi-functional catalysts can convert MEK to valuable chemicals in one step and in a single reactor, or whether the reaction should be executed in a two or three-stage process using different separated catalysts. This thesis attempts to address this question by studying multifunctional catalysts.

2.2 Making a Supported Catalyst (Chosen Catalyst)

Heterogeneous catalysts are solids or mixtures of solids which can accelerate chemical reactions without themselves accruing changes. However, this definition is too restrictive since the properties of catalysts can change remarkably with use: catalyst life time can vary from minutes to years [4].

Supported catalysts are composed of an active phase dispersed on a support as a carrier [5–7]. Supports are typically highly porous, high surface area, and thermally stable materials with suitable mechanical strength [8]. While generally the supports are considered as a means for dispersing the active phase, they can also play a role in the catalysis.

Common preparation methods for supported metal catalysts include impregnation (incipient wetness impregnation and wet impregnation), ion-exchange, coprecipitation and deposition-precipitation methods. In all of these methods, a metal

precursor is introduced onto the support to attach the metals to the support and to prevent dispersed metal crystals from coalescing. This step is followed by drying the support to eliminate the adsorbed liquid and activating the catalyst by calcination, reduction or other suitable treatments. [6,8].

There are two types of impregnation which can be distinguished according to the amount of solution used: incipient wetness impregnation (dry impregnation) and soaking impregnation (wet impregnation) methods. The incipient wetness impregnation method is the most common method used to prepare supported metal catalysts. This method is often used for catalyst manufacture industrially because it is simple and economical [8].For the incipient wetness impregnation method, the volume of the metal precursor solution does not exceed the pore volume of the support. The maximum loading is limited by the solubility of the metal precursor in the solution which can be overcome by performing successive impregnation steps. In contrast, the wet impregnation method includes the use of an excess of solution with respect to the support pore volume [8]. Then, the solid is separated and the excess solvent is removed via drying after a certain time [4]. The advantage of incipient wetness impregnation is that the weight of the added metal incorporated in the catalyst can be controlled easily. However, its disadvantage is that the dispersed metal may not be as uniform as that prepared by wet impregnation [9].

After impregnation, the material undergoes thermal treatments which involve drying, calcination and reduction treatments. The drying step consists of evaporating the

solvent (typically water) from the pores of the support. In general, this treatment is carried out at temperatures between 80 °C and 200 °C.

The second step comprises of a calcination process. This treatment includes heating the catalysts in air at a temperature usually higher than those used during catalytic reactions. The purpose of calcination is to decompose the metal precursor to form an oxide and to remove gaseous products including water, CO_2, and the cations or anions found in the precursor salt. Besides decomposition, a sintering of the precursor or of the formed oxide and a reaction of the latter with the support can happen during calcination.

The final step is reduction. In this step, the metal oxide or sometimes the metal precursor is transformed into a metal via thermal treatment in the presence of hydrogen. Some variables such as the rate of heating, final temperature, time of reduction, concentration and flow of hydrogen can affect the reduction of the catalyst, so they have to be carefully chosen, considering the type of metal, catalytic system and reaction to be carried out. The flow of hydrogen has to be high enough to remove the water, formed during the reduction, from the support since water vapor can be detrimental for a high dispersion of the metal [8].

In this work, all the catalysts were prepared using the incipient wetness method. The metal precursor solution was prepared by dissolving the metal precursor in a sufficient amount of water to fill the pores of the support using dropwise addition with manually mixing. The volume of liquid needed to fill these pores was determined by

adding small quantities of the solvent slowly to a weighted amount of the support with stirring until the mixture became slightly liquid. After that, this ratio of weight:volume was used to prepare a metal precursor solution with a suitable concentration to achieve the desired metal loading [10]. Next, the catalysts were dried in an oven overnight at 100 °C then heated in a furnace at 110 °C for 2 h and calcined at 550 °C for 4 h. A ramp rate of 2 °C/min was used up to 110 °C and 1 °C/min up to 550 °C. After the calcination process, the catalysts were crushed and sieved to the desired sizes.

2.3 Testing the Catalyst Activity

The catalytic reactions in this work were carried out in a continuous flow fixed-bed reactor made of stainless steel (id=0.85 cm) under atmospheric pressure. A reactant stream, in the gas phase, and hydrogen were fed into the reactor and contacted with the catalyst at a suitable reaction temperature using heating tape as a heating supply. Prior to the reaction, the catalyst was reduced in the reactor with hydrogen and nitrogen for 1 h. For the reaction, the reactant (MEK or C_8 ketone) was fed through the top of reactor at a feed rate of 1 (mL/h) via a micro pump (Eldex 1SMP) together with H_2 and N_2 at a specific flow rate and reaction temperature which were controlled using mass flow controllers and a heat controller respectively. The effluent product compositions were analyzed using an on-line gas chromatograph (SRI 8610C) with an MXT-1 column (100% dimethyl polysiloxane (nonpolar phase), 60 m, ID 0.53 mm), and FID and TCD detectors for the analysis of hydrocarbons and natural gases. The temperature of the product effluent from the bottom of the reactor was maintained above 200 °C to avoid the condensation of

liquid products, which were injected into the GC through the sample loop controlled by a high temperature ten-port valve. The GC oven was held at 40 °C for 5 min, and then raised to 120 °C at a ramp rate of 40 °C/min, finally raised to 250 °C at a rate of 20 °C/min, and held at this temperature for 10 min. The products were identified via gas chromatography with a mass spectrometer (GC-MS) analyzer using an Agilent 7890A GC system equipped with an Agilent 5975C MS detector. The experimental setup is shown in scheme 2.1.

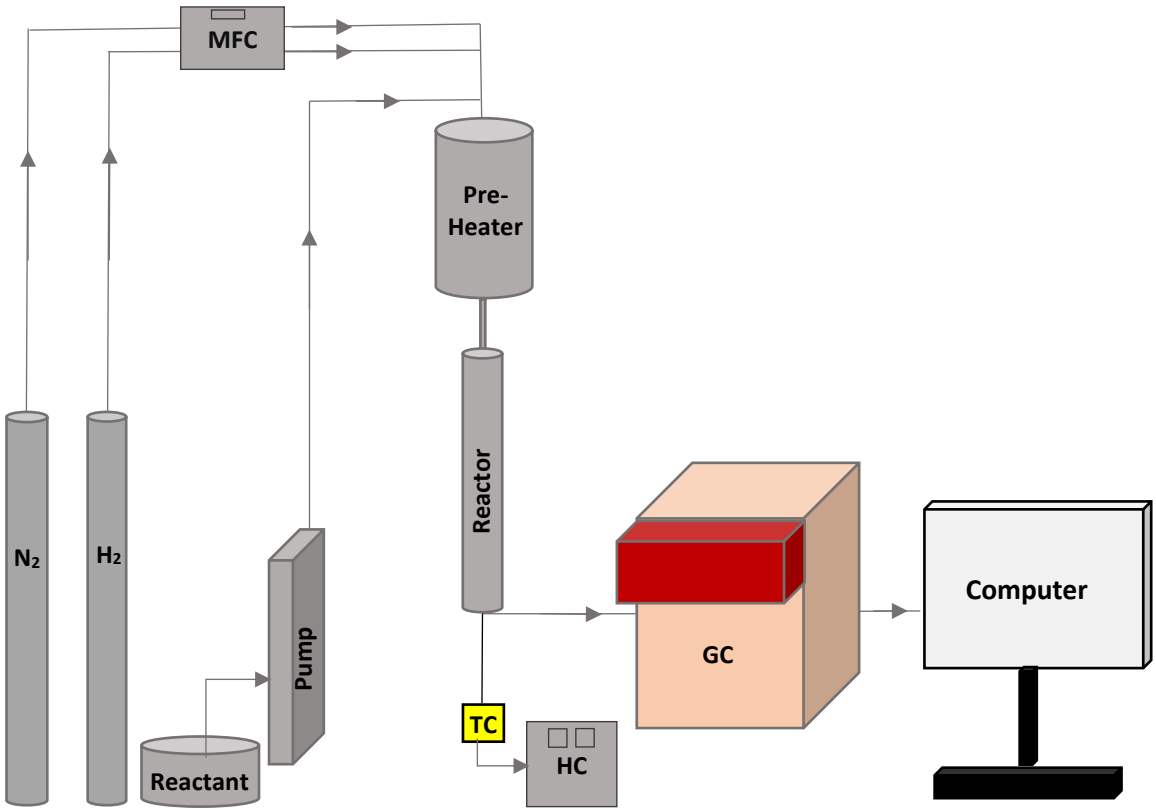

Scheme 2.1. The experimental setup. MFC; mass flow controller, TC; thermocouple, HC; heat controller and GC; mass chromatography.

2.4 Catalyst Characterization

In catalysis research, many physical and chemical methods were used to characterize solid catalysts. These techniques provide information on texture, surface chemical composition, catalyst structure, particle size, and surface chemistry (i.e. acidity and basicity). The characterization of catalyst surfaces is critical to correlate catalyst structure to catalytic performance in order to improve selectivity and reactivity and better comprehend the role of the catalyst in a chemical reaction. In the present study, X-ray diffraction (XRD), Temperature-Programmed Reduction (H_2-TPR), Temperature-Programmed Desorption (NH_3-TPD and CO_2-TPD) measurements were conducted to study the nature and properties of catalysts.

2.4.1 X-ray Diffraction (XRD)

XRD involves scattering phenomenon from crystalline materials. It can disclose information on crystal structure, crystalline quality, orientation and crystal size. Commonly, X-ray diffraction (XRD) is used to define the bulk structure as well as the composition of heterogeneous catalysts with crystalline structures [11]. Typically, the characteristic patterns related with individual solids make XRD ideal for identification of the bulk crystalline components of solid catalysts. However, since most catalysts are in the form of polycrystalline powders, XRD analysis is limited to distinguishing specific lattice planes which produce peaks at their corresponding angular positions 2θ [12]. Also, it fails to provide useful information about amorphous or highly dispersed solid phases, which are common in catalysts [13].

The principle of this method is based on X-ray diffraction from periodic atomic planes and the energy-resolved detection of the diffracted signal. The interpretation of the XDR phenomena was given by Bragg's law (Equation 2.1) and shown in scheme 2.2 [14,15].

$n\lambda = 2d_{hkl} \sin(\theta)$ …… (2.1)

where:

n is the order of the diffraction, λ is the wavelength of the incident beam, d_{hkl} the lattice spacing, and θ is the angle of the diffracted beam in degree.

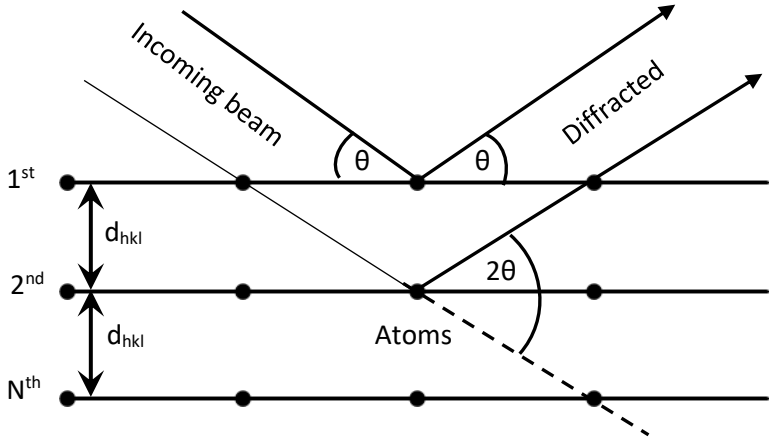

Scheme 2.2. Geometric conditions for diffraction from a total of N lattice planes.

XRD can be used to approximate the average crystalline size of catalysts [16]. In this study, XRD measurements were conducted using a Rigaku Miniflex II desktop X-ray diffractometer with Cu Kα radiation (λ = 0.15406 nm) in an operation mode of 30 kV and 15 mA. Scans of two theta angles were from 6^o to 80^o with a step size of 0.02^o and a scan speed of $2\ ^o$/min. The crystallite sizes of catalysts were determined using the Scherrer formula (Equation 2.2):

$$d = K\lambda / B \cos\theta \qquad \ldots\ldots (2.2)$$

where K is an empirical constant (0.9 as the particles were spherical), λ is the wavelength of the X-ray source (0.15406 nm), B is the full width at half-maximum (FWHM), and θ is the Bragg angle.

2.4.2 Temperature Programmed Reduction (H_2-TPR)

Temperature-programmed reduction (H_2-TPR) is used to investigate the reducibility of metals loaded on supports and to further explain the nature of the metal species in these catalysts. The TPR profile gives details on the interaction between the metal ions and the support and provides information on the dispersion of metal species over the support [17] in addition to finding the most effective reduction conditions. In this technique, reducible catalysts are exposed to a flow of reducing gas mixture, typically hydrogen diluted in some inert gas such as argon or nitrogen. The reduction rates are measured continuously via monitoring changes in the composition of the reducing gas mixture (H_2 content) at the outlet of the reactor [18].

Usually, low reduction temperature peaks are assigned to highly dispersed surface metal oxides species while high reduction temperature peaks are ascribed to bulk metal oxides [17,19–22]. Also, reduction peaks at low temperatures can be attributed to weak interactions between metal oxides and the support while high reduction temperature peaks indicate a stronger interaction between the metal oxides species and the support [23–28].

H_2-TPR was performed using an Altamira AMI-200 system. 0.1 g of sample was loaded in a quartz U-tube reactor and treated with argon at 500 °C with a flow rate of 40 mL/min for an hour followed by cooling to 50 °C. Then, the temperature was raised from 50 °C to 600 °C at a ramp rate of 10 °C /min using H_2/Ar (10 v/v %) with a flow of 40 mL/min. Consumed H_2 as a function of temperature was detected by a thermal conductivity detector (TCD).

2.4.3 Temperature Programmed Desorption (NH_3-TPD and CO_2-TPD)

Additional chemical information can be obtained from adsorption–desorption measurements. Temperature-Programmed Desorption (TPD) is commonly used to obtain information about specific sites in catalysts [29,30]. The desorption temperature indicates the strength of adsorption while the amount of gas consumed in the uptake indicates the concentration of the surface sites. NH_3 and CO_2 are the most common molecules used in TPD which probe acidic and basic sites, respectively [31–33]. Therefore, NH_3-TPD and CO_2-TPD characterizations are useful in investigating the surface acidity and basicity of catalysts and calculating the number of acid and base sites.

NH_3-TPD was conducted using an Altamira AMI-200 system. Prior to adsorption, 0.1 g of supported metal catalyst was loaded in a quartz U-tube reactor then pre-treated at 550 °C under helium for 1 h followed by cooling to 100 °C. After that, the catalyst was reduced in a flow of H_2/Ar (10 v/v %) at 300 °C at a constant ramp rate of 10 °C /min and then held for 2 h followed by cooling to 100 °C. 1% NH_3/He with flow of 50 mL/min was then introduced at 100 °C for 1 h. The sample was flushed in a He flow at 100 °C for 2 h to remove physically adsorbed NH_3 molecules. Finally, the temperature was raised to 700 °C at a ramp rate of 10 °C /min. CO_2-TPD was performed using the same instrument as the one used in the NH_3-TPD measurements. 0.1 g of the sample was preheated and reduced in the same series of steps as that described for NH_3-TPD except the cooling temperature after reducing the catalyst was 50 °C. After reducing, the sample was saturated with 10% CO_2 in Helium with a flow of 50 mL/min at 50 °C and was flushed with a He flow at 50 °C for 2 h to remove physisorbed CO_2 molecules. Finally, the temperature was raised to 700 °C at a ramp rate of 10 °C/min. Desorbed NH_3 and CO_2 from the samples were detected by a thermal conductivity detector (TCD).

References

1. Yashima, T.; Suzuki, H.; Hara, N. Decomposition of 2-propanol over alkali cation exchanged zeolites. *J. Catal.* **1974**, *33*, 486–492.

2. Hattori, H. Heterogeneous basic catalysis. *Chem. Rev.* **1995**, *95*, 537–558.

3. Yamaguchi, T.; Nakano, Y.; Iizuka, T.; Tanabe, K. Catalytic activity of ZrO_2 and ThO_2 for HD exchange reaction between methyl group of adsorbed isopropyl alcohol-d8 and surface OH group. *Chem. Lett.* **1976**, 677–678.

4. Campanati, M.; Fornasari, G.; Vaccari, A. Fundamentals in the preparation of heterogeneous catalysts. *Catal. Today* **2003**, *77*, 299–314.

5. Poncelet, G.; Jacobs, P. A.; Grange, P. *Preparation of catalysts III*; Elsevier, **1983**; Volume 16; ISBN 0080960510.

6. Perego, C.; Villa, P. Catalyst preparation methods. *Catal. Today* **1997**, *34*, 281–305.

7. Richardson, J. T. *Principles of catalyst development*; Springer, **2013**; ISBN 1489937250.

8. Pinna, F. Supported metal catalysts preparation. *Catal. Today* **1998**, *41*, 129–137.

9. Ross, J. R. H. *Heterogeneous catalysis: fundamentals and applications*; Elsevier, **2011**; ISBN 008095684X.

10. Augustine, R. L. *Heterogeneous catalysis for the synthetic chemist*; CRC Press, **1995**; ISBN 0824790219.

11. Paulus, E. F.; Gieren, A. Handbook of Analytical Techniques, **2001**; pp. 373.

12. Ma, Z.; Zaera, F. Characterization of heterogeneous catalysts. *Surf. Nanomolecular Catal.* **2006**, 1–37.

13. Xie, Y. C.; Tang, Y. Q. Spontaneous monolayer dispersion of oxides and salts onto surfaces of supports: applications to heterogeneous catalysis. In *Advances in catalysis*; 1**990**; 37, 1–43.

14. Hübschen, G.; Altpeter, I.; Tschuncky, R.; Herrmann, H.-G. *Materials characterization using Nondestructive Evaluation (NDE) methods*; Woodhead Publishing, **2016**; ISBN 008100057X.

15. Lee, M. *X-Ray Diffraction for Materials Research: From Fundamentals to Applications*; CRC Press, **2016**; ISBN 1771882999.

16. Matyi, R. J.; Schwartz, L. H.; Butt, J. B. Particle size, particle size distribution, and related measurements of supported metal catalysts. *Catal. Rev. Sci. Eng.* **1987**, *29*, 41–99.

17. der Grift, C. J. G. Van; Mulder, A.; Geus, J. W. Characterization of silica-supported copper catalysts by means of temperature-programmed reduction. *Appl. Catal.* **1990**, *60*, 181–192.

18. Fadoni, M.; Lucarelli, L. Temperature programmed desorption, reduction, oxidation and flow chemisorption for the characterisation of heterogeneous catalysts. Theoretical aspects, instrumentation and applications. *Stud. Surf. Sci. Catal.* **1999**, *120*, 177–225.

19. Chary, K. V. R.; Sagar, G. V.; Srikanth, C. S.; Rao, V. V. Characterization and catalytic functionalities of copper oxide catalysts supported on zirconia. *J. Phys. Chem. B* **2007**, *111*, 543–550.

20. Shimokawabe, M.; Asakawa, H.; Takezawa, N. Characterization of copper/zirconia catalysts prepared by an impregnation method. *Appl. Catal.* **1990**, *59*, 45–58.

21. Dow, W. P.; Wang, Y. P.; Huang, T. J. Yttria-stabilized zirconia supported copper oxide catalyst: I. Effect of oxygen vacancy of support on copper oxide reduction. *J. Catal.* **1996**, *160*, 155–170.

22. Robertson, S. D.; McNicol, B. D.; De Baas, J. H.; Kloet, S. C.; Jenkins, J. W. Determination of reducibility and identification of alloying in copper-nickel-on-silica catalysts by temperature-programmed reduction. *J. Catal.* **1975**, *37*, 424–431.

23. Roh, H. S.; Jun, K. W.; Dong, W. S.; Chang, J. S.; Park, S. E.; Joe, Y. I. Highly active and stable Ni/Ce–ZrO_2 catalyst for H_2 production from methane. *J. Mol. Catal. A Chem.* **2002**, *181*, 137–142.

24. Song, Y. Q.; Liu, H. M.; He, D. H. Effects of hydrothermal conditions of ZrO_2 on catalyst properties and catalytic performances of Ni/ZrO2 in the partial oxidation of methane. *Energy & Fuels* **2010**, *24*, 2817–2824.

25. Sun, L.; Tan, Y.; Zhang, Q.; Xie, H.; Han, Y. Tri-reforming of coal bed methane to syngas over the Ni-Mg-ZrO_2 catalyst. *J. Fuel Chem. Technol.* **2012**, *40*, 831–837.

26. Chen, S.; Luo, L.; Cheng, X. Influence of preparation method on the performance of Pd/ZrO_2-Al_2O_3 catalysts for HDS. **2009**, 16, 272–277.

27. Ivanova, A. S.; Slavinskaya, E. M.; Gulyaev, R. V; Zaikovskii, V. I.; Stonkus, O. A.; Danilova, I. G.; Plyasova, L. M.; Polukhina, I. A.; Boronin, A. I. Metal–support

interactions in Pt/Al_2O_3 and Pd/Al_2O_3 catalysts for CO oxidation. *Appl. Catal. B Environ.* **2010**, *97*, 57–71.

28. Lee, H. C.; Lee, D.; Lim, O. Y.; Kim, S.; Kim, Y. T.; Ko, E.-Y.; Park, E. D. ZrO_2-supported Pt catalysts for water gas shift reaction and their non-pyrophoric property. In *Studies in Surface Science and Catalysis*; Elsevier, 2007; Volume 167, pp. 201–206.

29. Cvetanović, R. J.; Amenomiya, Y. A temperature programmed desorption technique for investigation of practical catalysts. *Catal. Rev.* **1972**, *6*, 21–48.

30. Falconer, J. L.; Schwarz, J. A. Temperature-programmed desorption and reaction: applications to supported catalysts. *Catal. Rev. Sci. Eng.* **1983**, *25*, 141–227.

31. Bhatia, S.; Beltramini, J.; Do, D. D. Temperature programmed analysis and its applications in catalytic systems. *Catal. Today* **1990**, *7*, 309–438.

32. Gorte, R. J. Temperature-programmed desorption for the characterization of oxide catalysts. *Catal. Today* **1996**, *28*, 405–414.

33. Niwa, M.; Habuta, Y.; Okumura, K.; Katada, N. Solid acidity of metal oxide monolayer and its role in catalytic reactions. *Catal. today* **2003**, *87*, 213–218.

Chapter 3 - Conversion of Methyl Ethyl Ketone to Butenes over Bifunctional Catalysts

As accepted in Applied Catalysis A: General (2018) by Zahraa Al-Auda, Hayder Al-Atabi, Xu Li, Quanxing Zheng and Keith L. Hohn.

And as a non-provisional patent titled: **"Catalysts and methods for converting methyl ethyl ketone to butene"**

Abstract

The direct conversion of methyl ethyl ketone (MEK) to butene over supported copper catalysts was investigated in a fixed bed reactor over Cu-Al_2O_3, Cu-zeolite Y sodium (Cu-ZYNa) and Cu-zeolite Y hydrogen (Cu-ZYH). In this reaction, MEK is hydrogenated to 2-butanol over metal sites and further dehydrated on acid sites to produce butene. Experimental results showed that the selectivity for butene was the highest over Cu-ZYNa, and it was improved by finding the optimum reaction temperature, hydrogen pressure and the percentage of copper loaded on ZYNa. The highest selectivity of butene (97.9%) was obtained at 270 °C and 20 wt% Cu-ZYNa. Over Cu-Al_2O_3, the selectivity for butenes was less than Cu-ZYNa since subsequent hydrogenation of butene occurred to produce butane. It was also observed that with increasing H_2/MEK molar ratio, butane selectivity increased. However, when this ratio was decreased, hydrogenation of butene was reduced, but dimerization to C_8 alkenes and alkanes began to be favored. The main products over 20% Cu-Al_2O_3 were butene and butane, and a maximum selectivity of butene (87%) was achieved at an H_2/MEK molar ratio of five. The lowest selectivity of butene was obtained using Cu-ZYH, reaching ~40%. All catalysts were characterized by (NH_3-TPD), (CO_2-TPD), XPS and TPR to probe catalyst acidity, basicity and the reducibility of Cu loaded on the supports. It was found that the amount of acidity in Cu-ZYH is much higher than in Cu-ZYNa. This could have caused the selectivity of butene to decrease as a result of dimerization, oligomerization and cracking reactions.

Key Words

Methyl Ethyl Ketone (MEK); Hydrogenation-dehydration reactions; Cu supported on Al_2O_3; Cu supported on zeolite Y sodium.

3.1 Introduction

Recently, more attention has been paid to converting sustainable resources, like biomass, to hydrocarbons and chemicals because petroleum is a finite resource [1,2]. One approach for making fuels and chemicals from biomass is to combine biochemical and catalytic processes, where biochemical processes convert biomass-derived sugars to a useful intermediate and catalytic chemistry is then used to convert this intermediate to the final product. This approach takes advantage of the typically high selectivity of biochemical processes while using inorganic catalysts to make a product similar to current hydrocarbon-based products.

2,3-butanediol (2,3 BDO) has emerged as such a useful intermediate in recent years because it can be synthesized with high yield via ferementation of biomass-derived sugars with a variety of microorganisms (such as *Klebsiella pneumoniae* [3], *Entaerobacter aerogenes* [4] *Bacillus polymyxa* [5], *Aeromonas hydrophilia* and several species of *Serratia* [6]) and because it can be converted to a number of useful chemicals such as butene and butadiene [2,7]. Recently our research group has studied the conversion of 2,3 BDO to butene in a single reactor. This was considered a first step in converting 2,3 BDO to fuel-range hydrocarbons. Dimerization/oligomerization of 1-butene would be the

next step to obtain a “green” fuel [8]. In addition, 2-butene is important in increasing the octane number of gasoline when it is alkylated with isobutene to produce a mixture of highly branched paraffins which have high antiknock features and good stability [9,10].

Conversion of 2,3 BDO to butene in a single reactor is challenging because multiple reaction steps are involved in this transformation, which ultimately limits the butene selectivity achieved. Nonetheless, yields of up to 71% to butene have been achieved over copper supported on mesoporous supports [2].

It may be possible to improve the butene yield using multiple reactors with different catalysts in each reactor that are optimized for a specific reaction. This is the approach Sato and coworkers recently reported for achieving nearly a 95% selectivity to butadiene from 2,3 BDO [7]. In a first reactor, they converted 2,3 BDO to 3-butene-2-ol over Sc_2O_3, while the second reactor employed an acidic catalyst (Al_2O_3) to dehydrate the 3-buten-2-ol to butadiene. It is hypothesized that a similar approach will yield high selectivity in the conversion of 2,3 BDO to butene. The proposed approach is to convert 2,3 BDO to MEK in a first reactor, and then use a second catalytic process to convert MEK to butene.

Conversion of 2,3 BDO to MEK is well known in the literature and can be done with high yields. Molnar *et.al* [11] studied the dehydration of 2,3 BDO to MEK on NaX, NaY, NaHX and NaHY. They reported that the Y-zeolite gave the highest selectivity (80%) under suitable operating conditions (250 °C), and they attributed that to the differences in acid/base and electrostatic properties between X and Y zeolite. Biosynthesis of MEK from

2,3 BDO was studied by Multer *et al.* [12] via fermentation of glucose using bacteria *Klebsiella oxytoca* to produce 2,3 BDO followed by 2,3 BDO dehydration on HZSM-5. The yield of 2,3 BDO from total glucose consumed was about 0.63% g/g with a concentration of 0.03 mol/L and the selectivity to MEK was over 90% with 2-methyl propanal as the only other product detected. Emerson *et al.* [13] reported MEK yields of over 90% using sulfuric acid and suggested that aldol condensation limited MEK selectivity.

Since it is straightforward to produce MEK from 2,3 BDO with high selectivity, this work focuses on how to convert MEK to butene with high yields. An obvious pathway is to hydrogenate MEK to 2-butanol which can then be dehydrated to form butene. This pathway would require a bifunctional heterogeneous catalyst with both hydrogenation and dehydration activity.

Among potential hydrogenation catalysts, Cu is appealing because Cu catalysts selectively hydrogenate C=O bonds and are relatively inactive for hydrogenolysis of C–C bonds [14]. For example, Sitthisa and Resasco [15] studied the hydrodeoxygenation of furfural over Cu, Pd and Ni supported on SiO_2. The results showed that the Cu catalyst mainly produced furfuryl alcohol by hydrogenation of the carbonyl group because of the weak interaction of Cu with C=C. A number of studies have investigated the hydrogenation of MEK. Lilga *et.al* [16] tested the hydrogenation of MEK on several carbon-supported catalysts, including as Ru/C, Pt/C, Re/Ni/C and Pd/C. They found that the temperature of the reaction and the kind of the metal used affected the selectivity of 2-butanol. Using a Ru/C catalyst, the selectivity of 2-butanol was 97.5% and the optimum

temperature was at 120 °C, while using Pt/C, the selectivity was 68.5% at an optimum temperature of 180 °C. For Re/Ni/C and Pd/C, the selectivity was 81.7% and 34.8% and the optimum temperatures were 160 and 260 °C, respectively. Those results showed an excellent selectivity for 2-butanol over Ru/C with a lower temperature.

Generally, alcohols can be dehydrated to olefins and ethers over acidic catalysts and dehydrogenated to aldehydes or ketones over basic catalysts. However, sometimes, heterogeneous basic catalysts promote dehydration of 2-alcohols to obtain 1-olefins by mechanisms different from those for acid catalyzed dehydration. For example, ZrO_2 and ThO_2 are capable of converting 2-alcohols to 1-olefins with high selectivity. In contrast, the major products in the dehydration of 2-alcohols over strongly acidic catalysts like Al_2O_3 and SiO_2-Al_2O_3 catalysts are 2-alkenes [17]. For strongly basic catalysts such as MgO, CaO, the dehydrogenation of alcohols occurs to form ketones [18].

Yashima *et al.* [19] studied decomposition of 2-propanol over alkali cation-exchanged X and Y zeolites. They reported that for zeolites X and Y exchanged with Li^+ and Na^+, dehydration became appreciable, whereas for zeolites exchanged with K^+, Rb^+ and Cs^+ dehydrogenation reactions dominated, although the selectivity for dehydration surpassed that of dehydrogenation at 425 °C. Lilga *et.al* [16] studied the reaction of 2-butanol over HZSM-5 (30) at different reaction temperatures. They found at low temperatures (250 °C) the majority of the products are normal and branched olefins (C_5->C_{12}) with almost no aromatic products. However, at high temperatures (400 °C)

aromatics were formed, while at moderate temperatures (300 °C) the products were a mixture of both aromatics and normal and branched olefins.

Zheng *et al.* [2] investigated the conversion of MEK, as an intermediate in the conversion of 2,3 BDO to butene, to explore the role of MEK in the conversion of 2,3 BDO. Hydrogenation of MEK was performed under the same reaction conditions as those used for 2,3 BDO conversion over 19.2 wt% CuO/ZSM-5(280). The results showed that the selectivity for butene was about 50%, which is not as high as when 2,3 BDO was the reactant (71%). However, the results displayed that the selectivities of C_5–C_8 olefins are significantly higher in comparison with the result from 2,3 BDO as a result of oligomerization and cracking reactions which became dominant catalytic processes. Prasomsri *et al.* [20] studied the conversion of biomass-derived oxygenates, like acetone and 2-hexanone, to olefins over MoO_3. They reported that MoO_3 catalyzes the hydrodeoxygenation of acetone and 2-hexanone effectively to olefins. The main products from acetone as a reactant were propylene, C_4-C_6 olefins, and alkyl benzenes with carbon yields of 67.2%, 28.1% and 1.6%, respectively. In a similar manner, hexenes, C_3-C_5 olefins and hexadiene were obtained from 2-hexanone with carbon yields of 71.5%, 3% and 6.2%, respectively.

This chapter discusses the conversion of MEK to butene in a single reactor using bifunctional catalysts consisting of Cu supported on Al_2O_3, sodium-exchanged zeolite Y (referred to as ZYNa) and the hydrogen form of zeolite Y (referred to as ZYH). The impact of operating conditions like temperature, H_2/MEK molar ratio and Cu loading were

investigated in order to develop a catalytic process to obtain the highest selectivity of butene.

3.2 Experimental Work

3.2.1 Materials

MEK and the Cu precursor (copper(II) nitrate tri-hydrate [$Cu(NO_3)_2 \cdot 3H_2O$ (99%)]) were obtained from the Fisher Scientific Company. Al_2O_3 (catalyst support, high surface area, 1/8" pellet) and ZYNa (Powder, S.A. 900 m^2/g and 5.1:1 mole ratio of SiO_2:Al_2O_3) were purchased from Alfa Aesar. ZYH (Powder, S.A. 730 m^2/g and 5.1:1 mole ratio of SiO_2:Al_2O_3) was obtained from Zeolyst International.

3.2.2 Preparation of Supported Catalysts

The catalysts, consisting of copper loaded on Al_2O_3, ZYNa and ZYH, were synthesized using an incipient wetness impregnation method [21]. Different percentages of copper were loaded on ZYNa with the same method where the amount of precursor was changed to get metal loadings (by weight) of 8, 14, 20 and 26%. The precursor solutions were prepared by dissolving $Cu(NO_3)_2 \cdot 3H_2O$ (99%) in an amount of water just sufficient to fill the pores of the support. Then, the precursor solution was added to the support by dropwise addition and was mixed manually. The catalysts were dried first in an oven overnight at 100 °C. Next, the catalyst was placed into an alumina boat, loaded into a quartz tube and calcined in a tube furnace in air. The catalyst was heated at 110 °C for 2 h and calcined at 550 °C for 4 h. A ramp rate of 2 °C/min was used up to 110 °C and

1 °C/min up to 550 °C. For Al_2O_3, the pellet was crushed and sieved to obtain particles in size of ≤0.15 mm (≤mesh 100) before loading copper. After making the catalyst and the calcination process, the catalyst was crushed and sieved to < 0.15 mm for both Cu-ZYNa and Cu-ZYH and ≤ 0.15 mm for Cu-Al_2O_3.

3.2.3 Catalytic Reaction

The catalytic conversion of MEK was carried out in a continuous flow fixed-bed reactor made of stainless steel (id=0.85 cm) under atmospheric pressure. Prior to the reaction, a catalyst (1.0 g) was reduced in the reactor with flow rates of hydrogen and nitrogen equal to 48 and 15 mL/min, respectively, at 300 °C for 1 h. After the reduction process, MEK was mixed with hydrogen and nitrogen in a preheater at the desired reaction temperature before flowing into the reactor. The MEK was fed through the top of the reactor at a feed rate of 1 mL/h via a micro pump (Eldex 1SMP) together with H_2 and N_2 with flow rates of 68.5 and 16.5 mL/min, respectively. The reaction temperature was maintained between 230 °C to 290 °C, where heating was supplied by heating tape. The effluent product compositions were analyzed using an on-line gas chromatograph (SRI 8610C) with an MXT-1 column (100% dimethyl polysiloxane (nonpolar phase), 60 m, ID 0.53 mm) and FID and TCD detectors for the analysis of hydrocarbons and oxygenates. The temperature of the product effluent from the bottom of the reactor was maintained above 200 °C to avoid the condensation of liquid products. The products were injected into a GC through a sample loop controlled by a high temperature ten-port valve. The oven was kept at 40 °C for 5 min, and then raised to 120 °C at a ramp rate of 40 °C/min,

finally raised to 250 °C at a rate of 20 °C/min and held at this temperature for 10 min. To identify products detected by the GC, an Agilent 7890A GC-MS system equipped with an Agilent 5975C MS detector was used.

The conversion of MEK and selectivity for products were calculated using Equation 3.1 and 3.2 respectively:

$$\text{Conversion } \% = \frac{(\text{ Moles of MEK})_{in} - (\text{Moles of MEK})_{out}}{(\text{ Moles of MEK})_{in}} * 100 \qquad \ldots (3.1)$$

$$\text{Selectivity } \% = \frac{(\text{ Moles of product})}{(\text{ Moles of total products})} * 100 \qquad \ldots (3.2)$$

3.2.4 Catalyst Characterization

3.2.4.1 X-ray Diffraction (XRD)

X-ray diffraction measurements were conducted using a Rigaku Miniflex II desktop X-ray diffractometer with Cu Kα radiation (λ = 0.15406 nm) in an operation mode of 30 kV and 15 mA. Scans of two theta angles were from 6° to 70° for all catalysts with a step size of 0.02° and scan speed of 2 °/min.

3.2.4.2 Brunauer–Emmett–Teller (BET)

Surface area measurements of catalysts were performed according to the Brunauer–Emmett–Teller (BET) gas (N_2) adsorption method. N_2 adsorption/desorption

analyses were carried out using a Quantachrome Autosorb-1 instrument at -196 °C and analyzed with Autosorb-1 software. The samples were degassed at 350 °C for 4 h before the adsorption analysis. The total surface area was determined by the BET method with relative pressure from 0.007 to 0.03.

3.2.4.3 Temperature Programmed Reduction (H_2-TPR)

H_2-TPR was performed in an Altamira AMI-200 system. 0.1 g of sample was loaded in a quartz U-tube reactor and treated using argon at 500 °C with a flow of 40 mL/min for an hour followed by cooling to 50 °C. Then, the temperature was raised from 50 °C to 550 °C at a ramp rate of 10 °C /min using H_2/Ar with flow of 40 mL/min (10 v/v %). Consumed H_2 as a function of temperature was detected by a thermal conductivity detector (TCD).

3.2.4.4 N_2O Adsorption

Copper surface area (SA_{Cu}) and dispersion (D_{Cu}) were estimated by a TPR_1–N_2O passivation–TPR_2 procedure at 90 °C [22–24] using the same system as H_2-TPR. In the first step of the experiment, the catalysts (0.1 g) were treated in Ar at 550 °C and a flow of 40 mL/min for an hour followed by cooling to 50°C, then by a reduction from 50 °C to 350 °C at a ramp rate of 10 °C/min in 10 v/v% H_2/Ar with flow of 40 mL/min by the H_2-TPR procedure described above and cooling to 90°C in Ar (30 mL/min). In this step, the amount of hydrogen consumption was denoted as X (in moles) and assuming the stoichiometry of $CuO + H_2 \rightarrow Cu^0 + H_2O$. The total reducible Cu content (in wt %) was determined from TPR_1 hydrogen consumption as:

$Cu_{reduced}$ (wt%)$= \frac{X*Mwt_{Cu}*100}{W_{Cat}}$ … (3.3),

where Mwt_{Cu} is the atomic weight of Cu (63.546 g mol^{-1}) and W_{cat} is the weight of catalyst (in grams).

The second step in the experiment includes exposing the pre-reduced catalysts to a flow of 5 v/v% N_2O/He (40 mL/min) isothermally at 90 °C for 1 h to chemisorb a layer of O on metallic Cu in order to oxidize surface copper atoms to Cu_2O, followed by cooling to 50 °C in Ar (30 mL/min) by assuming the stoichiometry of N_2O + Cu-Cu → N_2 + Cu_2O.

The last step of the experiment consists of a second reduction H_2-TPR_2 (following N_2O passivation) from 50 °C to 400 °C at a ramp rate of 10 °C/min in 10 v/v% H_2/Ar flow (40 mL/min) in order to reduce Cu_2O back to metallic Cu. The hydrogen consumption in this step was denoted as Y (in moles) by assuming the stoichiometry of Cu_2O + H_2 → $2Cu^0$ + H_2O. The metallic Cu content was calculated from TPR_2 hydrogen consumption as:

Cu_{metal} (wt%)$= \frac{2*Y*Mwt_{Cu}*100}{W_{Cat}}$ … (3.4)

Copper metal dispersion (D_{Cu}) is determined as $D_{Cu} = \frac{Cu_{metal}}{Cu_{reduced}}$, which is defined as the ratio of the surface copper atoms to the total copper atoms present in the catalyst.

Copper surface area SA_{Cu} (m^2/g_{Cu}) is estimated by the following equation [23,24]:

$SA_{Cu} = \frac{Cu_{metal}*N_{av}}{Cu_{reduced}*Mwt_{Cu}*SD_{Cu}}$ … (3.5)

where SD_{Cu} is the copper surface density (1.47×10^{19} atoms/m^2) (the average value for Cu(1 1 1), Cu(1 1 0), and Cu(1 0 0) crystal surfaces) and N_{av} is Avogadro's constant (6.02×10^{23} atoms/mol).

3.2.4.5 Temperature Programmed Desorption (NH_3-TPD and CO_2-TPD)

The surface acidity and basicity of catalysts were investigated by temperature programmed desorption of ammonia (NH_3-TPD) and carbon dioxide (CO_2-TPD), respectively. NH_3-TPD was conducted in an Altamira AMI-200 system. Prior to adsorption, 0.1 g of supported copper catalyst was loaded in a quartz U-tube reactor then pre-treated at 550 °C under helium for 1 h followed by cooling to 100 °C. After that, the catalyst was reduced in a flow of H_2/Ar (10 v/v %) up to 300 °C at a constant ramp rate of 10 °C /min and then held for 2 h followed by cooling to 100 °C. 1% NH_3/He with a flow of 50 mL/min was then introduced at 100 °C for 1 h. The sample was flushed in a He flow at 100 °C for 2 h to remove physically adsorbed ammonia molecules. Finally, the temperature was raised to 600 °C at a ramp rate of 10 °C /min. CO_2-TPD was conducted using the same instrument employed in the NH_3-TPD measurements. 0.1 g of the sample was preheated and reduced using the same procedure as that described for NH_3-TPD except that the cooling temperature after reducing the catalyst was 50 °C. Then the sample was saturated with 10% CO_2 in Helium with a flow of 50 mL/min at 50 °C. The sample was flushed with a He flow at 50 °C for 2 h to remove physisorbed CO_2 molecules. In the end, the temperature was raised to 600 °C at a ramp rate of 10 °C/min. Desorbed NH_3 and CO_2 from the samples were detected by a thermal conductivity detector (TCD).

3.2.4.6 X-ray Photoelectron Spectroscopy (XPS)

XPS measurements were obtained with a PerkinElmer PHI 5400 using achromatic Al Kα radiation (1486.60 eV). The pressure in the analysis chamber at which the scanning of the spectra was done was less than 3×10^{-8} Torr. The binding energy of carbon 284.6 eV was used as the standard to correct the experimental binding energies, and Cu 2p3/2 (932.7 eV) and Au 4f7/2 (84.0 eV) were used as standards for calibration of the binding energy (BE) range.

3.3 Results and Discussions

3.3.1 Characterization of Catalysts

3.3.1.1 XRD

Figures 3.1a and 3.1b show the XRD patterns of copper loaded on three different supports and with different weight loadings. As seen in Figure 3.1a, all the characteristic peaks of the parent supports (Al_2O_3, ZYNa and ZYH) were observed in the supported copper catalysts. These peaks were maintained when copper was introduced; however, a slight decrease in the intensity of the main peaks was noticed. Two characteristic peaks related to CuO (35.43°and 38.57°) were observed on all catalysts, indicating that at least some of the copper was present as copper oxide clusters. Figure 3.1b shows the XRD patterns of the calcined catalysts with different copper loadings on ZYNa. Generally, the intensity of the peaks for the parent support decrease as copper weight loading increases.

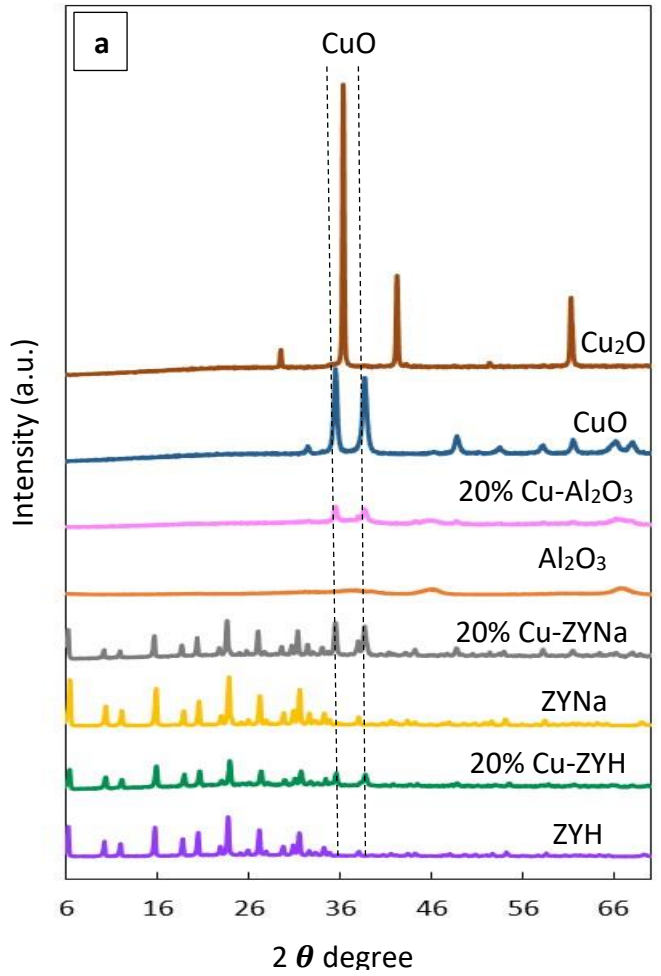

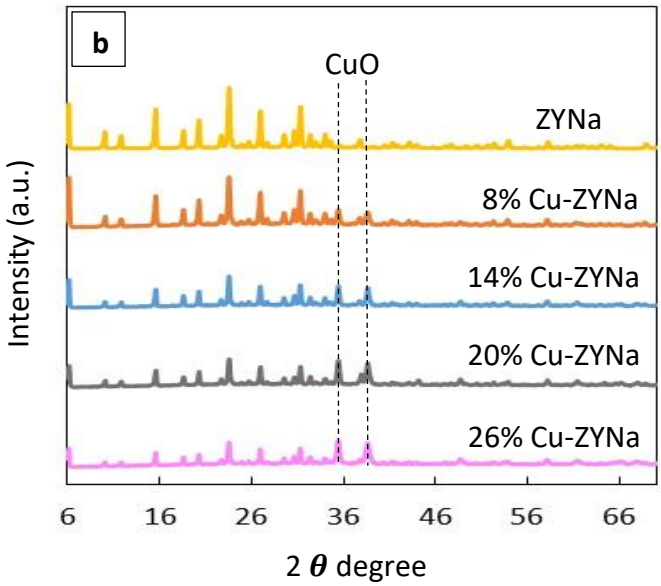

Figure 3.1. (a) XRD pattern for the different catalysts and their support and standards of copper, (b) XRD pattern for Cu-ZYNa with different percentages of copper.

The crystallite sizes of CuO were determined using the Scherrer formula:

$d = K\lambda / B \cos\theta$ … (3.6)

Where K is an empirical constant (0.9 as the particles were spherical), λ is the wavelength of the X-ray source (0.15406 nm), B is the full width at half-maximum (FWHM), and θ is the Bragg angle. Crystallite sizes are reported in Table 3.1.

Table 3.1. Physical properties of supported Cu catalysts.

Catalyst	Surface Area (m^2/g)[a]	Particle size of copper (nm)[b]	SA_{Cu} (m^2/g_{Cu})[c]	D_{cu}[d]
Al_2O_3	225	_	_	_
20% Cu-Al_2O_3	168	22	65.4	0.1
ZYH	730	_	_	_
20% Cu-ZYH	622	28	56.8	0.08
ZYNa	900	_	_	_
8% Cu-ZYNa	850	26	153.1	0.23
14% Cu-ZYNa	802	27	53.9	0.08
20% Cu-ZYNa	655	29	36.1	0.056
26% Cu-ZYNa	539	31	32.3	0.050

[a] Calculated from BET results.
[b] Calculated from XRD results.
[c & d] Calculated from N_2O adsorption method.

3.3.1.2 N_2 Adsorption

The BET surface areas of all of the catalysts are summarized in Table 3.1. This table shows that increasing the loading of Cu on ZYNa leads to a decrease in the surface area. Generally, surface area decreases with an increase in the percentage of metal loaded on a support when the impregnation method is used in preparing catalysts [25] which is in accordance with the presented results.

3.3.1.3 N_2O Adsorption

Copper surface area (SA_{Cu}) and the dispersion (D_{Cu}) of copper loaded on different supports were calculated by the N_2O decomposition method [23,24] as shown in Table 3.1. As can be seen, 20% Cu-Al_2O_3 has a higher copper dispersion (0.1) compared to the same copper loading on ZYNa and ZYH. On Cu-ZYNa, the dispersion of copper decreases from 0.23 to 0.05 with increasing CuO loadings from 8% to 26%. Also, the surface area of copper (SA_{Cu}) decreased with increasing CuO loadings.

3.3.1.4 H_2-TPR

H_2-TPR measurements were performed to investigate the reducibility of the Cu loaded on the three different supports. The TPR profile gives details on the interaction between the metal ions and the support and provides information on the dispersion of metal species over the support [26]. Figure 3.2a displays the TPR profiles of Cu-Al_2O_3, Cu-ZYNa and Cu-ZYH. For 20% Cu-Al_2O_3, two peaks were observed. The first one, centered at 199 °C, can be attributed to the reduction of highly dispersed CuO in one step to Cu^0 in

addition to reduction of isolated Cu^{2+} ions to Cu^{+}. The second peak which is around 243 °C is ascribed to the reduction of bulk CuO. Also, the TPR profile for 20% Cu-ZYNa and 20% Cu-ZYH exhibit two peaks centered on (242 °C and 300 °C) and (212 °C and 324 °C) respectively. The first peak at low temperature is assigned to the well dispersed CuO on the supports while the second peak at high temperature is attributed to the reduction of bulk CuO. It was reported that surface copper oxide on supports is reduced more easily than bulk CuO [27,28]. Also, it can be seen that among all catalysts, the reduction temperature of Cu-Al_2O_3 was the lowest.

Figure 3.2b shows the TPR profiles of Cu-ZYNa catalysts with different percentages loading of coper on support. Two main peaks of reduction were distinguished for all copper loadings indicating that there are mainly highly dispersed CuO in the low-temperature region in addition to bulk CuO particles in the high temperature region.

The total intensity of the reduction peak increases with increased copper loading from 8 wt% to 26 wt%. The reduction peaks shifted to higher temperatures as the copper loading increases and can be attributed to an increase in crystallite size of CuO, as confirmed by the XRD results [29] (see Figure 3.1b and Table 3.1). The hydrogen consumption values, and maximum temperature of reduction are shown in Table 3.2.

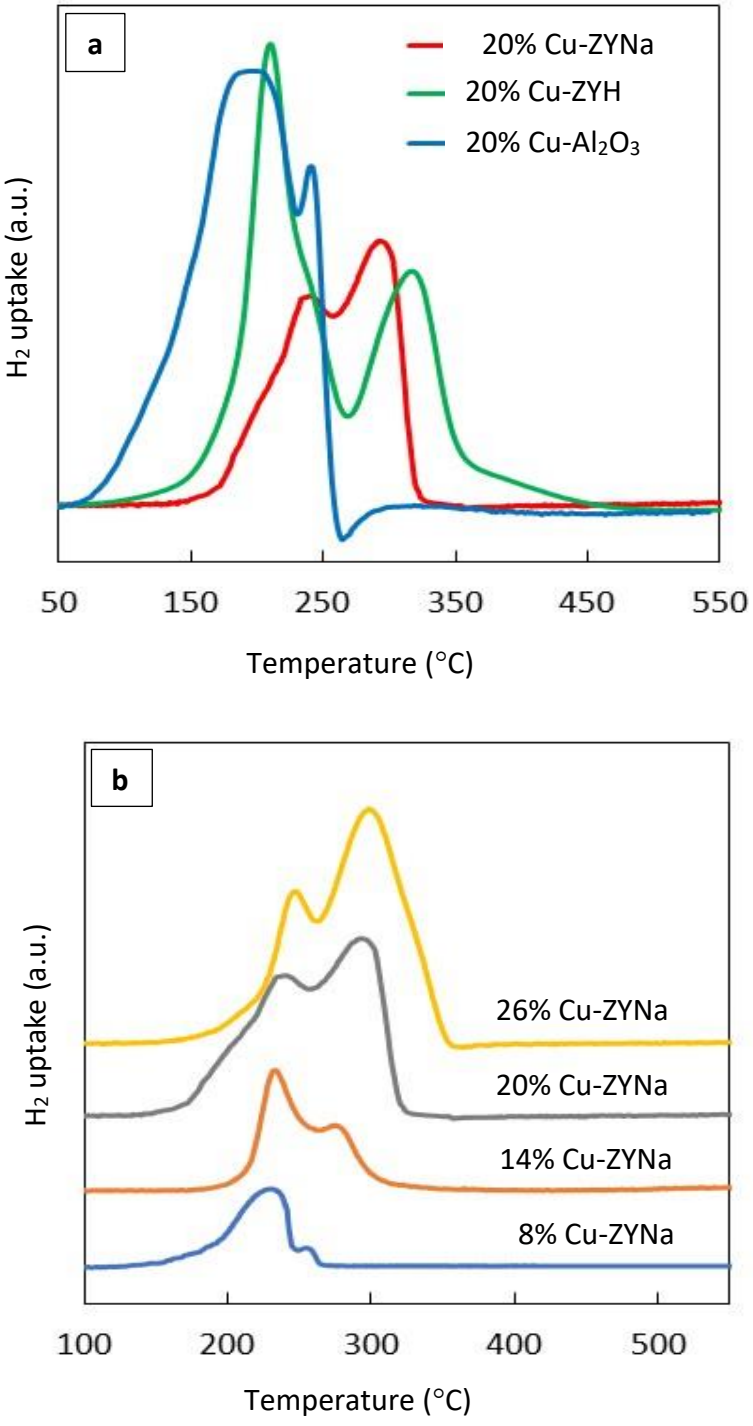

Figure 3.2. (a) (H_2-TPR) profiles of copper loaded on different supports, (b) (H_2-TPR) profiles of copper loaded with different percentages on ZYNa.

Table 3.2. Total consumption of H_2 and the maximum peak temperatures during TPR experiments for different catalysts.

Catalyst	H_2 uptake (mmol/g)	RT_{peak} (°C)
20% Cu-Al_2O_3	1.93	199, 243
20% Cu-ZYH	1.5	212, 324
8% Cu-ZYNa	0.59	235, 259
14% Cu-ZYNa	0.91	236, 279
20% Cu-ZYNa	1.37	242, 300
26% Cu-ZYNa	2.06	251, 303

3.3.1.5 (NH_3-TPD) and (CO_2-TPD)

The acidity and basicity of the reduced supported copper catalysts were studied by NH_3-TPD and CO_2-TPD respectively. Table 3.3 shows the number of moles of NH_3 and CO_2 adsorbed for different catalyst supports. Figures 3.3a and 3.3b display the NH_3-TPD and CO_2-TPD profiles of the reduced Cu-Al_2O_3, Cu-ZYNa and Cu-ZYH catalysts. Also, NH_3-TPD and CO_2-TPD measurements were performed on reduced Cu-ZYNa catalysts with different copper loadings, and their profiles are shown in Figures 3.3c and 3.3d respectively.

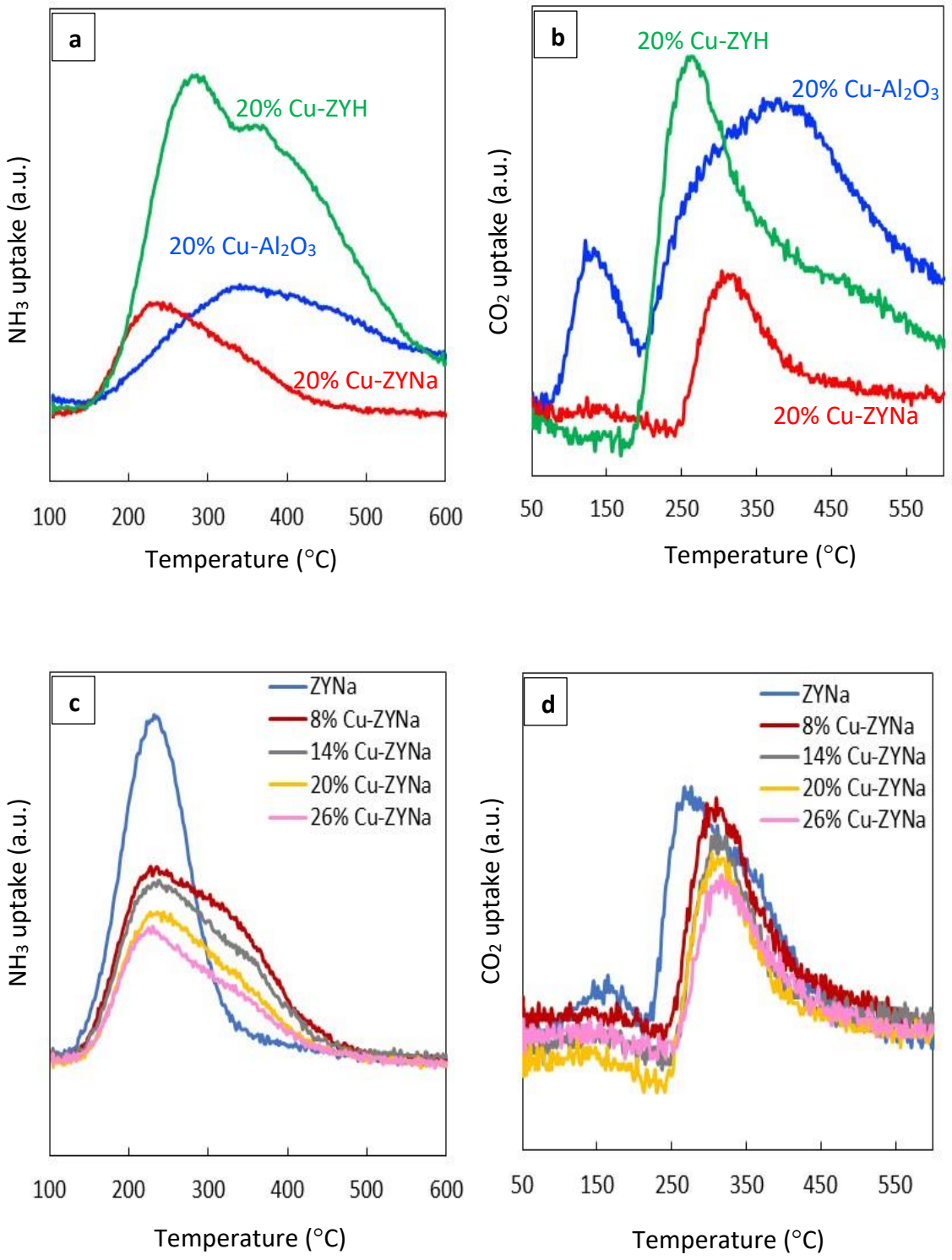

Figure 3.3. (a) (NH_3-TPD) profiles of copper loaded on different supports, (b) (CO_2-TPD) profiles of copper loaded on different supports, (c) (NH_3-TPD) profiles of copper on ZYNa with different Cu weight loadings, (d) (CO_2-TPD) profiles of copper on ZYNa with different Cu weight loadings.

As can be seen from Figure 3.3a, the maximum NH_3 desorption temperature for Cu-ZYNa was lower than Cu-ZYH and Cu-Al_2O_3, centering around 232 °C. The peak of Cu-Al_2O_3 was located nearby at 336 °C. For Cu-ZYH, two peaks were observed, centered around 283 °C and 370 °C. The two peaks could be indicative of different acidic sites of varying strength. The increase in the NH_3 desorption temperature suggests that the strength of the acidic sites in Cu-Al_2O_3 and Cu-ZYH are higher than in Cu-ZYNa. Also, from this figure, it is obvious that the peak of Cu-ZYH was the biggest, indicating that the total amount of acidic sites on it was the highest among all catalysts as shown in Table 3.3.

Figure 3.3b displays the (CO_2-TPD) profiles of reduced copper loaded on different supports. For both Cu-ZYNa and Cu-ZYH, there is only one distinct peak (at 319 °C and 267 °C for Cu-ZYNa and Cu-ZYH, respectively), which suggests that there are weakly basic sites on the surface of these catalysts. However, for Cu-Al_2O_3, two clear peaks (at 125 °C and 378 °C) are observed, indicating the presence of both weak and strong basic sites. The concentration of basic sites on Cu-Al_2O_3 was largest among the different catalysts as shown in Table 3.3.

As can be seen in Figure 3.3c, by increasing the percentage of copper loaded on the supports, the peak intensity of NH_3 desorption decreases. The total acid concentration decreases from 0.6 to 0.36 mmol/g_{cat} when the copper loadings increases from 8 wt% to 26 wt% (see Table 3.3). The maximum temperature desorption slightly decreases with increasing copper loading, indicating a slight decrease in the strength of the acidic sites.

These results can be attributed to the formation of larger copper clusters that cover acidic sites on the support.

From Figure 3.3d, it can be seen that the concentration of basic sites slightly decreases with increased copper loading. The amount of CO_2 adsorbed onto catalysts for different percentages of copper loaded and the maximum temperature of desorption are shown in Table 3.3

Table 3.3. Total acidity and basicity of the copper loaded on different catalysts (amount of desorbed NH_3 and CO_2) and the maximum peak temperatures.

Cu loading wt%	NH_3 uptake mmol/g_{cat}	RT $_{peak}$ (°C)	CO_2 uptake mmol/g_{cat}	RT $_{peak}$ (°C)
ZYNa	0.63	237	0.057	278
8% Cu-ZYNa	0.6	235	0.04	319
14% Cu-ZYNa	0.52	234	0.036	319.7
20% Cu-ZYNa	0.43	232.2	0.035	319.7
26% Cu-ZYNa	0.36	228	0.034	319
20% Cu-Al_2O_3	0.54	336	0.155	125, 378
20% Cu-ZYH	1.83	283, 370	0.146	267

3.3.1.6 XPS

The XPS measurements were conducted on reduced copper loaded on Al_2O_3, ZYNa and ZYH to study the strength of the basic sites for the different catalysts where the XPS binding energy of oxygen reflects the basic strength of the oxygen.

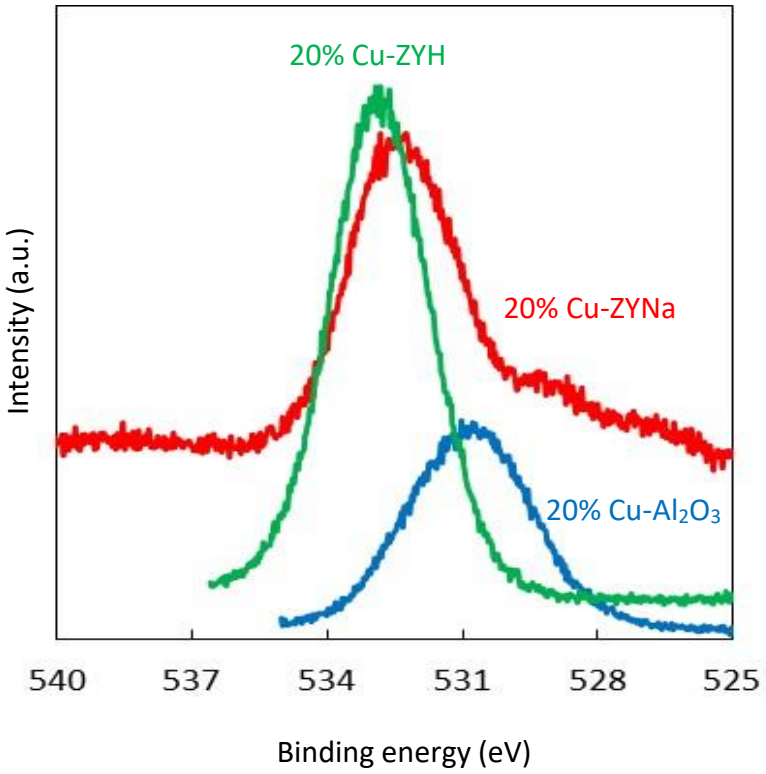

Figure 3.4. XPS analysis of O 1s orbital of different catalysts.

As can be seen from Figure 3.4, the binding energy of the O 1s orbital of the Cu-Al_2O_3 catalyst shifted to the lowest binding energy (530.8 eV) compared to that of the Cu-ZYNa (532.3 eV) and Cu-ZYH (532.8 eV) catalysts. This can be attributed to an increase in the electron pair donating ability of surface oxygen atoms. This increased electron pair

donating ability is responsible for the formation of basic sites, suggesting that the formation of stronger basic sites occurs when electron pair donation becomes stronger (i.e. a decrease in the binding energy of O 1s [30,31]). These results were in agreement with the results from CO_2-TPD.

3.3.2 Catalytic Reaction of MEK to Butene in a Fixed Bed Reactor

3.3.2.1 Reaction of MEK over Copper Loaded on Different Supports

Experiments were conducted using copper loaded on three different supports: Al_2O_3, ZYNa and ZYH. The percentage of copper loaded on the supports was 20 wt%. The temperature of the reaction was 270 °C, the total flow rate of H_2 and N_2 was 85 mL/min, the flow rate of MEK was 1 mL/h and the molar ratio of H_2/MEK was 15. Catalyst performance was compared after one hour of the reaction as summarized in Figure 3.5.

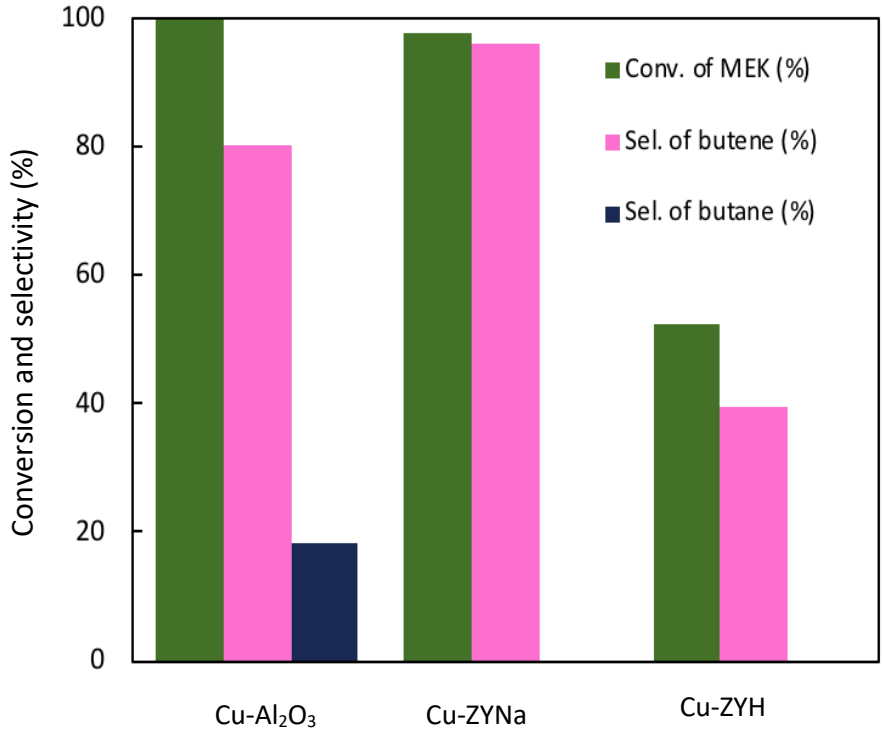

Figure 3.5. Catalytic results for the conversion of MEK to butene over Copper loading on different supports. Reaction conditions: catalyst weight, 1 g; feed rate of MEK, 1.0 mL/h; H_2/MEK molar ratio, 15; reaction temperature, 270 °C; total flow rate of H_2 & N_2, 85 mL/min.

Figure 3.5 shows that the nature of the zeolite used to support copper has a significant impact on the products produced. Cu-Al_2O_3 and Cu-ZYNa give similar results, with nearly complete conversion of MEK and a high selectivity for butene. However, the selectivity to butene is lower on Cu-Al_2O_3, due to production of butane. Cu-ZYH, on the other hand, gives a much lower MEK conversion and a comparatively low butene selectivity. Butene makes up less than 40% of the total products, while a variety of other oxygenates and hydrocarbons are produced. Note that the lower butene selectivity measured for Cu-ZYH is noted even when lower amounts of Cu-Al_2O_3 and Cu-ZYNa are used to give roughly the same conversion. The selectivity for butene was higher (91%)

when using Cu-ZYNa than Cu-Al_2O_3 (64%) at approximately 60% conversion (60.2% and 58.3%, respectively) (see Figure 3.6).

These results clearly indicated that using ZYH as a support led to quite different catalytic chemistry than ZYNa or Al_2O_3. These differences are likely attributable to the amount of acidity in Cu-ZYH much higher than the other two catalysts as shown in Figure 3.3a and in Table 3.3. It is also seen that the conversion of MEK is much lower in copper loaded on ZYH than the other two supports. Previous research by our group has indicated that Cu-ZYH catalysts give low selectivity for butene in the reaction of 2,3 BDO with hydrogen because this catalyst tends to dehydrogenate 2-butanol to MEK at a similar rate to which it dehydrates butanol to butene [32]. This is consistent with the low MEK conversions noted in these studies. The distribution of major products is tabulated in Table 3.4.

Table 3.4. Catalytic activity in the conversion of MEK to main products over several catalysts.

Catalysts	MEK Conv. (%)	Mix-Butene Sel. (%)	Butane Sel. (%)	Others Sel. (%)
20% Cu-Al_2O_3	100	80.11	18.32	1.57 [a]
20% Cu-ZYNa	97.67	96.21	0	3.79[b]
20% Cu-ZYH	52.45	39.66	0	60.34[c]

Reaction conditions: catalyst weight, 1 g; feed rate of MEK, 1.0 mL/h; H_2/MEK molar ratio, 15; reaction temperature, 270 °C; total flow rate of H_2&N_2, 85 mL/min.

Others include:

[a] C_8 alkene, C_8 alkane and xylene, etc.

[b] 2,3 butanedione, 3-hydroxy 2-butanone, MVK, 2,3 BDO and light and heavy olefin (C_3, C_5, C_6, C_7 & C_8).

[C] Acetone, 2,3 butanedione, MVK, 3-hydroxy 2-butanone, C_8 ketone, C_8 alcohol, light and heavy olefins (C_3, C_5, C_6, C_7 & C_8), condensation products, etc.

The catalytic results for Cu-Al_2O_3 and Cu-ZYNa are similar, except for the higher amount of butane from Cu-Al_2O_3 as a result of hydrogenation of butene to butane suggesting that the two catalysts catalyze similar reaction pathways. To look at the mechanisms at play for these two supports, experiments were conducted with lower amounts of catalysts to ensure the MEK conversion less than 100%. Figure 3.6 shows the results of these trials, where major product selectivities are plotted as functions of MEK conversion for the two catalysts.

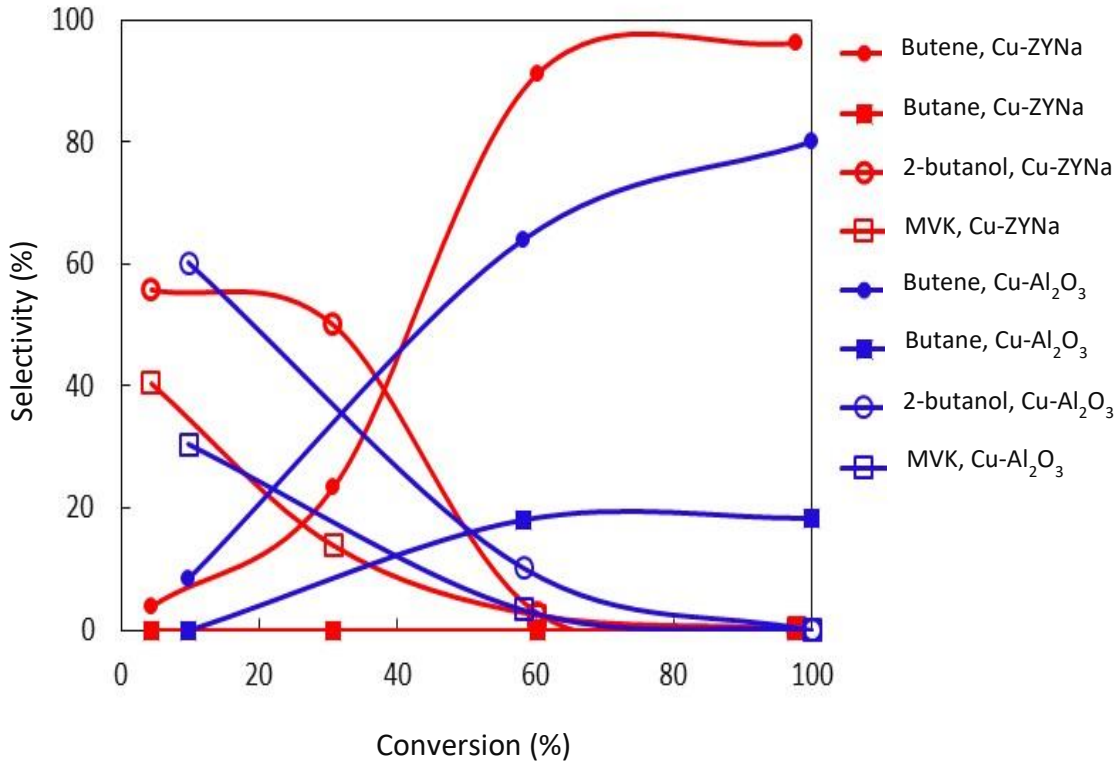

Figure 3.6. Product selectivities as functions of MEK conversion for 20% Cu-ZYNa and 20% Cu-Al_2O_3. Data were obtained with different catalyst weights: 10, 100, 300 and 1000 mg (Cu-ZYNa) and 11, 100, and 1000 mg (Cu-Al_2O_3). Feed rate of MEK, 1.0 mL/h; H_2/MEK molar ratio, 15; reaction temperature, 270 °C; total flow rate of H_2 & N_2, 85 mL/min.

The results shown in Figure 3.6 are consistent with a two-step reaction where MEK is hydrogenated to 2-butanol and then dehydrated to butene, which can further be hydrogenated to butane. At low conversion, 2-butanol selectivity is highest, but it decreases as the conversion increases and selectivities for butene and, eventually, butane increase. At low conversions, significant amounts of methyl vinyl ketone (MVK) are formed. This is consistent with previously reported results for 2,3 BDO where the dehydrogenation product, acetoin, was produced at low space times [32]. 2,3 BDO was reversibly dehydrogenated on copper sites in competition with dehydration on acid sites.

The same chemistry may be at play here: dehydrogenation to MVK may compete with hydrogenation to butanol on copper sites on Cu-Al_2O_3 and Cu-ZYNa. With sufficient space time, MEK is hydrogenated to 2-butanol and further converted to butene and butane.

The major difference between Cu-Al_2O_3 and Cu-ZYNa is that the former produces much more butane than the latter. This is born out in Figure 3.6 where Cu-Al_2O_3 products progressively shift towards butane with increased conversions (space time). No butane, on the other hand, is observed for Cu-ZYNa for any conversion. This is likely due to greater activity for Cu-Al_2O_3. The turnover frequency (TOF (h^{-1})) using Cu-Al_2O_3 and Cu-ZYNa were 34.2 and 27.5 h^{-1}, respectively. It is not possible with this data to calculate the rate of 2-butanol dehydration or butene hydrogenation, but it is certainly possible that these rates are also faster on Cu-Al_2O_3. Faster hydrogenation rates on Cu-Al_2O_3 make sense given the TPR results shown in Figure 3.2a.

3.3.2.2 Effect of Reaction Temperature

The effect of temperature on the conversion of MEK and the distribution of products for Cu-ZYNa was studied for a temperature range of 230 to 290 °C. Figure 3.7 shows the changes in the conversion of MEK and the selectivity for butene with different reaction temperatures after two hours on stream. As seen in this figure, the conversion of MEK first increased with increasing temperature until 270 °C**.** Beyond that temperature, conversion decreases, which is attributed to rapid deactivation, likely because of coke formation [2,33]. Data taken for a reaction time of ten minutes (not shown) showed a slightly higher MEK conversion at 290 °C (99.86%) than at 270 °C

(99.83%), implying that from ten minutes to two hours, catalyst activity dramatically dropped at 290 °C to 86.68%, while the conversion at 270 °C only dropped to 97.05% after two hours.

The distribution of products changed with varying reaction temperatures as shown in Figure 3.7. As displayed in this figure, the selectivity for butene increases with increasing temperature, and the maximum selectivity is about (97%) at 270 °C.

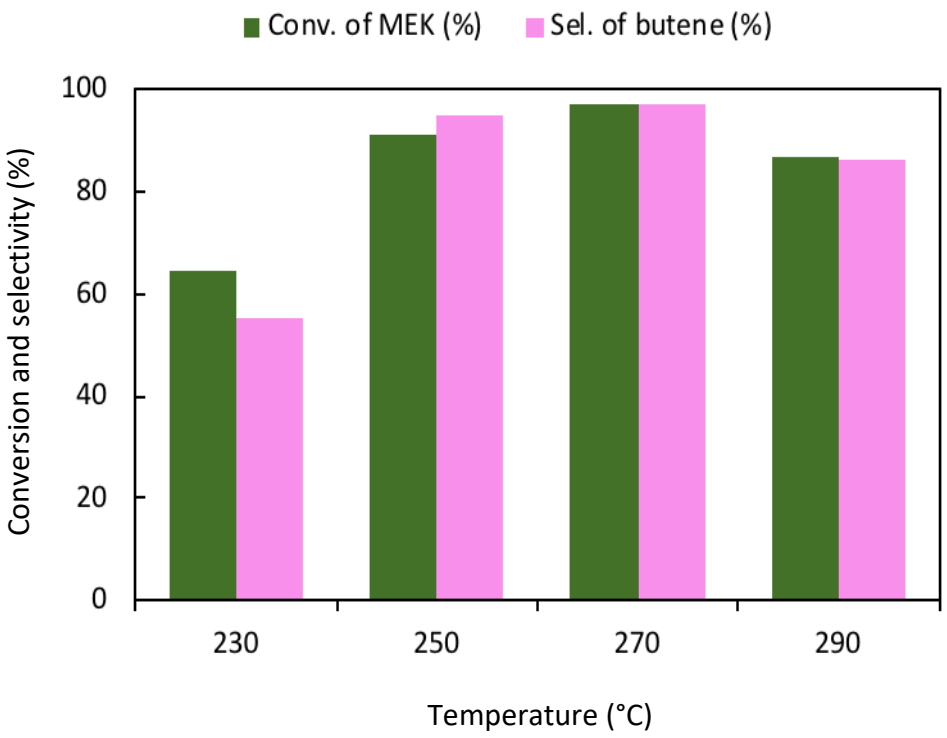

Figure 3.7. Catalytic results for the conversion of MEK to butene over different temperatures after 2h. Reaction conditions: catalyst weight, 1 g (20% Cu-ZYNa); feed rate of MEK, 1.0 mL/h; H_2/MEK molar ratio, 15; total flow rate of H_2 & N_2, 85 mL/min. Other products include 2,3 butanedione, MVK, 2,3 BDO, 3-hydroxy 2-butanone, C_8 ketone, light and heavy olefins (C_2, C_5, C_6, C_7 & C_8), etc.

At low temperatures, product selectivities shifted to products such as MVK, 2,3 BDO and C_8 ketone as a result of dehydrogenation, hydration and condensation reactions. However, at the highest temperature of 290 °C, the selectivity for butene decreased and light and heavy olefins (C_3, C_5, C_6, C_7 and C_8) increased, which was probably due to subsequent oligomerization and cracking reactions of butenes. The potential reaction pathways starting with MEK are summarized in Scheme 3.1.

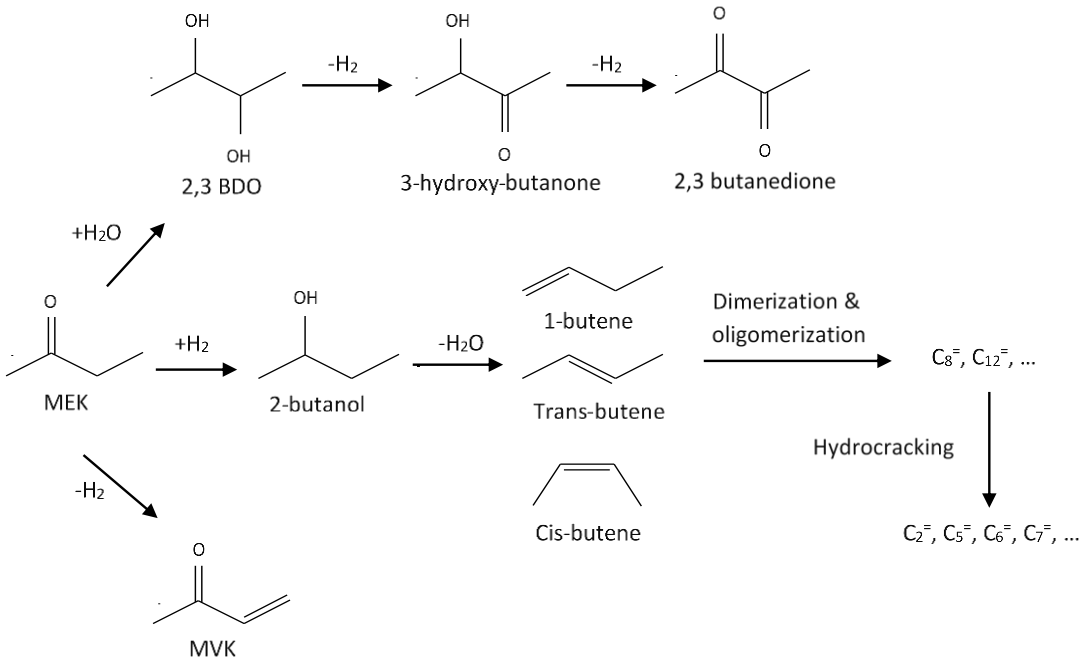

Scheme 3.1. The potential reaction pathway in the reaction of MEK to products.

The main pathways involve hydrogenation and dehydration reactions. MEK is converted to 2-butanol over copper sites through a hydrogenation reaction. Then, 2-butanol is dehydrated to form butene over acidic sites via a dehydration reaction. These butene compounds can be dimerized and oligomerized to form dimers and trimers by a

carbenium-ion mechanism [34] which can further be hydrocracked to other olefins like $C_2^=$, $C_5^=$, $C_6^=$ and $C_7^=$. In addition, small amounts of 2,3 BDO can be produced from MEK hydration, which can then be converted to 3-hydroxy-2-butanone and 2,3-butandione via dehydrogenation reactions on copper sites. It is believed that water formed in the dehydration of 2-butanol to butene is available for the hydration reaction of MEK to 2,3 BDO.

3.3.2.3 Effect of Copper Content

The effect of Cu loading on the catalytic conversion of MEK was investigated by varying the percentage of CuO supported on ZYNa between 8 and 26 wt %. The major results are shown in Figure 3.8. As seen in this figure, the conversion of MEK increases with increasing amounts of CuO supported on ZYNa. However, by increasing the copper loading to 26%, the conversion of MEK decreases. Figure 3.8 also shows that by decreasing the amount of CuO, the selectivity of butene decreases while the selectivity for other products like light and heavy olefins (C_2, C_5, C_6, C_7 & C_8), MVK, 2,3 BDO, 2,3 butanedione, 3-hydroxy 2-butanone and C_8 ketones increases.

The trend noted in MEK conversion can be understood by recognizing that the first step in the reaction mechanism, as described above, likely occurs on metal sites. The metal loading, therefore, should play an important role in MEK conversion. However, as noted in Table 3.1, there are actually more copper sites available for this reaction at the lowest Cu loadings because of their higher dispersion, so one might expect conversion to drop with increased loadings. This discrepancy is likely due to the complicated nature of

MEK conversion. While the copper sites catalyze MEK hydrogenation to 2-butanol, they can also catalyze the dehydrogenation of MEK to MVK (see Scheme 3.1). For the catalysts with the lowest loadings, the highly dispersed particles led to faster rates of dehydrogenation to MVK. This is reflected in the product selectivities. 8% Cu-ZYNa gives a selectivity to MVK of 7.5% as compared to 1.7% and 0.2% MVK selectivities for 14 and 20% Cu-ZYNa, respectively. MVK can be hydrogenated back to MEK, resulting in a lower apparent MEK conversion for the catalysts with more highly dispersed CuO particles. The drop in conversion noted from 20 to 26% Cu-ZYNa could reflect the presence of larger Cu particles in 26% Cu-ZYNa which may block some of the catalyst pores (see Table 3.1 BET, N_2O dispersion and XRD results).

The trends in product selectivities can be attributed to the bifunctional nature of the catalysts. Product composition is dependent on the relative contributions of copper and acidic/basic sites. When the CuO loading is low, acid/base catalyzed reactions can compete with hydrogenation chemistry, leading to the production of a variety of other products. The best results were noted for the catalyst with 20 wt% of CuO, which achieved MEK conversion above 97% and a butene selectivity of 97.3% after 2h.

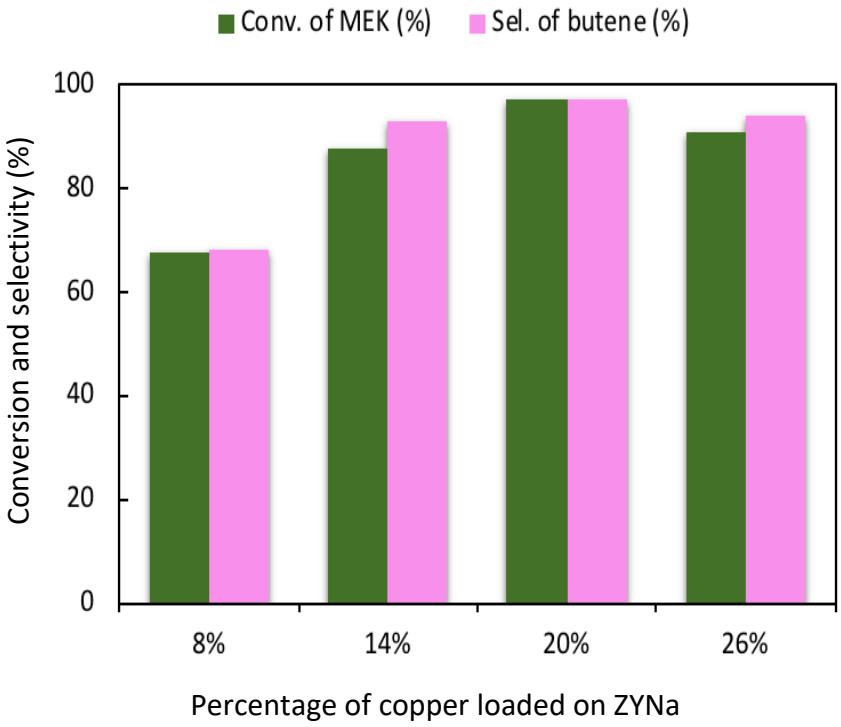

Figure 3.8. Catalytic results for the conversion of MEK to butene using different copper loadings on ZYNa after 2h. Reaction conditions: catalyst weight, 1 g; feed rate of MEK, 1.0 mL/h; H_2/MEK molar ratio, 15; reaction temperature, 270 °C; total flow rate of H_2 & N_2, 85 mL/min. Other products include light and heavy olefins (C_2, C_5, C_6, C_7 & C_8), MVK, 2,3 BDO, 2,3 butanedione, 3-hydroxy 2-butaneone, C_8 ketone, etc.

3.3.2.4 Effect of H_2/MEK Molar Ratio

Experiments were conducted to study the effect of changing the molar ratio of H_2 to MEK on the conversion of MEK and the selectivity for butene over both Cu-Al_2O_3 and Cu-ZYNa. The results are shown in Figures 3.9a and 3.9b, respectively.

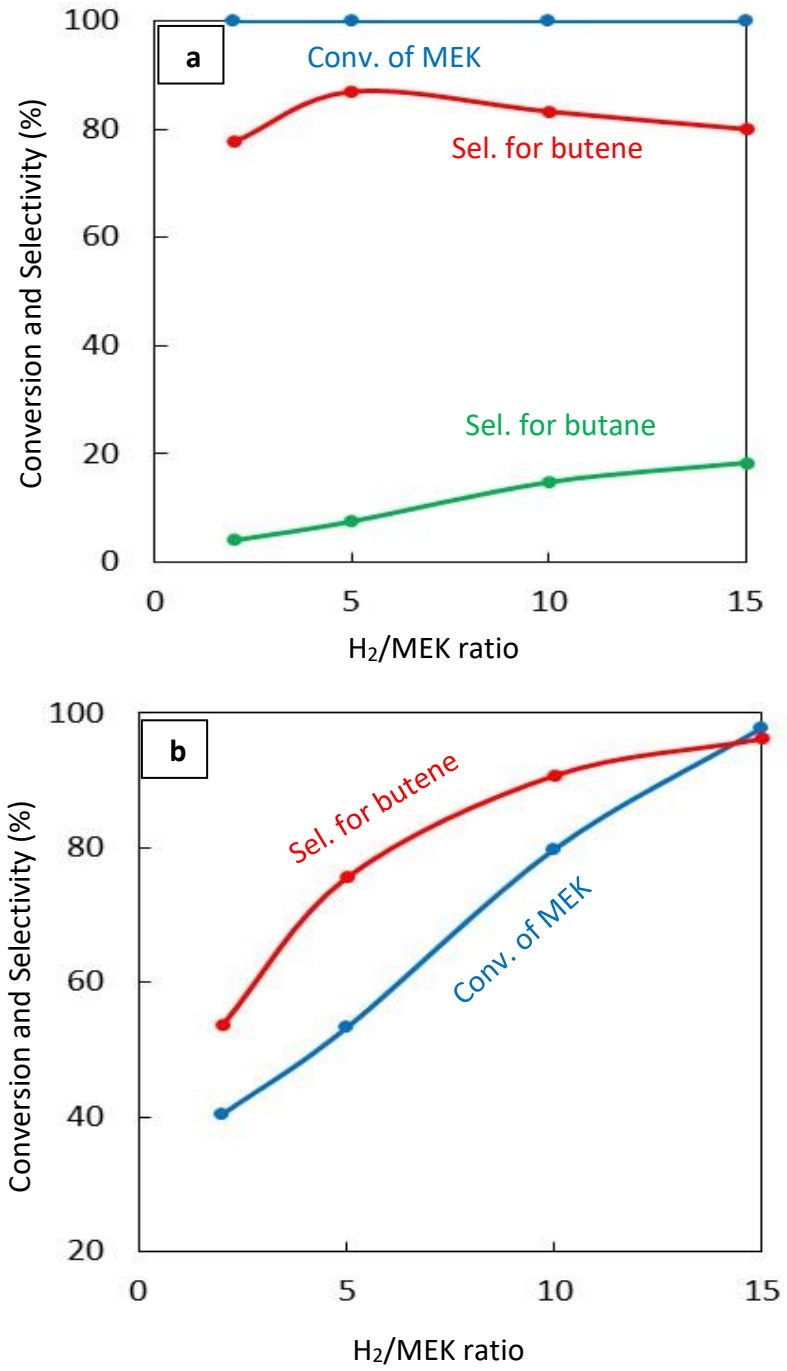

Figure 3.9. Catalytic results for the conversion of MEK to butene with different H_2/MEK ratios. Reaction conditions: catalyst weight, 1.0 g; feed rate of MEK, 1.0 mL/h; reaction temperature, 270 °C; total flow rate of H_2 & N_2, 85 mL/min. (a) over 20% Cu-Al_2O_3, other products detected include C_8 alkene, C_8 alkane, xylene, etc. (b) over 20% Cu-ZYNa, other products include light and heavy olefins (C_2, C_5, C_6, C_7 & C_8), MVK, 2,3 BDO, 2,3 butanedione, 3-hydroxy 2-butanone and C_8 ketones, etc.

As can be seen from Figure 3.9a, changing the H_2/MEK ratio did not affect the conversion of MEK, which is nearly 100% at all ratios. However, the ratio impacted the product selectivities. As the H_2/MEK ratio increased, the selectivity of butane increased due to subsequent hydrogenation of butene to butane. The highest selectivity of butene (87%) was found at a H_2/MEK ratio of 5. At lower ratios, dimerization reactions increased leading to larger hydrocarbons and consequently slightly lower butene selectivities. The impact of the H_2/MEK ratio on the catalytic performance of Cu-ZYNa is shown in Figure 3.9b. Increasing the H_2/MEK ratio from 2 to 15 increased the MEK conversion from 40.5% to 97.7%. This is in contrast to the results in Figure 3.9a for Cu-Al_2O_3 which showed essentially complete MEK conversion at all ratios. This is another indication of the higher activity of Cu-Al_2O_3. The butene selectivity progressively increased with increasing H_2/MEK ratio, increasing from 53.7% to 96.2% as the ratio was increased from 2 to 15. At lower ratios, oligomerization and dehydrogenation reactions of MEK were prominent, lowering the selectivity for butene. As the ratio was increased, these reactions became less important and the selectivity for butene was nearly 100%. Unlike Cu-Al_2O_3, Cu-ZYNa did not produce significant amounts of butane under the reaction conditions, even at the highest H_2/MEK ratio.

3.3.2.5 Catalyst Stability

The conversion of MEK and distribution of major products are shown in Figure 3.10 as a function of time on stream over 20% Cu-ZYNa.

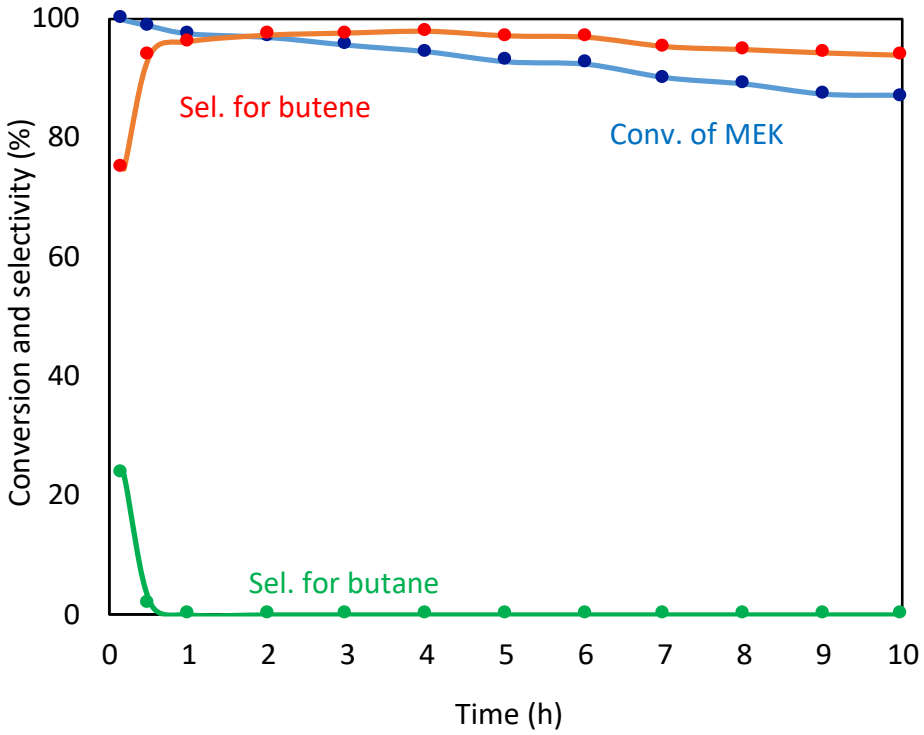

Figure 3.10. Catalytic results for the conversion of MEK to butene over 20% Cu-ZYNa with time. Reaction conditions: catalyst weight, 1 g; feed rate of MEK, 1.0 mL/h; reaction temperature, 270 °C; total flow rate of H_2 & N_2, 85 mL/min; H_2/MEK, 15.

As can be seen from this figure, the conversion of MEK decreases with time from 100% in the beginning of the reaction to 87 % after 10 h. This can be attributed to the formation of coke which is a non-desorbed product preventing access to the active sites of the catalyst [33,35]. Butane is produced only on a fresh catalyst for reaction times under an hour. Since multiple reaction pathways must occur to produce butane, it is not obvious whether the loss of butane selectivity is due to loss of activity in hydrogenation of butene to butane, in acid-catalyzed dehydration of 2-butanol, or hydrogenation of MEK to 2-butanol. The maximum selectivity of butene was obtained in the fourth hour of the reaction, reaching around 97.9%, before decreasing to 93.9% after 10 h. At the same time

butene selectivity was decreasing, the selectivities of other products (not shown) such as MVK, C_8 ketones, and 2,3 BDO increased. These trends are all related to catalyst deactivation, likely through the loss of active copper sites. As shown in Figure 3.6, MEK is readily dehydrogenated to MVK. Longer reaction times are needed before the reaction products shift from MVK to butene. Deactivation of the catalyst slows reactions that lead to butene, leading to more MVK production. The production of 2,3 BDO (from hydration of MEK) and C_8 ketone (from condensation of MEK) likely result from acid-base catalyzed pathways that become more important when the copper sites are deactivated.

3.4 Conclusion

The conversion of MEK to butenes in one step has been demonstrated using copper loaded on three different supports. The results showed that the highest selectivity for butene was obtained over Cu-ZYNa; 97% at nearly complete conversion. The optimum reaction temperature was 270 °C. At lower temperatures (230 °C) hydration, dehydrogenation and aldol condensation reactions became important, while higher temperatures (290 °C) led to oligomerization and cracking reactions and catalyst deactivation. The copper loading had a significant impact on catalytic results. Butene selectivity increased with copper loading, with the highest butene selectivity coming with a loading of 20 wt%. Catalyst deactivation was noted over 10 hours, probably because of coke formation. Using Cu-Al_2O_3, butane was produced in addition to butene due to the hydrogenation reaction of butene to butane. With increasing H_2/MEK ratio, the selectivity of butane increased. With lower H_2/MEK ratios, butane selectivity was decreased and

other products including C_8 alkenes were produced. Using Cu-ZYNa, the conversion of MEK and the selectivity for butene both increased with increasing H_2/MEK ratios. The lowest selectivity for butene was obtained over Cu-ZYH, likely because its highest amount of acidic sites catalyzing non-selective reaction pathways.

Acknowledgements

Financial support from Navy SBIR Phase II Contract #NG8335, in collaboration with TekHolding, Inc. and Higher Committee for Education Development in Iraq (HCED) is gratefully acknowledged.

References

1. Liu, D.; Chen, E. Y. X. Integrated catalytic process for biomass conversion and upgrading to C_{12} furoin and alkane fuel. ACS Catal. **2014**, 4, 1302–1310.

2. Zheng, Q.; Wales, M. D.; Heidlage, M. G.; Rezac, M.; Wang, H.; Bossmann, S. H.; Hohn, K. L. Conversion of 2,3-butanediol to butenes over bifunctional catalysts in a single reactor. J. Catal. **2015**, 330, 222–237.

3. Yu, E. K.; Saddler, J. N. Fed-batch approach to production of 2,3-butanediol by Klebsiella pneumoniae grown on high substrate concentrations. Appl. Environ. Microbiol. **1983**, 46, 630–635.

4. Zeng, A. P.; Biebl, H.; Deckwer, W. D. Effect of pH and acetic acid on growth and 2, 3-butanediol production of Enterobacter aerogenes in continuous culture. Appl. Microbiol. Biotechnol. **1990**, 33, 485–489.

5. Mas, C. De; Jansen, N. B.; Tsao, G. T. Production of optically active 2,3-butanediol by Bacillus polymyxa. Biotechnol. Bioeng. **1988**, 31, 366–377.

6. Ledingham, G. A.; Neish, A. C. Fermentative Production of 2,3 Butanediol. Industrial Fermentations, LA Underkofler and RJ Hickey, Eds. **1954**,2, 27–93.

7. Duan, H.; Yamada, Y.; Sato, S. Efficient production of 1, 3-butadiene in the catalytic dehydration of 2,3-butanediol. Appl. Catal. A Gen. **2015**, 491, 163–169.

8. Villegas, J.; Kumar, N.; Heikkilä, T.; Lehto, V. P.; Salmi, T.; Murzin, D. A study on the dimerization of 1-butene over Beta zeolite. Top. Catal. **2007**, 45, 187–190.

9. Haller, G. L. Chemistry of catalytic processes: By Bruce C. Gates, James R. Katzer, and G. C. A. Schuit. McGraw-Hill, New York. **1979**, 60, pp 464.

10. Gary, J. H.; Handwerk, G. E.; Kaiser, M. J. Petroleum refining: technology and economics; CRC press, 2007;

11. Molnár, Á.; Bucsi, I.; Bartók, M. Pinacol Rearrangement on Zeolites. Stud. Surf. Sci. Catal. 1988, 41, 203–210.

12. Multer, A.; McGraw, N.; Hohn, K.; Vadlani, P. Production of methyl ethyl ketone from biomass using a hybrid biochemical/catalytic approach. Ind. Eng. Chem. Res. 2012, 52, 56–60.

13. Emerson, R. R.; Flickinger, M. C.; Tsao, G. T. Kinetics of dehydration of aqueous 2,3-butanediol to methyl ethyl ketone. Ind. Eng. Chem. Prod. Res. Dev. 1982, 21, 473–477.

14. Brands, D. S.; Poels, E. K.; Bliek, A. Ester hydrogenolysis over promoted Cu/SiO_2 catalysts. Appl. Catal. A Gen. 1999, 184, 279–289.

15. Sitthisa, S.; Resasco, D. E. Hydrodeoxygenation of furfural over supported metal catalysts: a comparative study of Cu, Pd and Ni. Catal. Letters 2011, 141, 784–791.

16. Lilga, M. A.; Lee, G. S.; Lee, S. J. Conversion of 2,3-butanediol to 2-butanol, olefin and fuels. U.S. Patent No. 9,517,984. 2016.

17. Yamaguchi, T.; Nakano, Y.; Iizuka, T.; Tanabe, K. Catalytic activity of ZrO_2 and ThO_2 for HD exchange reaction between methyl group of adsorbed isopropyl alcohol-d8 and surface OH group. Chem. Lett. 1976, 677–678.

18. Szabó, Z. G.; Jover, B.; Ohmacht, R. The joint application of flow-system and micropulse techniques for a comparative study of 2-propanol decomposition over MgO, CaO and SrO. J. Catal. 1975, 39, 225–233.

19. Yashima, T.; Suzuki, H.; Hara, N. Decomposition of 2-propanol over alkali cation exchanged zeolites. J. Catal. 1974, 33, 486–492.

20. Prasomsri, T.; Nimmanwudipong, T.; Román-Leshkov, Y. Effective hydrodeoxygenation of biomass-derived oxygenates into unsaturated hydrocarbons by MoO_3 using low H_2 pressures. Energy Environ. Sci. 2013, 6, 1732–1738.

21. Hou, R.; Yu, W.; Porosoff, M. D.; Chen, J. G.; Wang, T. Selective hydrogenation of 1,3-butadiene on Pd Ni bimetallic catalyst: From model surfaces to supported catalysts. J. Catal. 2014, 316, 1–10.

22. Bond, G. C.; Namijo, S. N. An improved procedure for estimating the metal surface area of supported copper catalysts. J. Catal. 1989, 118, 507–510.

23. Van Der Grift, C. J. G.; Wielers, A. F. H.; Jogh, B. P. J.; Van Beunum, J.; De Boer, M.; Versluijs-Helder, M.; Geus, J. W. Effect of the reduction treatment on the structure and reactivity of silica-supported copper particles. J. Catal. 1991, 131, 178–189.

24. Bravo-Suárez, J. J.; Subramaniam, B.; Chaudhari, R. V Ultraviolet–Visible Spectroscopy and Temperature-Programmed Techniques as Tools for Structural Characterization of Cu in CuMgAlO x Mixed Metal Oxides. J. Phys. Chem. C 2012, 116, 18207–18221.

25. Marella, R. K.; Koppadi, K. S.; Jyothi, Y.; Rao, K. S. R.; Burri, D. R. Selective gas-phase hydrogenation of benzonitrile into benzylamine over Cu–MgO catalysts without using any additives. New J. Chem. 2013, 37, 3229–3235.

26. der Grift, C. J. G. Van; Mulder, A.; Geus, J. W. Characterization of silica-supported copper catalysts by means of temperature-programmed reduction. Appl. Catal. 1990, 60, 181–192.

27. Fierro, G.; Lojacono, M.; Inversi, M.; Porta, P.; Lavecchia, R.; Cioci, F. A study of anomalous temperature-programmed reduction profiles of Cu2O, CuO, and CuO-ZnO catalysts. J. Catal. 1994, 148, 709–721.

28. Zhou, R.; Yu, T.; Jiang, X.; Chen, F.; Zheng, X. Temperature-programmed reduction and temperature-programmed desorption studies of CuO/ZrO_2 catalysts. Appl. Surf. Sci. 1999, 148, 263–270.

29. Sagar, G. V.; Rao, P. V. R.; Srikanth, C. S.; Chary, K. V. R. Dispersion and Reactivity of Copper Catalysts Supported on $Al2O_3 – ZrO_2$. J. Phys. Chem. B 2006, 110, 13881–13888.

30. Hattori, H. Heterogeneous basic catalysis. Chem. Rev. 1995, 95, 537–558.

31. Kim, H. J.; Kang, B. S.; Kim, M. J.; Park, Y. M.; Kim, D. K.; Lee, J. S.; Lee, K. Y. Transesterification of vegetable oil to biodiesel using heterogeneous base catalyst. Catal. today 2004, 93, 315–320.

32. Zheng, Q.; Xu, J.; Liu, B.; Hohn, K. L. Mechanistic study of the catalytic conversion of 2,3-butanediol to butenes. J. Catal. 2018, 360, 221–239.

33. Wang, B.; Manos, G. A novel thermogravimetric method for coke precursor characterisation. J. Catal. 2007, 250, 121–127.

34. Kissin, Y. V Chemical mechanisms of catalytic cracking over solid acidic catalysts: Alkanes and alkenes. Catal. Rev. 2001, 43, 85–146.

35. Cerqueira, H. S.; Caeiro, G.; Costa, L.; Ribeiro, F. R. Deactivation of FCC catalysts. J. Mol. Catal. A Chem. 2008, 292, 1–13.

Chapter 4 - Metals on ZrO_2: Catalysts for the Aldol Condensation of Methyl Ethyl Ketone (MEK) to C_8 Ketone

As submitted in Catalysts (2018) by Zahraa Al-Auda, Hayder Al-Atabi and Keith Hohn

As a part of provisional patent application titled: "**Method for converting unsymmetrical and/or symmetrical ketones to higher hydrocarbons"**

Abstract

Methyl ethyl ketone (MEK) was converted to higher ketones in one step using a multifunctional catalyst having both aldol condensation (aldolization and dehydration) and hydrogenation properties. 15% Cu supported zirconia (ZrO_2) was investigated in the catalytic gas phase reaction of MEK in a fixed bed reactor. The results showed that the main product was 5-methyl-3-heptanone (C_8 ketone), with side products including 5-methyl-3-heptanol, 2-butanol and other heavy products (C_{12} and up). Effects of various reaction parameters like temperature and molar ratio of reactants (H_2/MEK) on overall product selectivity were studied. It was found that with increasing temperature, the selectivity for C_8 ketone increased while selectivity for 2-butanol decreased. The hydrogen pressure played a significant role on the selectivity of products. It was observed that with increasing H_2/MEK molar ratio, 2-butanol selectivity increased due to hydrogenation while decreasing this ratio led to increasing aldol condensation products. In addition, it was noted that both conversion and selectivity for the main product increased using a low loading percentage of copper, 1% Cu-ZrO_2. The highest selectivity of 5-methyl-3-heptanone reached (60%) was obtained at temperatures around 180 °C and a molar ratio of H_2/MEK equal to 2. Other metals (Ni, Pd and Pt) supported on ZrO_2 also produced 5-methyl 3-heptanone as the main product with slight differences in selectivity, suggesting that a hydrogenation catalyst is important for producing the C_8 ketone, but the exact identity of the metal is less important.

Key Words

Methyl ethyl ketone, higher ketone, aldol condensation reaction, copper, zirconia.

4.1 Introduction

With declining petroleum resources, more attention has been paid to developing biomass as a sustainable source of renewable fuels and chemicals. In general, the aldol condensation reaction is considered one of the most powerful C–C bond forming reactions [1] for the production of large organic molecules. In the fine chemical industry, base–catalyzed aldol condensations are a common method of coupling organic molecules [2]. C-C bond formation proceeds via condensation between a molecule containing a carbonyl group and another molecule containing an activated methylene group under suitable operating conditions [3]. Aldol condensations involve reactions forming β-hydroxy aldehydes (β-aldol) or β-hydroxy ketone (β-ketol) either via self-condensations or mixed condensations of aldehydes and ketones. Then, via dehydration of the intermediate β-aldol or β-ketol, α,β-unsaturated aldehydes or α,β-unsaturated ketones are formed [4]. Finally, further hydrogenation yields higher aldehydes or higher ketones. In fact, aldol condensation reactions are commercially significant in the production of intermediates needed to produce other commercially important products.

The largest volume aldol reaction product of acetone is Methyl isobutyl ketone (MIBK) which is an excellent solvent for cellulose, vinyl, epoxy and acrylic resins, in addition to resin based coating systems [5]. Industrially, MIBK is manufactured in three

steps: (i) an aldolization reaction of acetone to produce diacetone alcohol (DAA). (ii) a dehydration of DAA to mesityl oxide (MO); and (iii) hydrogenation of the olefin double bond of MO to give MIBK [6].

These processes are intricate and require high operating costs, so recently a one-step process to convert acetone to MIBK has become commercially possible. Reichle [7] described the condensation of aldehydes and ketones in the gas phase, especially acetone over catalysts consisting of lithium ions supported on a complex magnesium-aluminum oxide-hydroxide mixture. The reactions formed *iso*-phorone and mesityl oxide with isophorone/mesityl oxide ratios>1. Kelly [5] studied aldol condensation reaction of acetone over two beds of catalysts consisting of 3 mL of the K-SiO_2 catalyst followed by a 3 mL bed of a hydrogenation catalyst consisting of 1% palladium supported on carbon. The main product was MIBK in addition to mesityl oxide and *iso*-phorone. He also investigated aldol condensation of MEK using different catalysts. He reported that, using Na-SiO_2 and Cs-SiO_2, the major product was an α,β-unsaturated ketone (5-methyl-4-hepten-3-one), with both isomers (*cis* and *trans*) being formed at temperatures between 325 and 400 °C. He further tested aldol condensation of MEK over two beds comprised of Na-SiO_2 and Cu-Zn. The main products were 5-methyl-3-heptanone and 5-methyl-3-heptanol which were the result of a subsequent hydrogenation of an α,β-unsaturated ketone. However, over just one bed consisting of Cu-Zn alone, the main products were believed to be bicyclo-[3,3,0]-octane-3,7-dione resulting from a dehydrogenation reaction of two molecules of MEK with little evidence of aldol condensation compounds.

It is comparatively easy to hydrogenate α,β-unsaturated carbonyls into saturated carbonyls rather than into unsaturated alcohols [8–10] since thermodynamics favor the hydrogenation of C=C bonds over C=O bonds [11,12]. For kinetic reasons, the reactivity of the C=C bond for hydrogenation is higher than the C=O bond, leading to saturated aldehydes or saturated alcohols via subsequent hydrogenation of the aldehydes over conventional supported hydrogenation catalysts (Pt, Ru, Ni, etc.) [12]. The catalysts used for hydrogenation of double bonds in α,β-unsaturated ketones can be divided in to two groups: one which includes platinum metals as a main component or a modifier, and the other group consisting of Ni, Cu or Co [13]. Cu catalysts are often more selective for the hydrogenation of the C=C bond rather than the C=O bond when used in the reduction of α,β-unsaturated carbonyls [11].

Szöllősi, *et al.* [14] carried out a comparative study to determine the activity and selectivity for gas-phase hydrogenation of 3-penten-2-one to form 2-pentanone on well-defined SiO_2 (Cab-O-Sil)-supported metals: Ni, Cu, Ru, Rh, Pd and Pt. The activity of the metals investigated for the hydrogenation of 3-penten-2-one followed the order: Pt > Pd > Rh >> Ru > Ni > Cu at 120 °C and Pt > Pd > Rh >Ru - Ni >> Cu at 200 °C. However, Ravasio, Nicoletta *et al.* [15] reported that Cu-Al_2O_3 is an effective catalyst for the selective reduction of different α,β-unsaturated carbonyl compounds. Ravasio, Nicoletta *et al.* [16] also reported that Cu-SiO_2 was selective for the hydrogenation of unsaturated ketones.

The coupling reaction of small molecules to produce large molecules is a commercially attractive method to form a range of products having specific structures and properties. For this reason, this chapter utilized aldol condensation for upgrading MEK to higher ketones. MEK is an attractive feedstock since it can be derived from renewable resources, for example by dehydrating 2,3 butanediol [17–24], which can be produced in high yields from biomass-derived sugars [25–32]. The process studied includes a single step to create C-C bonds between two equivalents of biomass-derived MEK via heterogeneous catalysis using a multifunctional catalyst having aldol condensation (aldolization and dehydration) and hydrogenation properties to produce a higher ketone (C_8) in a single reactor. The main product, 5-methyl-3-heptanone, is an important intermediate used to produce higher aliphatic alcohols (5-methyl-3-heptanol) via hydrogenation reactions. It can also be used to produce C_8 alkenes and alkane for use as fuels through hydrogenation-dehydration reactions.

Our aim in this chapter was to develop a catalyst that can condense MEK into higher ketones in a single step. ZrO_2 was chosen as a support since it has both acidic and basic properties. A cooperative effect of acidic and basic sites makes ZrO_2 function as an effective catalyst [33]. It is hypothesized that the basic sites on ZrO_2 can catalyze the aldol condensation reaction, while its acidic sites are suitable for dehydration reactions [34]. Supported metals like copper have been investigated for the hydrogenation of aldol condensation products (α,β-unsaturated ketones) to give saturated ketones. We hypothesized that Cu/ZrO_2 would be capable of catalyzing the three steps needed to produce C_8 ketones from MEK. Optimizing the operating conditions like temperature,

H_2/MEK molar ratio and Cu loading were studied to obtain the highest selectivity of 5-methyl-3-heptanone. The effect of different metals (Ni, Pd and Pt) loaded on ZrO_2 was also considered.

4.2 Experimental Work

4.2.1 Materials

Methyl ethyl ketone, the copper precursor (copper(II) nitrate tri-hydrate [$Cu(NO_3)_2 \cdot 3H_2O$ (99%)]) and the nickel precursor (nickel(II) nitrate hexahydrate [$Ni(NO_3)_2 \cdot 6H_2O$ (99%)]) were obtained from Fisher Scientific, while the Pt precursor (tetraammineplatinum(II) nitrate [$Pt(NH_3)_4(NO_3)_2$]), Pd precursor (palladium(II) nitrate hydrate [$N_2O_6Pd \cdot xH_2O$]) and zirconium oxide (catalyst support, S.A 51 m^2/g, 1/8" pellet) were obtained from Alfa Aesar.

4.2.2 Preparation of Supported Catalysts

All catalysts presented (Cu, Ni, Pd and Pt supported on ZrO_2) were synthesized using an incipient wetness impregnation method. Before loading the metal, the support pellet was crushed and sieved to obtain particles < 0.15 mm in size (mesh 100). Next, a metal salt solution was prepared by dissolving the metal precursor in an amount of water just sufficient to fill the pores of amount of the support. This solution was added to the support by dropwise addition and was mixed thoroughly between droplets. The catalysts were dried first in an oven overnight at 100 °C then heated in a furnace at 110 °C for 2 h and calcined at 550 °C for 4 h in air. A ramp rate of 2 °C/min was used up to 110 °C and 1

°C/min up to 550 °C. After the calcination process, the catalyst was crushed and sieved to < 0.15 mm for all catalysts.

4.2.3 Catalytic Reaction

Catalysts prepared as described above were used for the aldol condensation of MEK. The catalytic conversion of MEK was performed in the gas phase in a continuous flow fixed-bed reactor made of stainless steel (id=0.85 cm) under atmospheric pressure. Before the reaction, a catalyst (1.0 g) was reduced in the reactor with flow rates of H_2 and N_2 equal to 68.5 and 16.5 mL/min, respectively, at 300 °C for 1 h for Cu, Pd and Pt supported ZrO_2 and at 500 °C for Ni-ZrO_2. After the reduction step, MEK was mixed with hydrogen and nitrogen in a preheater at the desired reaction temperature prior to flowing into the reactor. The MEK was fed through the top of the reactor at a feed rate of 1 mL/h via a micro pump (Eldex 1SMP) together with H_2 and N_2 with flow rates of 9.2 and 75.8 mL/min respectively, and the molar ratio of H_2/MEK was 2. The reaction temperature was maintained at 180 °C. The temperature of the product effluent from the bottom of the reactor was maintained above 230 °C to avoid the condensation of liquid products. Product analysis was conducted using an on-line gas chromatograph (SRI 8610C) with an MXT-1 column (100% dimethyl polysiloxane (nonpolar phase), 60 m, ID 0.53 mm) and FID and TCD detectors for the analysis of hydrocarbons and oxygenates. The oven was held at 40 °C for 5 min, raised to 120 °C at a ramp rate of 40 °C/min, then raised to 250 °C at a rate of 20 °C/min and held at this temperature for 10 min. An Agilent 7890A GC-MS

system equipped with an Agilent 5975C MS detector was used to identify the products detected by the GC.

The conversion of MEK and the selectivity for products were calculated using Equation 4.1 and 4.2 respectively:

$$\text{Conversion } \% = \frac{(\text{ Moles of MEK})in - (\text{Mole of MEK})out}{(\text{ Moles of MEK})in} * 100 \qquad \ldots (4.1)$$

$$\text{Selectivity } \% = \frac{(\text{ Moles of product})}{(\text{ Moles of total products})} * 100 \qquad \ldots (4.2)$$

4.2.4 Catalyst Characterization

4.2.4.1 X-ray Diffraction (XRD)

X-ray diffraction patterns were obtained using a Rigaku Miniflex II desktop X-ray diffractometer, using Cu Kα radiation (λ = 0.15406 nm) at 30 kV and 15 mA. Scans of two theta angles were from 10° to 80° for all catalysts with rate of 2 °/min and a step size of 0.02°.

4.2.4.2 Temperature Programmed Reduction (H_2-TPR)

H_2-TPR was performed in an Altamira AMI-200. In a typical experiment, 0.1 g of sample was loaded in a quartz U-tube reactor and argon was passed at 500 °C with a flow of 40 mL/min for an hour to pretreat the catalyst sample followed by cooling to 50 °C.

After treatment, the temperature was raised from 50 °C to 600 °C at a ramp rate of 10 °C/min using H_2/Ar with flow of 40 mL/min (10 v/v %). Consumed H_2 as a function of temperature was detected via a thermal conductivity detector (TCD).

4.2.4.3 Temperature Programmed Desorption (NH_3-TPD and CO_2-TPD)

Temperature programmed desorption of ammonia (NH_3-TPD) and carbon dioxide (CO_2-TPD) were performed on an Altamira AMI-200 system to investigate the surface acidity and basicity of catalysts. Before (NH_3-TPD) studies, 0.1 g of supported metal catalyst was loaded in a quartz U-tube reactor and pretreated at 550 °C under helium for 1 h followed by cooling to 100 °C. After that, the catalyst was reduced by passing H_2/Ar (10 v/v %) with a flow of 40 mL/min up to 300 °C at a constant ramp rate of 10 °C /min and then held for 2 h followed by cooling to 100 °C. After reducing the sample, 1% NH_3/He with a flow of 50 mL/min was then introduced at 100 °C for 1 h to saturate the sample with NH_3 and was subsequently flushed in a He flow at 100 °C for 2 h to remove physically adsorbed NH_3 molecules. Finally, the temperature was raised to 700 °C at a ramp rate of 10 °C /min. CO_2-TPD was performed using the same instrument used in the NH_3-TPD measurements. 0.1 g of the sample was preheated and reduced in the same series of steps as that described for NH_3-TPD except that the cooling temperature after reducing the catalyst was 50 °C. After reducing, the sample was saturated with 10% CO_2 in Helium with a flow of 50 mL/min at 50 °C and was flushed with a He flow at 50 °C for 2 h to remove physisorbed CO_2 molecules. Finally, the temperature was raised to 700 °C at

a ramp rate of 10 °C/min. Desorbed NH_3 and CO_2 from the samples were detected by a thermal conductivity detector (TCD).

4.3 Results and Discussions

4.3.1 Characterization of Catalysts

4.3.1.1 XRD

The XRD patterns of pure ZrO_2 and calcined different metals (Cu, Ni, Pt and Pd) over ZrO_2 in addition to different loadings of copper on ZrO_2 are shown in Figure 4.1.

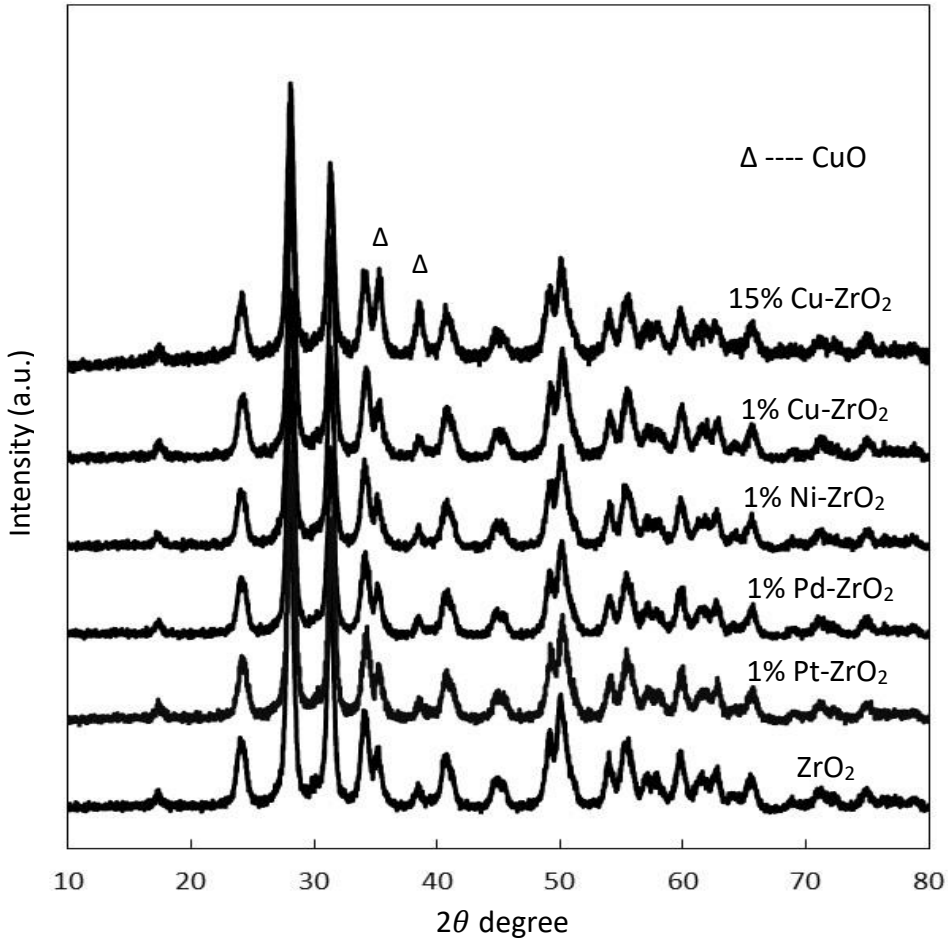

Figure 4.1. XRD patterns for pure ZrO_2 and different metals supported on ZrO_2.

As shown in this figure, the zirconia displays a monoclinic phase in all the samples. ZrO_2 peaks were observed at 2θ= 24.05°, 31.47°, 35.3°, 38.5°, 40.72° and 61.37° [JCPDS 37-1484]. There are no distinguishable diffraction peaks representing crystalline CuO at low Cu loading (1 wt% Cu-ZrO_2) either because the copper particles are smaller than 40 Å in size, the detection limit of XRD [35,36], or because the peaks are obscured by ZrO_2 peaks at similar diffraction angles**.**

For 15% Cu-ZrO_2, peaks attributed to crystalline CuO at 2θ= (35.5°, 38.7°) can be distinguished from the characteristic ZrO_2 peaks near these diffraction angles, confirming presence of CuO as clusters at higher loadings of Cu. This is in accordance with the results obtained from TPR measurements described below. For 1% Ni-ZrO_2, no obvious diffraction peaks were observed for NiO, suggesting that NiO was dispersed well on the surface of the support. Also, no diffraction peaks for palladium or platinum oxide were detected in the diffraction profiles of 1% Pd-ZrO_2 and 1% Pt-ZrO_2 indicating that these metals have been well dispersed at low loadings on the support.

4.3.1.2 H_2-TPR

H_2-TPR measurements were performed to investigate the reducibility of different metals (Cu, Ni, Pt and Pd) supported on ZrO_2 and the dispersion of the metals on the support. The TPR profile provides information on the dispersion of metal species over the support and gives details of the interaction between the metal ions and the support [37], and it is well suited for studying systems with high metal dispersion whose characteristics are beyond the detectability limits of XRD [35]. Figure 4.2a exhibits the TPR profiles of

pure ZrO_2 and Cu supported on ZrO_2. As can be seen, ZrO_2 displays no reduction peaks while 1% Cu-ZrO_2 exhibits three reduction peaks centered at 176.41 °C, 378.12 °C and 441.34 °C. Shimokawable *et al.* [38] and Dow *et al.* [39] have studied the reduction behavior of Cu-ZrO_2 and CuO-YSZ (Y_2O_3-stabilized ZrO_2) catalysts respectively. They have elucidated that the lower temperature peaks are because of highly dispersed CuO and/or Cu^{2+} ions with an octahedral environment. Robertson *et al.* [40] and Van der Grift *et al.* [37] have studied Cu-SiO_2 catalysts. These authors have demonstrated that highly dispersed CuO species are more easily reduced than bulk CuO. Based on the literature data and the XRD results, it can be concluded that the first peak is attributed to highly dispersed CuO species, while the second and third peaks are assigned to the small CuO clusters with different particle sizes. For 15% Cu-ZrO_2, it can be seen that there are four peaks. The first and second peaks at low reduction temperatures (103.07 °C and 155.92 °C) can be ascribed to well dispersed CuO, whereas the large peaks (third and fourth) at high reduction temperatures (222.87 °C and 241.71 °C) are attributed to bulk CuO. A considerable shift was observed for the high temperature peaks at high Cu loading, likely due to the weakening of the metal-support interaction.

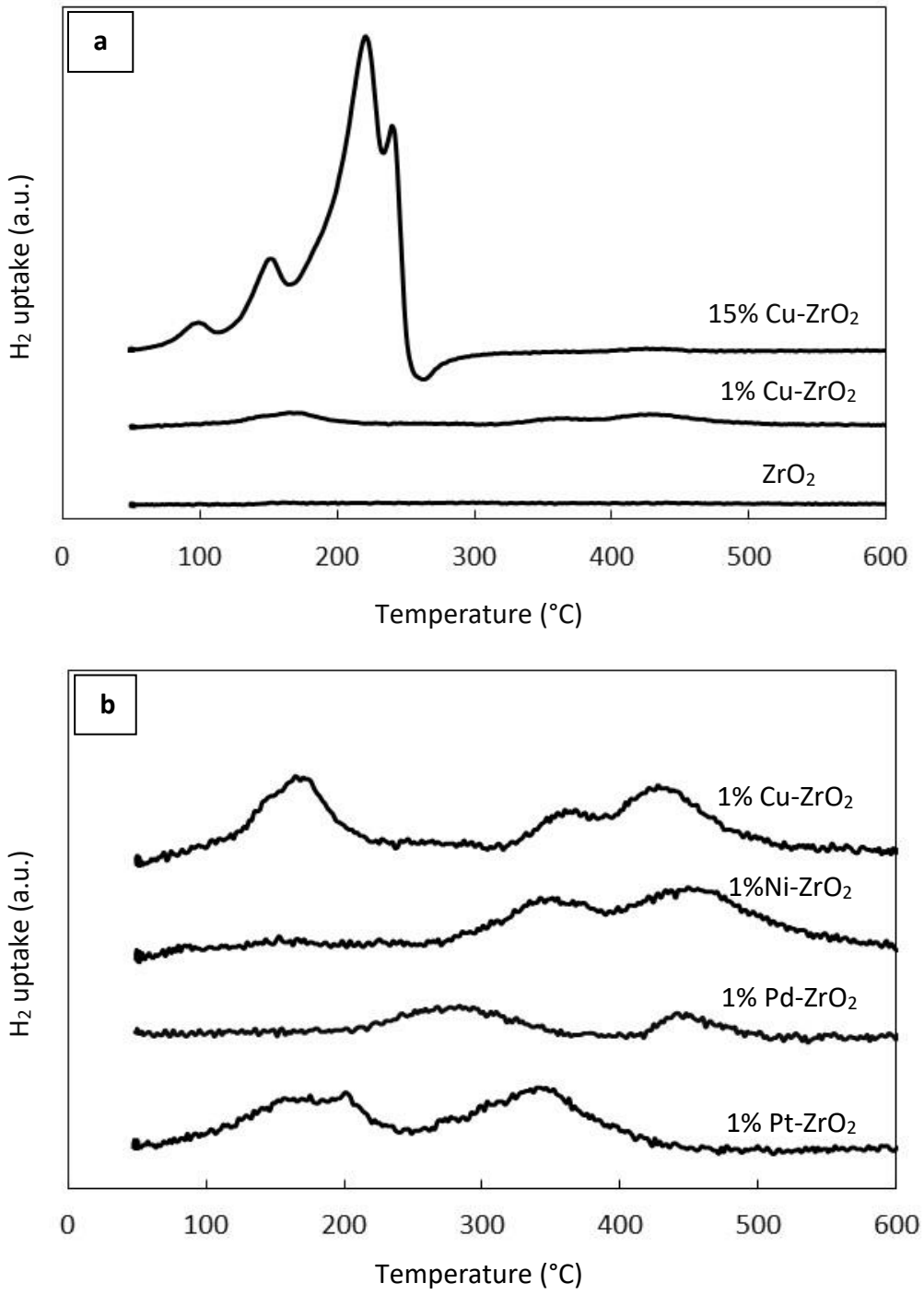

Figure 4.2. (a) (H_2-TPR) profiles of pure ZrO_2 and ZrO_2 loaded with different Cu percentages, (b) (H_2-TPR) profiles of different metals loaded on ZrO_2.

The TPR profiles of the different metals (Cu, Ni, Pt and Pd) supported over ZrO_2 are demonstrated in Figure 4.2b. For 1% Ni- ZrO_2, two peaks were distinct around 356.5 °C and 461.2 °C. The first peak at lower reduction temperatures is assigned to relatively free NiO on the surface of ZrO_2, and the second higher reduction temperature peak is attributed to NiO that interacts strongly with ZrO_2 [41–43].

Two peaks were observed for Pd-ZrO_2 which can be attributed to different interactions between Pd and the support. The first one which is centered at 279.88 °C and can be attributed to superficial PdO on the catalyst [44] while the second peak which is at a higher reduction temperature (445.76 °C) is related to the reduction of PdO clusters which interact more strongly with the support [45].

For Pt-ZrO_2, two peaks appeared centered at 179.43 °C and 344.41 °C that could be related to different dispersions of platinum. The first peak can be ascribed to the reduction of weak interaction between platinum oxide with the support while the second peak could be attributed to platinum sites with strong interaction with the support [46]. The amount of H_2 consumed for different catalysts are shown in Table 4.1.

Table 4.1. Total consumption of H_2, NH_3 and CO_2 for different catalysts.

Catalyst	H_2 uptake mmol/g	NH_3 uptake mmol/g	CO_2 uptake mmol/g
ZrO_2	_	0.12	0.053
15% Cu-ZrO_2	1.46	0.27	0.092
1% Cu-ZrO_2	0.17	0.17	0.075
1% Ni-ZrO_2	0.18	0.15	0.064
1% Pd-ZrO_2	0.05	0.16	0.071
1% Pt-ZrO_2	0.13	0.16	0.066

4.3.1.3 (NH_3-TPD) and (CO_2-TPD)

(NH_3-TPD) and (CO_2-TPD) experiments were carried out to investigate the acid-base properties of the reduced catalysts. Figure 4.3a shows the NH_3-TPD profile of pure ZrO_2, as well as the catalysts with different reduced metals (Cu, Ni, Pd and Pt) loaded on the ZrO_2, and Cu-ZrO_2 catalysts with different Cu loadings. Figure 4.3b displays the CO_2-TPD profile for the same catalysts.

As can be seen from Figure 4.3a, the broad NH_3 desorption peaks over ZrO_2 and the different supported metal catalysts at low loadings extend from 160 °C to 580 °C. Also, there is an obvious peak at 328 °C for 1% Cu-ZrO_2 while the sharp peak appeared at 270.2 °C for 15% Cu-ZrO_2 with a broad shoulder extending out to 600 °C. For all supported catalysts, the amount of acidic sites slightly increased as compared to the support alone.

A notable increase in the number of acidic sites can be seen over 15% Cu-ZrO_2 (see Table 4.1).

Figure 4.3b shows the CO_2-TPD profiles of the different catalysts. For pure ZrO_2 and 1% Pd-ZrO_2, two obvious peaks were distinct around (143.3 °C and 393 °C) and (151.32 °C and 378.21 °C), respectively. The two peaks can be indicative of different basic sites of varying strength which suggests that there are both weak and strong basic sites on these catalysts. 1% Ni-ZrO_2 exhibits one clear peak around 146.28 °C. For 1% Pt-ZrO_2 and 1% Cu-ZrO_2 catalysts, broad CO_2 desorption peaks appeared with a long tail that extend to higher desorption temperatures. Increasing the Cu loading percentage (15% Cu-ZrO_2) led to a split in the desorption peak to two peaks. The amount of basic sites were higher for supported metals catalysts than for the support. The number of moles of NH_3 and CO_2 adsorbed for different catalysts are reported in Table 4.1.

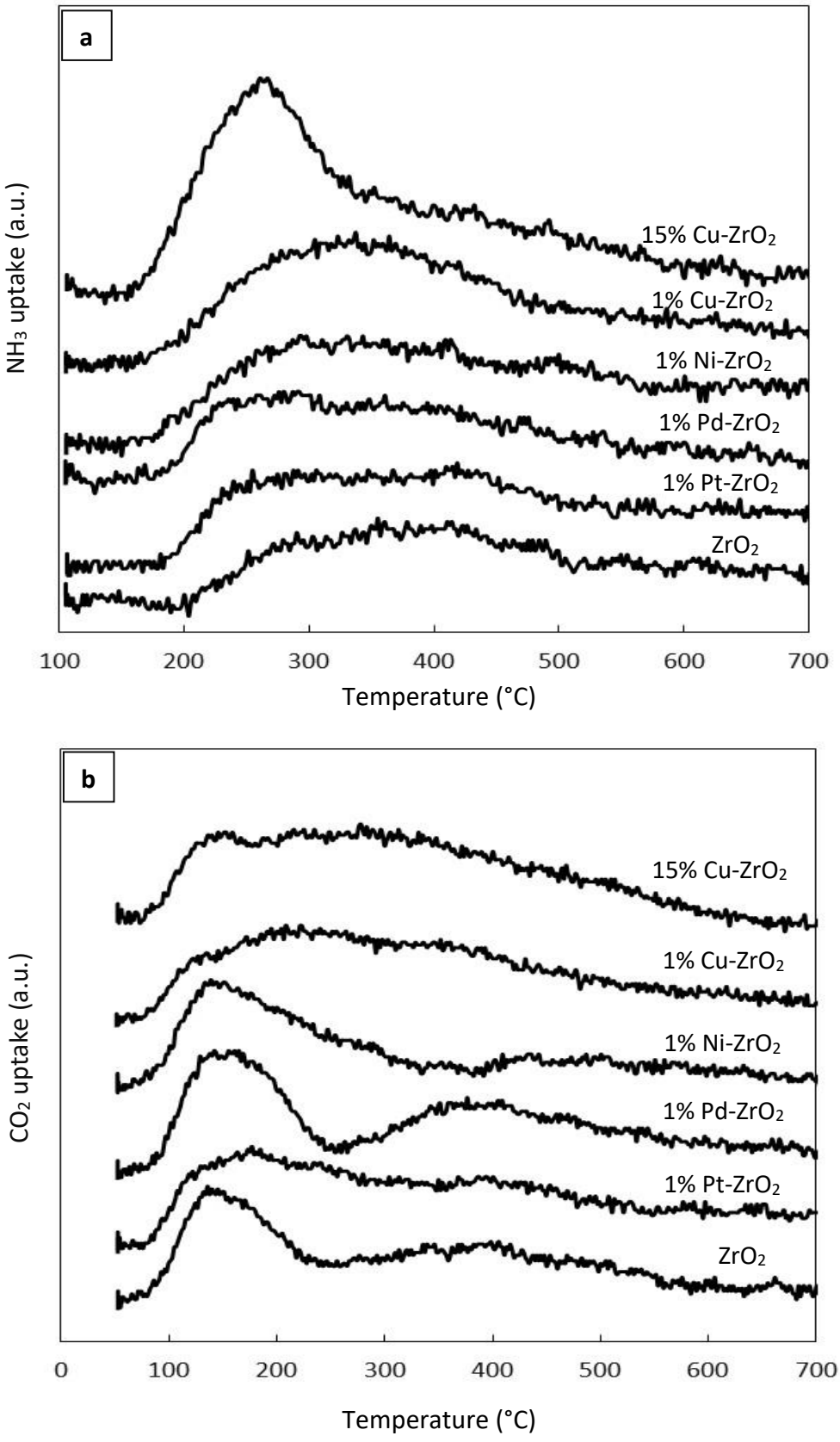

Figure 4.3. (a) (NH_3-TPD) profiles of different catalysts, (b) (CO_2-TPD) profiles of different catalysts.

4.3.2 Catalytic Reaction of MEK to Higher Ketone in a Fixed Bed Reactor

4.3.2.1 Effect of Reaction Temperature

The effect of reaction temperature on the conversion of MEK and the distribution of major products over 15% Cu-ZrO_2 was investigated for a temperature range of 140 °C to 200 °C. Figure 4.4 shows the changes in the conversion of MEK and the selectivity for different products with different reaction temperatures after one hour on stream. As can be seen from this figure, the conversion of MEK increased from 56% to 84.9% as the temperature increased from 140 °C to 200 °C**.** Also, the distribution of products was strongly affected by reaction temperature. C_8 ketone production increased to over 61% at 180 °C. Higher temperatures also led to more heavy products, including C_{12} ketones, C_{12} alcohols and C_{16} ketones. 2-butanol production was favored at lower temperatures, going from 74.5 % at 140 °C to 4.26% at 200 °C, indicating that lower temperatures favored hydrogenation of MEK to 2-butanol, while higher temperatures promoted coupling reactions.

The conversion of MEK to 2-butanol is a reversible reaction (see Figure 4.7) where the main product from the conversion of 2-butanol is MEK (the backward reaction). This means that with increasing temperature, dehydrogenation of 2-butanol to MEK is more favorable. The equilibrium constant was calculated at different temperatures using Van't Hoff Equation:

$$K_{(T)} = K_{(r)} + e^{\frac{-\Delta_f H^o}{R}\left(\frac{1}{T} - \frac{1}{T_{(r)}}\right)} \qquad \ldots\ldots (4.3)$$

where $K_{(T)}$ is the equilibrium constant at temperature T, $K_{(r)}$ is the equilibrium constant at reference temperature $T_{(r)}$ (25 °C), $\Delta_f H^o$ is the standard enthalpy of formation under standard conditions at the specified temperature (25 °C), and R is the gas constant.

The equilibrium constant decreased from 0.136 at 140 °C to 0.018 at 200 °C, explaining the trend seen in Figure 4.4 where the selectivity of 2-butanol decreases with increasing temperature.

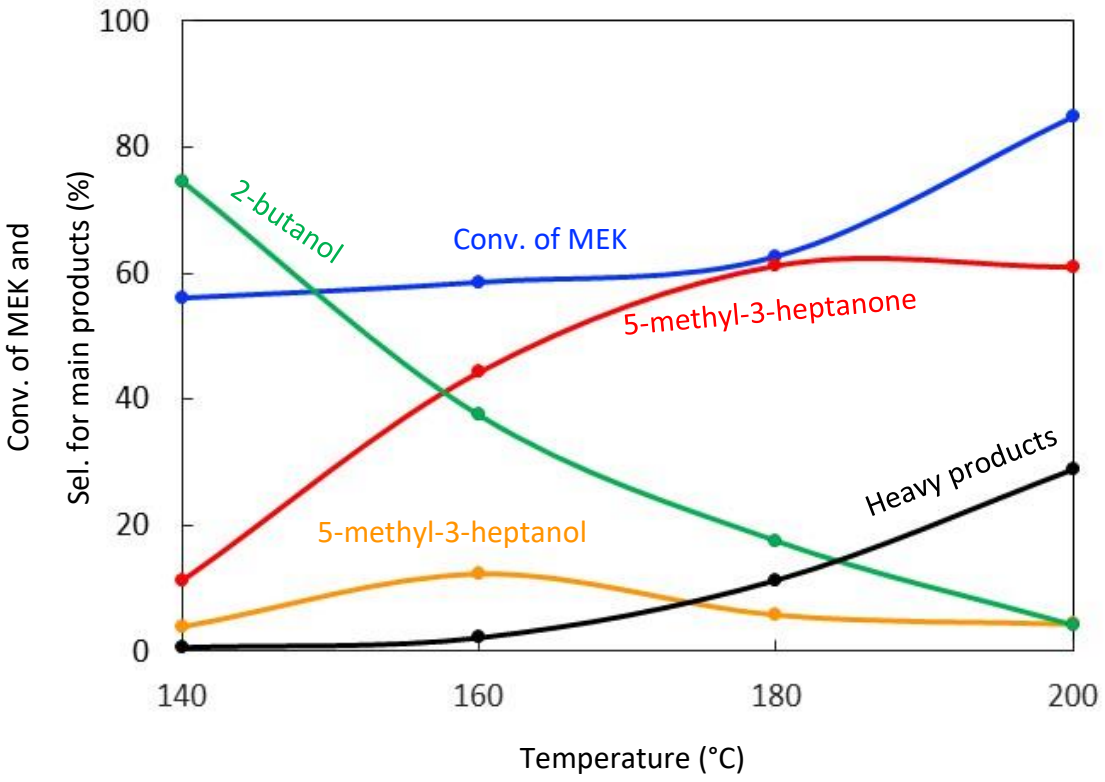

Figure 4.4. Catalytic results for the conversion of MEK to several products at different temperatures. Reaction conditions: catalyst weight, 1.0 g (15% Cu-ZrO_2); feed rate of MEK, 1.0 mL/h; H_2/MEK molar ratio, 2.

4.3.2.2 Effect of H_2/MEK Molar Ratio

Experiments were performed to study the effect of changing the molar ratio of H_2 to MEK on the conversion of MEK and the selectivity for different products over 15% Cu-ZrO_2. The results are shown in Figure 4.5. Increasing the molar ratio of H_2/MEK slightly increased the conversion of MEK, but there was a significant impact on selectivity of the catalyst on changing this ratio. It was observed that higher H_2/MEK ratios led to increased amounts of 2-butanol and lower amounts of C_8 ketones. This suggested that higher amounts of hydrogen changed the relative rates between hydrogenation and aldol condensation of MEK, leading to higher amounts of 2-butanol. Higher amounts of hydrogen also led to further hydrogenation of C_8 ketone, as evidenced by increased conversions of C_8 ketone to C_8 alcohol with increasing H_2/MEK molar ratios from 2 to 15. With increased molar ratios, C_8 ketone selectivity decreased from 61.23% to 11.2%, which was associated with increased 2-butanol from 17.6% to 75.5%. Also, it was noted that the amount of heavy products produced decreased from 11.34% to 0% with excess hydrogen.

As seen in Figure 4.5, the selectivity for C_8 ketone increased while conversion was fairly flat as the H_2/MEK ratio decreased. This begs the question of whether removing hydrogen would further improve the C_8 ketone yield. For this reason, an experiment was conducted without H_2 (H_2/MEK molar ratio=0) (not shown in the figure). For this experiment, MEK conversion was quite low: less than 15%. The main products that formed were condensation products like cyclic trimers and aromatics (39%), MVK resulting from dehydrogenation of MEK (27%), and unsaturated ketones (20%).

Interestingly, C_8 ketone was formed (13.5%) that should result from hydrogenation of unsaturated C_8 ketone even though there was no hydrogen in the feed. It is hypothesized that the H_2 formed from the dehydrogenation of MEK to MVK was responsible for the hydrogenation reaction leading to produce C_8 ketone.

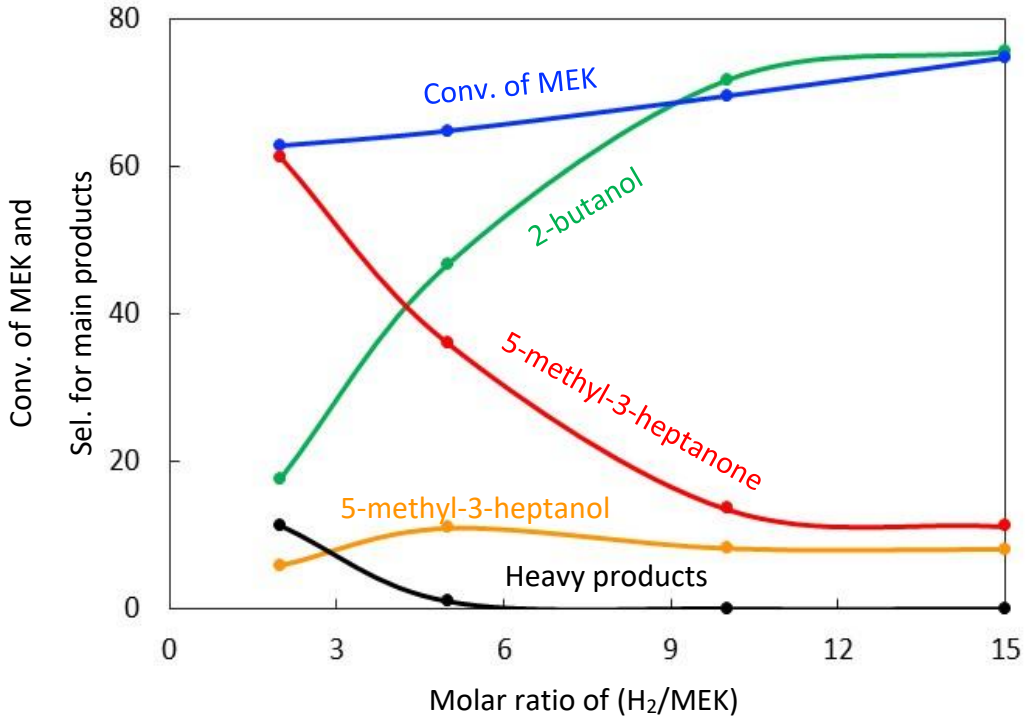

Figure 4.5. Catalytic results for the conversion of MEK to the main products with different H_2/MEK molar ratios. Reaction conditions: catalyst weight, 1.0 g (15% Cu- ZrO_2); feed rate of MEK, 1.0 mL/h; reaction temperature, 180 °C.

4.3.2.3 Effect of Space Time

The effect of space time (W/FA_0 where W is the weight of catalyst (g), and FA_0 is the molar flow rate of MEK (mol. h^{-1})) was evaluated to better understand the reaction mechanism of MEK. Figure 4.6 shows the change in conversion of MEK and the distribution of products over 15 wt% Cu-ZrO_2 with changing of space times at a feed rate

of MEK of 1 mL/h in the presence of H_2 at 180 °C after 1 h. As can been seen, the conversion of MEK increased from 46.8 % to 74.2% when the space time increased from 17.7 to 115.5 g.mol^{-1}.h. The selectivity for C_8 ketone increased with increasing space time, reaching a maximum of 61.2% when the space time W/FA_0 was 88.8 g.mol^{-1}.h, then decreased as the selectivity for heavy products increased. For low space times, MEK was hydrogenated to produce 2-butanol with a selectivity above 48%. 2-butanol selectivity decreased with increasing space times to reach about 12.8% at a space time of 115.5 g. mol^{-1}.h. MVK was produced as a result of dehydrogenation of MEK at low space times but its selectivity decreased with increasing space times.

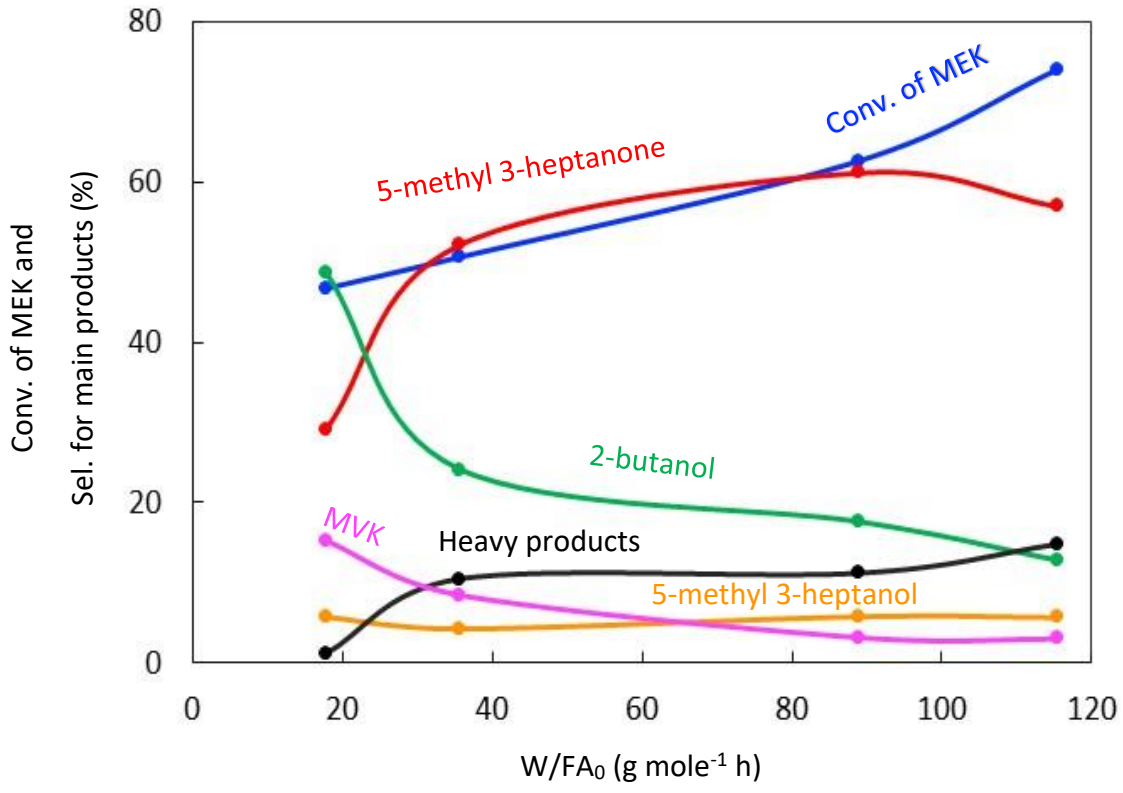

Figure 4.6. Catalytic results for the conversion of MEK to several products with different space times after 1 h of the reaction. Reaction conditions: catalyst weight, 1.0 g (15 wt% Cu-ZrO_2); feed rate of MEK, 1.0 mL/h; H_2/MEK molar ratio, 2; reaction temperature, 180 °C.

The results in Figure 4.6 could be interpreted to imply that 2-butanol is a key intermediate in producing C_8 ketones: 2-butanol was the most prevalent product at low space times, but its selectivity decreased as space time increased in favor of 5-methyl-3-heptanone. It is possible that C_8 ketone resulted from the Guerbet condensation [47,48] of 2-butanol followed by dehydrogenation of C_8 alcohol. For these reasons, the reaction of 2-butanol on 15 wt% Cu-ZrO_2 was carried out with different space times. As can be seen from Figure 4.7, the conversion of 2-butanol increased from 36.9% to 76.4% with increasing space times from 3.6 to 91 g mol^{-1} h. However, the selectivity of MEK produced from dehydrogenation of 2-butanol decreased with increasing space times from 86.7% to 53.4% and was associated with increasing C_8 ketone from 0% to 30%. This suggests that MEK was responsible for producing C_8 ketone instead of obtaining C_8 ketone from 2-butanol directly via a Guerbet condensation. It is also important to note that at low space times, where mainly primary reactions should occur, no C_8 ketones or alcohols were detected. MVK and 2,3 BDO were detected at low space times as a result of dehydrogenation and hydration of MEK, respectively, and both decreased with increasing space times.

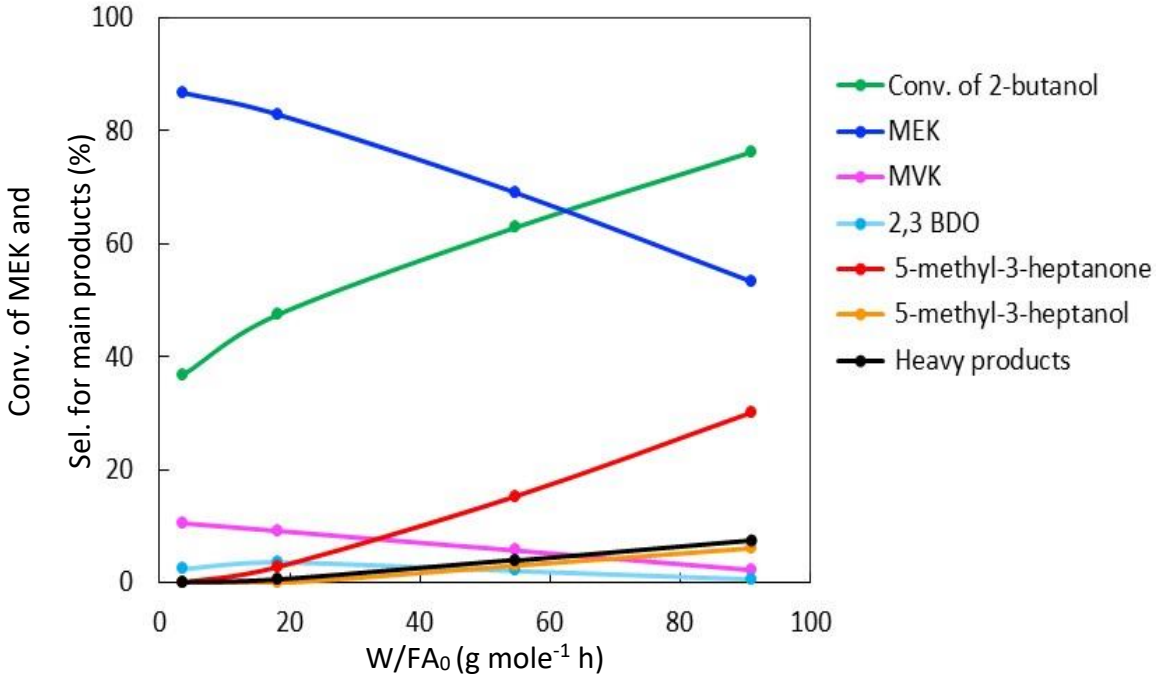

Figure 4.7. Catalytic results for the conversion of 2-butanol to a variety of products with different space time after 1 h of the reaction. Reaction conditions: catalyst weight, 1.0 g (15 wt% Cu-ZrO_2); feed rate of 2-butanol, 1.0 mL/h; H_2/2-butanol molar ratio, 2; reaction temperature, 180 °C.

4.3.2.4 Effect of Copper Loading on the Support

The effect of copper loading was investigated by conducting experiments with just the support (ZrO_2) and with copper supported on it at high and low loadings (15% and 1%). Table 4.2 shows that only minor amounts of C_8 ketone were obtained from MEK condensation over pure ZrO_2. However, heavy products were obtained like cyclic trimers and aromatics. The selectivity for C_8 ketone increased dramatically when the reaction was conducted over 1% Cu-ZrO_2. It is believed that adding Cu on ZrO_2 facilitates the hydrogenation of C=C bonds in α,β-unsaturated C_8 ketone immediately after the dimeric condensates form preventing the dimer condensates from undergoing conjugate addition

with ketone enolates to produce heavy condensation products. Increasing the percentage of Cu supported on ZrO_2 from 1 wt % to 15 wt % did not have an important impact on the distribution of products where the amount of C_8 ketone actually decreased from 63.48% to 61.23% with an increased percentage of copper loaded on the support along with increased production of 2-butanol and C_8 alcohol. However, it was obvious that increasing this percentage led to decreased MEK conversions probably because the hydrogenation of MEK is reversible, while condensation is not. With more copper, MEK can be hydrogenated to 2-butanol, but then the 2-butanol can be dehydrogenated to MEK. This makes it look like less MEK was converted as illustrated in Figure 4.7. The conversion of MEK and the distribution of major products are shown in Table 4.2.

Table 4.2. Catalytic activity for the conversion of MEK to a desirable product (C_8 ketone) over several catalysts.

Catalysts	Conv. of MEK (%)	Sel. for 2-butanol (%)	Sel. for C_8 ketone (%)	Sel. for C_8 alcohol (%)	Others (%)
ZrO_2	26.1	0	5	0	95[a]
1%Cu-ZrO_2	78.38	12.09	63.48	7.43	17[b]
15%Cu-ZrO_2	62.7	17.6	61.23	5.87	15.3[b]

[a] Others include MVK, unsaturated C_8 ketone, cyclic trimers condensate and aromatics.
[b] Others include C_{12} ketone, C_{12} alcohol and condensation products.

4.3.2.5 Reaction of MEK over Different Metals Loaded on ZrO_2

Different metals (Cu, Ni, Pd and Pt) supported on ZrO_2 were investigated in this chapter to see the effect of the metal on catalytic performance. The conversion of MEK and the distribution of products after 1 h using 1 g of the catalyst are shown in Figure 4.8.

As seen in this figure, all four catalysts gave similar results. All four produced 5-methyl-3-heptanone as the main product, with smaller amounts of 5-methyl-3-heptanol and 2-butanol. The main difference was in the conversion of MEK. Perhaps surprisingly, the conversion of MEK was highest on Ni-ZrO_2 and Cu-ZrO_2 (82% and 78%, respectively). Pt-ZrO_2 and Pd-ZrO_2, which would be expected to be the most active hydrogenation catalysts, both yielded MEK conversion of ~65%.

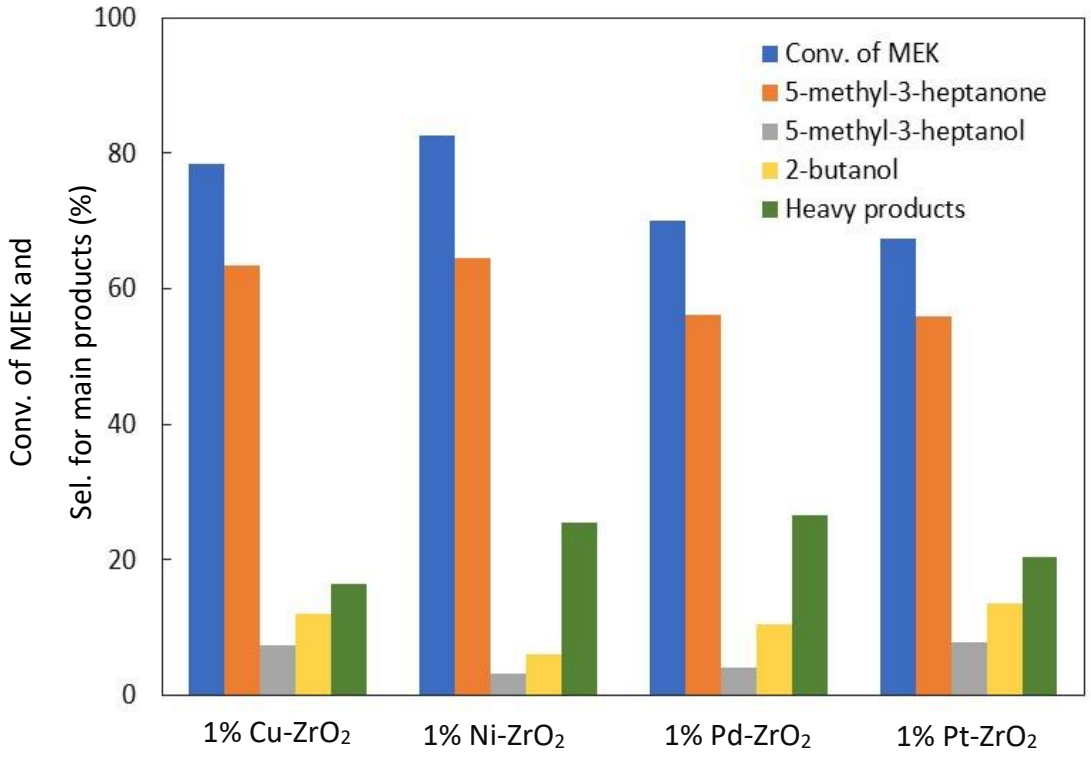

Figure 4.8. Catalytic results for the conversion of MEK to a variety of products over different catalysts. Reaction conditions: catalyst weight, 1.0 g; feed rate of MEK, 1.0 mL/h; H_2/MEK molar ratio, 2; reaction temperature, 180 °C.

We hypothesize that the trend in MEK conversion is attributed to metal hydrogenation activity, but not in the expected way. Reaction of MEK on these multifunctional catalysts is due to multiple reaction pathways, which is detailed in

Scheme 4.1. The metal sites catalyze MEK hydrogenation to 2-butanol, while the ZrO_2 support catalyzes Aldol condensation of MEK to an α,β-unsaturated C_8 ketone (5-methyl-3-heptenone). Subsequently, hydrogenation of the α,β-unsaturated C_8 ketone over metal sites produces the saturated C_8 ketone and, further, a C_8 alcohol. Hydrogenation of MEK to 2-butanol is believed to be reversible, and 2-butanol is not expected to be converted further to other products. For this reason, the lower MEK conversion noted for Pt and Pd catalysts may actually represent higher activity for those metals: they are more active in converting MEK to 2-butanol, and 2-butanol back to MEK. The aldol condensation reaction on ZrO_2 is, therefore, decreased and the ultimate C_8 ketone yield is decreased.

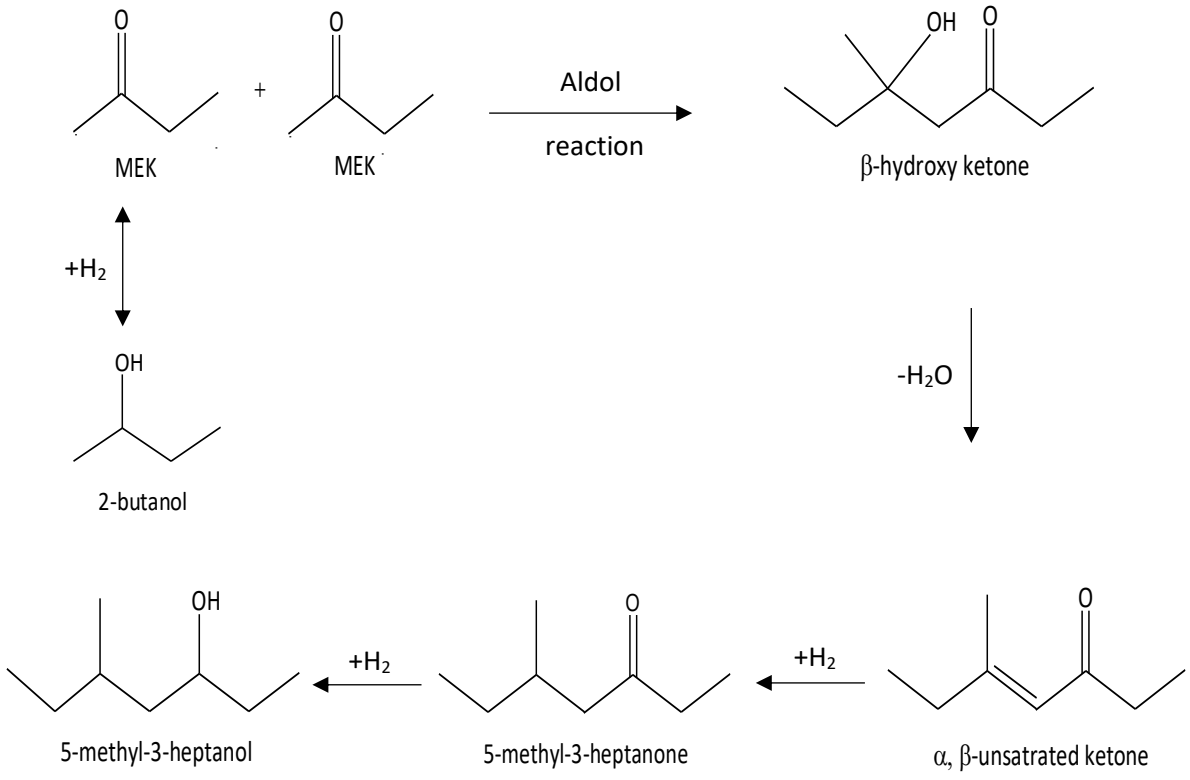

Scheme 4.1. The potential reaction pathways in the reaction of MEK to C_8 ketone and C_8 alcohol

4.4 Conclusion

The conversion of MEK to 5-methyl-3-heptenone in one step has been demonstrated over Cu-ZrO_2. Temperature and H_2/MEK molar ratio play a significant role in the selectivity of the catalyst. The selectivity for C_8 ketone increased with increasing temperature while at lower temperatures hydrogenation of MEK was favored, leading to increased production of 2-butanol. In addition, it was found that with increasing H_2/MEK molar ratio, 2-butanol production increased, limiting the aldol condensation of MEK and decreasing the selectivity for C_8 ketone. Also, the results showed that using Cu-ZrO_2 at low loadings of Cu (1 wt%) led to an increase in the conversion of MEK and a higher selectivity for C_8 ketone. Catalytic results were similar for four different supported metals (Cu, Ni, Pd and Pt) supported on ZrO_2, suggesting that all the metals catalyzed the same catalytic routes in generating 5-methyl-3-heptenone as the main product.

Acknowledgements

Higher Committee for Education Development in Iraq (HCED) is gratefully acknowledged in addition to the financial support from Navy SBIR Phase II Contr #NG8335, in collaboration with TekHolding, Inc.

References

1. Yoshikawa, N.; Yamada, Y. M. A.; Das, J.; Sasai, H.; Shibasaki, M. Direct catalytic asymmetric aldol reaction. *J. Am. Chem. Soc.* **1999**, *121*, 4168–4178.

2. Roelofs, J.; van Dillen, A. J.; Jong, K. P. De Base-catalyzed condensation of citral and acetone at low temperature using modified hydrotalcite catalysts. *Catal. Today* **2000**, *60*, 297–303.

3. Cosimo, J. I. Di; Diez, V. K.; Apesteguía, C. R. Base catalysis for the synthesis of α,β-unsaturated ketones from the vapor-phase aldol condensation of acetone. *Appl. Catal. A Gen.* **1996**, *137*, 149–166.

4. Nielsen, A. T.; Houlihan, W. J. The aldol condensation. *Org. React.* **1968**, 16, pp 2–3.

5. Kelly, G. J. Aldol condensation reaction and catalyst therefor. U.S. patent No. 6,706,928. **2004.**

6. Melo, L.; Giannetto, G.; Alvarez, F.; Magnoux, P.; Guisnet, M. Effect of the metallic/acid site (nPt/nA) ratio on the transformation of acetone towards methyl isobutyl ketone. *Catal. Letters.* **1997**, *44*, 201–204.

7. Reichle, W. T. Catalytic aldol condensations. U.S. patent No. 4,165,339. **1979.**

8. Vannice, M. A.; Sen, B. Metal-support effects on the intramolecular selectivity of crotonaldehyde hydrogenation over platinum. *J. Catal.* **1989**, *115*, 65–78.

9. Claus, P. Selective hydrogenation of α,β-unsaturated aldehydes and other C=O and C=C bonds containing compounds. *Top. Catal.* **1998**, *5*, 51–62.

10. Zhu, L.; Lu, J. Q.; Chen, P.; Hong, X.; Xie, G. Q.; Hu, G. S.; Luo, M. F. A comparative study on Pt/CeO_2 and Pt/ZrO_2 catalysts for crotonaldehyde hydrogenation. *J. Mol. Catal. A Chem.* **2012**, *361*, 52–57.

11. Gallezot, P.; Richard, D. Selective hydrogenation of α,β-unsaturated aldehydes. *Catal. Rev.* **1998**, *40*, 81–126.

12. Mohr, C.; Claus, P. Hydrogenation properties of supported nanosized gold particles. *Sci. Prog.* **2001**, *84*, 311–334.

13. Sul'man, E. Selective hydrogenation of unsaturated ketones and acetylene alcohols. *Russ. Chem. Rev.* **1994**, *63*, 923–936.

14. Szöllősi, G.; Mastalir, A.; Molnár, Á.; Bartók, M. Hydrogenation of α,β-unsaturated ketones on metal catalysts. *React. Kinet. Catal. Lett.* **1996**, *57*, 29–36.

15. Ravasio, N.; Antenori, M.; Gargano, M.; Rossi, M. Chemoselectivity and regioselectivity in the hydrogenation of α,β-unsaturated carbonyl compounds promoted by Cu/Al_2O_3. *J. Mol. Catal.* **1992**, *74*, 267–274.

16. Ravasio, N.; Antenori, M.; Gargano, M.; Mastrorilli, P. $CuSiO_2$: an improved catalyst for the chemoselective hydrogenation of α,β-unsaturated ketones. *Tetrahedron Lett.* **1996**, *37*, 3529–3532.

17. Molnár, Á.; Bucsi, I.; Bartók, M. Pinacol Rearrangement on Zeolites. *Stud. Surf. Sci. Catal.* **1988**, *41*, 203–210.

18. Multer, A.; McGraw, N.; Hohn, K.; Vadlani, P. Production of methyl ethyl ketone from biomass using a hybrid biochemical/catalytic approach. *Ind. Eng. Chem. Res.* **2012**, *52*, 56–60.

19. Emerson, R. R.; Flickinger, M. C.; Tsao, G. T. Kinetics of dehydration of aqueous 2,3-butanediol to methyl ethyl ketone. *Ind. Eng. Chem. Prod. Res. Dev.* **1982**, *21*, 473–477.

20. Zhang, W.; Yu, D.; Ji, X.; Huang, H. Efficient dehydration of bio-based 2,3-butanediol to butanone over boric acid modified HZSM-5 zeolites. *Green Chem.* **2012**, *14*, 3441–3450.

21. Bucsi, I.; Molnár, Á.; Bartók, M.; Olah, G. A. Transformation of 1,2-diols over perfluorinated resinsulfonic acids (Nafion-H). *Tetrahedron* **1994**, *50*, 8195–8202.

22. Török, B.; Bucsi, I.; Beregszászi, T.; Kapocsi, I.; Molnár, Á. Transformation of diols in the presence of heteropoly acids under homogeneous and heterogeneous conditions. *J. Mol. Catal. A Chem.* **1996**, *107*, 305–311.

23. Nikitina, M. A.; Ivanova, I. I. Conversion of 2,3-Butanediol over Phosphate Catalysts. *ChemCatChem* **2016**, 8, 1346–1353.

24. Lee, J.; Grutzner, J. B.; Walters, W. E.; Delgass, W. N. The conversion of 2,3-butanediol to methyl ethyl ketone over zeolites. *Stud. Surf. Sci. Catal.* **2000**, *130*, 2603–2608.

25. Yu, E. K.; Saddler, J. N. Fed-batch approach to production of 2,3-butanediol by Klebsiella pneumoniae grown on high substrate concentrations. *Appl. Environ. Microbiol.* **1983**, *46*, 630–635.

26. Zeng, A. P.; Biebl, H.; Deckwer, W. D. Effect of pH and acetic acid on growth and 2,3-butanediol production of Enterobacter aerogenes in continuous culture. *Appl. Microbiol. Biotechnol.* **1990**, *33*, 485–489.

27. Mas, C. De; Jansen, N. B.; Tsao, G. T. Production of optically active 2,3-butanediol by Bacillus polymyxa. *Biotechnol. Bioeng.* **1988**, *31*, 366–377.

28. Ledingham, G. A.; Neish, A. C. Fermentative Production of 2,3 Butanediol Industrial Fermentations, LA Underkofler and RJ Hickey, Eds. **1954**, 2, pp 27–93.

29. Jansen, N. B.; Flickinger, M. C.; Tsao, G. T. Production of 2,3-butanediol from D-xylose by Klebsiella oxytoca ATCC 8724. *Biotechnol. Bioeng.* **1984**, *26*, 362–369.

30. Qureshi, N.; Cheryan, M. Effects of aeration on 2,3-butanediol production from glucose by Klebsiella oxytoca. *J. Ferment. Bioeng.* **1989**, *67*, 415–418.

31. Ji, X. J.; Huang, H.; Du, J.; Zhu, J. G.; Ren, L. J.; Hu, N.; Li, S. Enhanced 2,3-butanediol production by Klebsiella oxytoca using a two-stage agitation speed control strategy. *Bioresour. Technol.* **2009**, *100*, 3410–3414.

32. Saha, B. C.; Bothast, R. J. Production of 2,3-butanediol by newly isolated Enterobacter cloacae. *Appl. Microbiol. Biotechnol.* **1999**, *52*, 321–326.

33. Hattori, H. Heterogeneous basic catalysis. *Chem. Rev.* **1995**, *95*, 537–558.

34. Yamaguchi, T.; Nakano, Y.; Iizuka, T.; Tanabe, K. Catalytic activity of ZrO_2 and ThO_2 for HD exchange reaction between methyl group of adsorbed isopropyl alcohol-d8 and surface OH group. *Chem. Lett.* **1976**, 677–678.

35. Chary, K. V. R.; Sagar, G. V.; Srikanth, C. S.; Rao, V. V. Characterization and catalytic functionalities of copper oxide catalysts supported on zirconia. *J. Phys. Chem. B.* **2007**, *111*, 543–550.

36. Sagar, G. V.; Rao, P. V. R.; Srikanth, C. S.; Chary, K. V. R. Dispersion and Reactivity of Copper Catalysts Supported on Al_2O_3–ZrO_2. *J. Phys. Chem. B.* **2006**, *110*, 13881–13888.

37. der Grift, C. J. G. Van; Mulder, A.; Geus, J. W. Characterization of silica-supported copper catalysts by means of temperature-programmed reduction. *Appl. Catal.* **1990**, *60*, 181–192.

38. Shimokawabe, M.; Asakawa, H.; Takezawa, N. Characterization of copper/zirconia catalysts prepared by an impregnation method. *Appl. Catal.* **1990**, *59*, 45–58.

39. Dow, W. P.; Wang, Y. P.; Huang, T. J. Yttria-stabilized zirconia supported copper oxide catalyst: I. Effect of oxygen vacancy of support on copper oxide reduction. *J. Catal.* **1996**, *160*, 155–170.

40. Robertson, S. D.; McNicol, B. D.; De Baas, J. H.; Kloet, S. C.; Jenkins, J. W.

Determination of reducibility and identification of alloying in copper-nickel-on-silica catalysts by temperature-programmed reduction. *J. Catal.* **1975**, *37*, 424–431.

41. Roh, H. S.; Jun, K. W.; Dong, W. S.; Chang, J. S.; Park, S. E.; Joe, Y. I. Highly active and stable Ni/Ce–ZrO_2 catalyst for H_2 production from methane. *J. Mol. Catal. A Chem.* **2002**, *181*, 137–142.

42. Song, Y. Q.; Liu, H. M.; He, D. H. Effects of hydrothermal conditions of ZrO_2 on catalyst properties and catalytic performances of Ni/ZrO_2 in the partial oxidation of methane. *Energy & Fuels.* **2010**, *24*, 2817–2824.

43. Sun, L.; Tan, Y.; Zhang, Q.; Xie, H.; Han, Y. Tri-reforming of coal bed methane to syngas over the Ni-Mg-ZrO_2 catalyst. *J. Fuel Chem. Technol.* **2012**, *40*, 831–837.

44. Chen, S.; Luo, L.; Cheng, X. Influence of preparation method on the performance of Pd/ZrO_2-Al_2O_3 catalysts for HDS. **2009**, 16, 272–277.

45. Ivanova, A. S.; Slavinskaya, E. M.; Gulyaev, R. V; Zaikovskii, V. I.; Stonkus, O. A.; Danilova, I. G.; Plyasova, L. M.; Polukhina, I. A.; Boronin, A. I. Metal–support interactions in Pt/Al_2O_3 and Pd/Al_2O_3 catalysts for CO oxidation. *Appl. Catal. B Environ.* **2010**, *97*, 57–71.

46. Lee, H. C.; Lee, D.; Lim, O. Y.; Kim, S.; Kim, Y. T.; Ko, E. Y.; Park, E. D. ZrO_2-supported Pt catalysts for water gas shift reaction and their non-pyrophoric property. Stud Surf Sci Catal. **2007**, 167, 201–206.

47. Kozlowski, J. T.; Davis, R. J. Heterogeneous catalysts for the Guerbet coupling of alcohols. *ACS Catal.* **2013**, *3*, 1588–1600.

48. Gabriëls, D.; Hernández, W. Y.; Sels, B.; Voort, P. Van Der; Verberckmoes, A. Review of catalytic systems and thermodynamics for the Guerbet condensation reaction and challenges for biomass valorization. *Catal. Sci. Technol.* **2015**, *5*, 3876–3902.

Chapter 5 - Conversion of 5-methyl-3-heptanone to C_8 Alkenes and Alkane over Bifunctional Catalysts

As a part of provisional patent application titled: "**Method for converting unsymmetrical and/or symmetrical ketones to higher hydrocarbons**"

Abstract

A one-step catalytic process has been used to produce a mixture of 5-methyl-3-heptene, 5-methyl-2-heptene (C_8 alkene) and 3-methyl heptane (C_8 alkane) from 5-methyl-3-heptanone (C_8 ketone) via hydrogenation-dehydration reactions. The C_8 ketone is hydrogenated to 5-methyl-3-heptanol over metal sites, followed by dehydration of 5-methyl-3-heptanol on acidic sites to obtain a mixture of C_8 alkenes. These C_8 alkenes can be further hydrogenated on metal sites to make a C_8 alkane. Conversion of C_8 ketone to the desired products was achieved over single bed of a supported catalyst consisting of one transition metal (Cu or Pt) loaded on alumina (Al_2O_3) as a bifunctional heterogeneous catalyst.

The experiments were conducted under mild operating conditions (reaction temperatures were varied between 180 °C to 260 °C and the pressure was 1 atm) with high conversions of reactant and selectivity for the desired products. Experimental results showed that the main products over 20% Cu-Al_2O_3 were a mixture of 5-methyl-3-heptene, 5-methyl-2-heptene in addition to 3-methyl heptane in different amounts depending on the operating conditions. However, using 1% Pt-Al_2O_3 the major product was 3-methyl heptane with a selectivity up to 97% and a conversion of 99.9%. Both reaction temperature and the hydrogen pressure played an important role in the catalytic chemistry. Over 20% Cu-Al_2O_3, it was observed that increasing the reaction temperature led to an increase in the selectivity for C_8 alkane as a result of hydrogenation of C_8 alkenes. Also, it was observed that with increasing H_2/C_8 ketone molar ratio, C_8 alkane selectivity increased. However, when this ratio was decreased, the hydrogenation of C_8 alkenes to C_8 alkane was reduced. The highest selectivity for C_8 alkenes (81.7%) was obtained at 220

°C and a H_2/C_8 ketone ratio of 2. Both conversion and the selectivity for the main products decreased when less copper, 1% Cu-Al_2O_3, was used. Over 1% Pt-Al_2O_3, C_8 alkanes were the major products at different temperatures indicating that the further hydrogenation reaction of C_8 alkenes was promoted. At low temperatures, for both Cu-Al_2O_3 and Pt-Al_2O_3, significant amounts of C_8 alcohols were formed because subsequent reactions did not proceed at a fast enough rate. However, with 1% Pt-Al_2O_3 the main product was still C_8 alkane at all H_2/C_8 ketone ratios.

Key Words

Hydrogenation-dehydration reactions, bifunctional catalyst, Cu supported on Al_2O_3, Pt supported on Al_2O_3, 5-methyl-3-heptanone.

5.1 Introduction

Recently, significant effort has been devoted to the development of alternative pathways of producing biofuel and chemicals from biomass as a sustainable source because of declining petroleum resources and rising oil prices. Synthesizing fuel-range hydrocarbons from biomass is of particular interest because it offers the potential for a drop-in replacement of petroleum-based fuels. A number of different routes have been considered for such a conversion of biomass to biofuel and chemicals. For instance, furanic compounds like furfural and hydroxymethyl furfural (HMF) can be produced from the dehydration of aqueous solutions of sugar (xylose and fructose) with high selectivity (90%) [1,2]. These furanic aldehydes can be converted to large hydrocarbons via aldol

condensation reactions followed by hydrogenation-dehydration reactions. Another intermediate compound is levulinic acid, produced from the treatment of lignocellulosic biomass with acidic solutions. This acid undergoes catalytic reduction to produce γ-valerolactone, an intermediate for the production of nonane which is appropriate for diesel fuel or branched alkanes suitable for jet fuel. In addition, γ-valerolactone can be converted to butene and CO_2, as well as dimerized and oligomerized to produce higher alkenes [3].

This chapter envisions that fuel-range hydrocarbons can be produced with a C_8 ketone as the key intermediate. 5-methyl-3-heptanone is produced by dehydrating 2,3 butanediol (2,3 BDO), which can be produced in high yields from biomass-derived sugars [4–11], to methyl ethyl ketone (MEK) [12–19] followed by aldol condensation and hydrogenation reactions [20]. This C_8 ketone can then be converted to C_8 alkenes and C_8 alkanes, which can be used as gasoline blended components. This work extends previous work in our laboratory to convert 2,3 BDO and MEK to light alkenes (butene) [21–23], an intermediate to higher alkenes, and MEK to chemicals such as C_8 ketone [24].

Hydrodeoxygenation of C_8 ketones to C_8 alkenes and C_8 alkanes requires removing an oxygen atom from the ketone, for example by hydrogenation of the C=O bond via metal sites followed by dehydration of the produced alcohol by acidic sites. C=O hydrogenation catalysts also have high hydrogenation activity of C=C bonds, causing the produced C=C bonds (alkene) to be further hydrogenated to alkane. An exception is Cu which is relatively inactive for the hydrogenolysis of C–C bonds [25].

A variety of metals, including Pt, Ru, Rh, Ni, Cu, catalyze the hydrogenation of carbonyl groups [26]. Cu [26–29] and Pt [30–33] based catalysts have been extensively studied for the hydrogenation of carbonyl groups. For example, Nagaraja *et al*. [28] reported the hydrogenation of furfural to furfuryl alcohol over a Cu-MgO catalyst made with different methods (coprecipitation, impregnated and solid–solid wetting) at atmospheric pressure. The results showed that high conversions of furfural (98%) and high selectivity for furfuryl alcohol (98%) could be obtained over Cu-MgO prepared by a coprecipitation method. Fan *et al.* [26] investigated Cu-γAl_2O_3 and Ni-γAl_2O_3 to hydrogenate 2,2,6,6-tetramethylpiperidin-4-one to 2,2,6,6 tetramethylpiperidin-4-ol at 140 °C. The results demonstrated that Cu-γAl_2O_3 gave much better activity and selectivity than Ni-γAl_2O_3. They also studied the effect of introducing Cr into Cu-γAl_2O_3 and found that Cu-Cr/γAl_2O_3 displayed better catalytic performance over Cu-γAl_2O_3. Poondi *et al.* [30] studied the hydrogenation of phenylacetaldehyde over Pt loaded on different supports (TiO_2, SiO_2 and Al_2O_3). The selectivity for 2-phenylethanol increased remarkably over Pt-TiO_2, giving 70% selectivity at conversions of 60%. Vannice *et al.* [32] investigated Pt supported on various supports (TiO_2, SiO_2 and Al_2O_3) for the hydrogenation of benzaldehyde to benzyl alcohol. The most active catalyst among all the Pt catalysts was Pt-TiO_2 giving a selectivity for benzyl alcohol of 100% and a conversion up to at least 80%.

Al_2O_3 is a traditional choice for alcohol dehydration [34–36] and has been well known for centuries [37]. Kostestkyy *et al.* [38] studied the dehydration of simple alcohols such as 1-propanol, 2-propanol and 2-methyl-2-propanol on TiO_2, ZrO_2 and γAl_2O_3 oxide

catalysts. They reported that γAl_2O_3 is more active in catalyzing the dehydration reactions than either TiO_2 or ZrO_2.

It is well known that the hydrodeoxygenation of ketones to alkanes is a significant reaction in the production of biofuels [39]. However, hydrodeoxygenation reactions are seldom used in industrial chemistry, and the development of successful catalytic systems has been explored only in recent years.

Ma *et al.* [40] investigated the hydrodeoxygenation of hypnone to phenylethane over different catalysts (Ni-γAl_2O_3, Cu-γAl_2O_3 and Cu-Cr/γAl_2O_3) at 200 °C. They found that the catalytic performance of Cu-γAl_2O_3 was better than Ni-γAl_2O_3 and its activity can be improved by adding Cr to it. Kong *et al.* [41] investigated the hydrodeoxygenation of cyclohexanone to cyclohexane using Ni loaded on (γAl_2O_3, parent HZSM-5 (HZSM-5-P) and alkali-treated HZSM-5 (HZSM-5-At)) at a reaction temperature 160 °C and under a H_2 pressure of 2 MPa. The highest selectivity was obtained over Ni-HZSM-5-At (above 99 %) while the lowest selectivity of cyclohexane was 7.3% over Ni-γAl_2O_3 as a result of poor dehydration of cyclohexanol, as an intermediate compound, produced with a selectivity that reached 83.7%. Yang *et al.* [42] studied the hydrodeoxygenation of 2-cyclopentylidene cyclopentanone, produced via the self-condensation of cyclopentanone [43–47], to bi-cyclopentane (bicyclopentyl) in a flow system at 230 °C. Higher yields of bicyclopentyl (≥90%) were obtained using Pd/SiO2 and Ni/SiO2 than Pd/SiO_2-Al_2O_3, Pd/H-zeolites (H-beta, H-ZSM-5), and Pd/zirconium phosphate, more acidic supports, which gave about ~80% yield at 230 °C.

The present chapter involves using a one-step catalytic process to produce 5-methyl-3-heptene, 5-methyl-2-heptene (C_8 alkenes) and 3-methyl-heptane (C_8 alkane) from biomass-derived 5-methyl-3-heptanone (C_8 ketone). The reaction uses a heterogenous catalyst comprised of a transition metal (Cu or Pt) loaded on Al_2O_3, chosen based on the above literature. This catalyst functions as a bifunctional catalyst with both hydrogenation and dehydration activity. This chapter shows that this approach can be quite selective to C_8 alkenes and C_8 alkane in the presence of hydrogen under mild operation conditions (reaction temperature between 180 °C to 260 °C and a pressure of 1 atm) in a single stage.

5.2 Experimental Work

5.2.1 Materials

5-methyl-3-heptanone was purchased from Tokyo Chemical Industry (TCI). The copper precursor (copper(II) nitrate tri-hydrate [$Cu(NO_3)_2 \cdot 3H_2O$ (99%)]) was obtained from Fisher Scientific, while the Pt precursor (tetraammineplatinum(II) nitrate [$Pt(NH_3)_4(NO_3)_2$]) and aluminum oxide (catalyst support, high surface area, 1/8" pellet) were obtained from Alfa Aesar.

5.2.2 Preparation of Supported Catalysts

Both catalysts (Cu-Al_2O_3 and Pt-Al_2O_3) were synthesized using an incipient wetness impregnation method. Prior to loading the metals, the support (Al_2O_3) was crushed and sieved to obtain particles ≤ 0.15 mm in size (mesh 100). The precursor solution of a metal was prepared through dissolving the metal precursor in an amount of water just sufficient

to fill the pores of the support by means of dropwise addition to it with manual mixing. The volume of liquid needed to fill these pores was determined by adding small quantities of the solvent slowly to the weighed amount of support with stirring until the mixture became slightly liquid. After that, this ratio of weight:volume was used to prepare a metal precursor solution with a suitable concentration to achieve the desired metal loading [48]. Next, the catalysts were dried first in an oven overnight at 100 °C then heated in a furnace at 110 °C for 2 h and calcined at 550 °C for 4 h. A ramp rate of 2 °C/min was used up to 110 °C and 1 °C/min up to 550 °C. After the calcination process, the catalysts were crushed and sieved to < 0.15 mm for Pt-Al_2O_3 and to ≤ 0.18 mm for Cu-Al_2O_3.

5.2.3 Catalytic Reaction

Catalysts prepared as described above were used for the conversion of C_8 ketone to C_8 alkenes and C_8 alkane. The catalytic conversion of C_8 ketone was performed in a continuous flow fixed-bed reactor made of stainless steel (id=0.85 cm) under atmospheric pressure. Prior to the reaction, 0.5 g of catalyst was reduced in the reactor with flow rates of hydrogen and nitrogen equal to 68.5 and 16.5 mL/min, respectively, at 300 °C for 1 h. After the reduction process, the C_8 ketone was mixed with hydrogen and nitrogen in a preheater at the desired reaction temperature before flowing into the reactor. The C_8 ketone was fed through the top of reactor at a feed rate of 1 (mL/h) via a micro pump (Eldex 1SMP) together with H_2 and N_2 with flow rates of 68.5 and 16.5 mL/min, respectively. The molar ratio of H_2/C_8 ketone was maintained around 25, and the temperature of the reaction was kept at 220 °C using heating tape as a heating source.

The effluent product compositions were analyzed using an on-line gas chromatograph (SRI 8610C) with an MXT-1 column (100% dimethyl polysiloxane (nonpolar phase), 60 m, ID 0.53 mm) with FID and TCD detectors for the analysis of hydrocarbons and oxygenates. The temperature of the product effluent from the bottom of the reactor was maintained above 230 °C to avoid condensation of liquid products. The products were injected into the GC through a sample loop controlled by a high temperature ten-port valve. The oven was maintained at 40 °C for 5 min, and then increased to 120 °C at a ramp rate of 40 °C/min, finally raised to 250 °C at a rate of 20 °C/min and kept at this temperature for 10 min.

An Agilent 7890A GC-MS system equipped with an Agilent 5975C MS detector was used to identify the products detected by the GC. The conversion of MEK and the selectivity for the products were determined using Equation 5.1 and 5.2 respectively:

$$\text{Conversion } \% = \frac{(\text{ Moles of MEK})\text{in-(Mole of MEK)out}}{(\text{ Moles of MEK})\text{in}} * 100 \qquad \ldots (5.1)$$

$$\text{Selectivity } \% = \frac{(\text{ Moles of product})}{(\text{ Moles of total products})} * 100 \qquad \ldots (5.2)$$

Two different C_8 alkenes were detected (5-methyl-3-heptene and 5-methyl-2-heptene), while a single C_8 alkane (3-methyl heptane) was detected in the product. For brevity, these will be referred to as C_8 alkenes and C_8 alkane in the rest of the chapter.

5.2.4 Catalyst Characterization

5.2.4.1 X-ray Diffraction (XRD)

X-ray diffraction measurements were conducted using a Rigaku Miniflex II desktop X-ray diffractometer with Cu Kα radiation (λ = 0.15406 nm) in an operation mode of 30 kV and 15 mA. Scans of two theta angles were from 6° to 70° for all catalysts with a step size of 0.02° and scan speed of 2 °/min.

5.2.4.2 Temperature Programmed Desorption (NH_3-TPD and CO_2-TPD)

Temperature Programmed Desorption of ammonia (NH_3-TPD) and carbon dioxide (CO_2-TPD) were performed to investigate the surface acidity and basicity of the catalysts. NH_3-TPD was conducted in an Altamira AMI-200 system. Before adsorption, 0.1 g of supported metal catalyst was loaded in a quartz U-tube reactor then pre-treated at 550 °C under helium for 1 h followed by cooling to 100 °C. After that, the catalyst was reduced by passing H_2/Ar (10 v/v %) with a flow of 40 mL/min and heating up to 300 °C at a constant ramp rate of 10 °C /min and then held for 2 h followed by cooling to 100 °C. Next, 1% NH_3/He with a flow of 50 mL/min was introduced at 100 °C for 1 h. The sample was flushed with a He flow at 100 °C for 2 h to remove physically adsorbed NH_3 molecules. In the end, the temperature was raised to 600 °C at a ramp rate of 10 °C /min. For CO_2-TPD experiments, they were conducted using the same instrument employed in the NH_3-TPD measurements. 0.1 g of the sample was preheated and reduced in the same series of steps as that described for NH_3-TPD except the cooling temperature after reducing the

catalyst was 50 °C. After reducing, the sample was saturated with 10% CO_2 in Helium as the adsorbate with a flow of 50 mL/min at 50 °C. The sample was flushed with a He flow at 50 °C for 2 h to remove physisorbed CO_2 molecules. Finally, the temperature was raised to 600 °C at a ramp rate of 10 °C/min. Desorbed NH_3 and CO_2 from the samples were detected by a thermal conductivity detector (TCD).

5.3 Results and Discussions

5.3.1 Characterization of Catalysts

5.3.1.1 XRD

The XRD patterns of pure Al_2O_3, 1% Cu-Al_2O_3, 1% Pt-Al_2O_3, and catalysts with a high loading of Cu (20 wt% Cu on Al_2O_3) with different calcination times (4h and 8h) are shown in Figure 5.1.

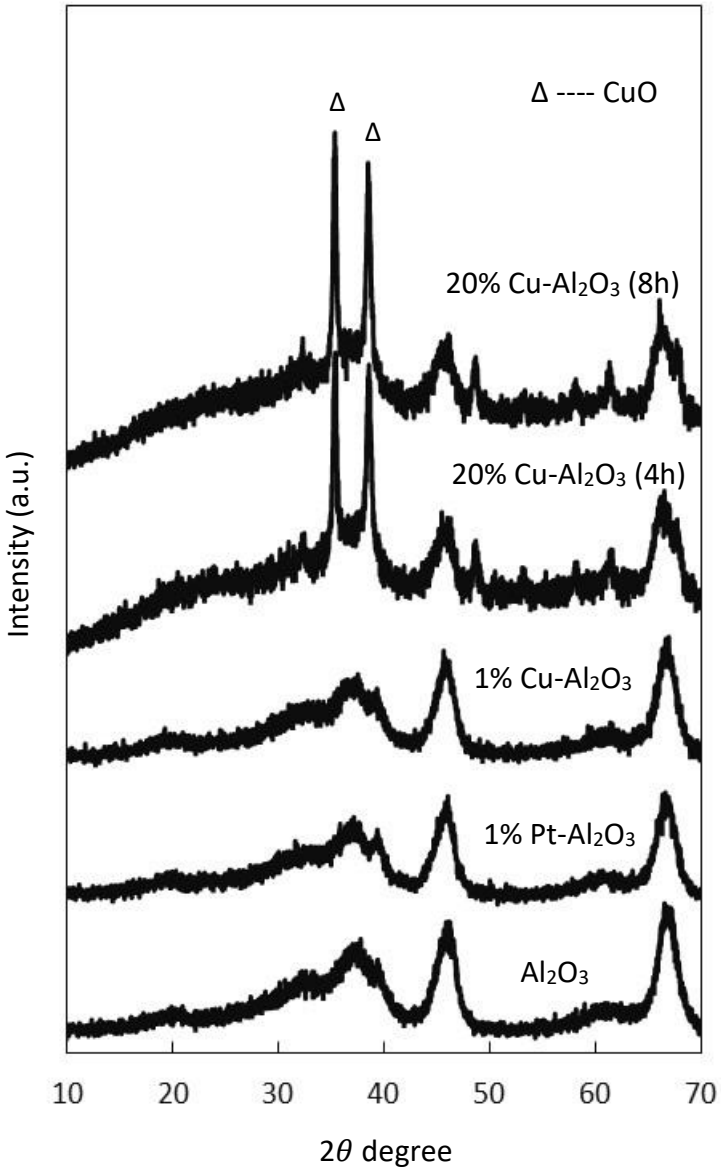

Figure 5.1. XRD pattern for pure Al_2O_3 and different supported catalysts.

As seen in this figure, all the characteristic peaks of the parent support (Al_2O_3) were observed in the supported metal catalysts. These peaks were maintained when metals were introduced; however, a slight decrease in the intensity of the main peaks was noticed at high Cu loadings. Two characteristic peaks related to CuO (35.5°and 38.6°) were observed on the Cu catalysts with 20 wt% Cu, confirming that at least some of the copper

was present as CuO clusters. However, there are no distinguishable diffraction peaks representing crystalline CuO peaks at low Cu loadings (1% Cu-Al_2O_3) probably because the copper particles are smaller than 40 Å in size, the detection limit of XRD [49,50]. Also for 1% Pt-Al_2O_3, no obvious diffraction peaks were observed, suggesting that the metal was well dispersed on the support. The crystallite sizes of CuO for 20% Cu-Al_2O_3 were determined using the Scherrer formula:

$$d = K\lambda / B \cos\theta \qquad \ldots (5.3)$$

where K is an empirical constant (assumed to be 0.9, the value for spherical particles), λ is the wavelength of the X-ray source (0.15406 nm), B is the full width at half-maximum (FWHM), and θ is the Bragg angle. Crystallite sizes are reported in Table 5.1.

Table 5.1. Calculations of particle size of the metal species using XRD, as well as acidity and basicity values from (NH_3-TPD and CO_2-TPD) experiments for the different catalysts.

Catalyst	Particle size of metal species (nm)[a]	NH_3 uptake (mmol/g)[b]	CO_2 uptake (mmol/g)[b]
1% Pt-Al_2O_3	_	0.44	0.114
1% Cu-Al_2O_3	_	0.21	0.066
20% Cu-Al_2O_3 (4h)	20	0.54	0.155
20% Cu-Al_2O_3 (8h)	20.5	0.4	0.115

[a] Calculated from XRD results
[b] Calculated from AMI measurements

5.3.1.2 (NH_3-TPD) and (CO_2-TPD)

NH_3-TPD and CO_2-TPD experiments were performed to investigate the acid-base properties of the reduced catalysts. Figure 5.2a shows the NH_3-TPD profile of different reduced metal supported catalysts calcined for 4 h and 8 h, while Figure 5.2b displays the CO_2-TPD profile for the same catalysts.

As can be seen from Figure 5.2a, broad NH_3 desorption peaks over 20% Cu-Al_2O_3 (4h) and 1% Pt-Al_2O_3 extended from 160 °C to 600 °C. However over 20% Cu-Al_2O_3 (8h), the peak was narrower and less intense than measured for 20% Cu-Al_2O_3 (4h). For these three mentioned catalysts, the maximum NH_3 desorption temperatures were centered around 360 °C while the peak for 1% Cu-Al_2O_3 was shifted to a higher temperature and centered around 425 °C. The increase in the NH_3 desorption temperature suggested that the strength of the acidic sites in 1% Cu-Al_2O_3 was higher than in the other. Also, it had the lowest concentration of acidic sites while the highest concentration was noted for 20% Cu-Al_2O_3 (4h) (see Table 5.1).

Figure 5.2b shows the CO_2-TPD profiles of the different catalysts. Two obvious peaks can be observed for all catalysts, suggesting the presence of different sites of varying base strength. 20% Cu-Al_2O_3 (4h and 8h) and 1% Pt-Al_2O_3 have very similar maximum CO_2 desorption temperatures (near 130 °C and 370 °C), although the first peak for 1% Pt-Al_2O_3 is shifted slightly to a lower temperature (around 124 °C). For 1% Cu-Al_2O_3, the first peak was proportionally bigger than the lower-temperature peak for the three other catalysts, while the second one was lower than them and shifted to a high

temperature (around 420 °C), suggesting that the amount of weakly basic sites is higher for this catalyst. However, the total amount of base sites is still the lower than the other catalysts as shown in Table 5.1.

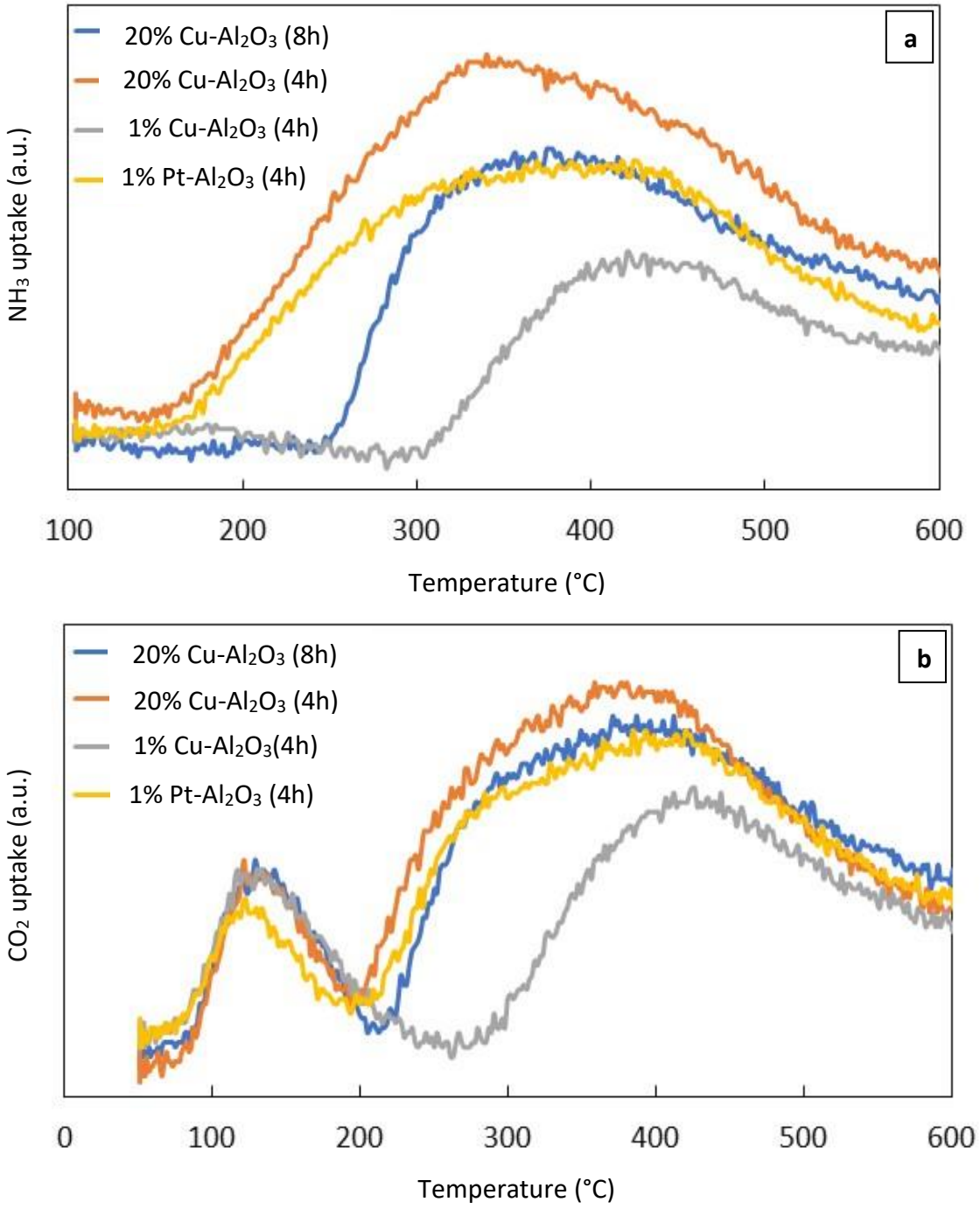

Figure 5.2. (a) (NH_3-TPD) profiles of the different catalysts, (b) (CO_2-TPD) profiles of the different catalysts.

5.3.2 Catalytic Conversion of C_8 Ketone to C_8 Alkenes and C_8 Alkane in a Fixed Bed Reactor

5.3.2.1 Effect of Different Supported Catalysts on the Reaction of C_8 Ketone

Experiments were conducted to study the effect of using different metals (Cu and Pt) supported Al_2O_3 on the conversion of C_8 ketone and the distribution of major products. Reaction of C_8 ketone over 20% Cu-Al_2O_3, 1% Cu-Al_2O_3 and 1% Pt-Al_2O_3 were investigated in the fixed bed reactor at 220 °C in the presence of H_2 as a reactant and N_2 as a diluent. The total flow rate of H_2 and N_2 was 85 mL/min with flow rate of H_2 and N_2 of 68.5 and 16.5 mL/min, respectively. The flow rate of C_8 ketone was 1 mL/h and the molar ratio of H_2/C_8 ketone was around 25. All the catalysts were calcined for 4h. Prior to introducing the reactants, the catalyst was reduced in the reactor at 300 °C for 1 h with H_2 and N_2 flowing at 68.5 and 16.5 mL/min, respectively. The catalytic results after 1 h using 0.5 g of catalyst are summarized in Table 5.2.

Table 5.2. Catalytic activity in the conversion of C_8 ketone to C_8 alkene and C_8 alkane over several catalysts.

Catalyst	Conv. of C_8 ketone (%)	Sel. for C_8 alkenes (%)	Sel. for C_8 alkane (%)	Others (%)[a]
20% Cu-Al_2O_3	100	44.7	54.58	0.72
1% Cu-Al_2O_3	50.9	65.9	10.4	23.7
1% Pt-Al_2O_3	99.9	0	97.7	2.3

[a] Others include Butene, Xylene, unsaturated C_8 ketone, condensation products and aromatics.

The results in Table 5.2 indicate that Pt was much more active than Cu. For the same weight loading, conversion over 1% Pt-Al_2O_3 was approximately double of that for 1% Cu-Al_2O_3. The other major difference for these two catalysts was that 1% Pt-Al_2O_3 gave nearly 98% selectivity for the C_8 alkane while 1% Cu-Al_2O_3 produced primarily C_8 alkenes, with lesser amounts of C_8 alkane and other products. When the amount of Cu loaded on the catalyst was increased to 20 wt%, an equivalent conversion was reached to that of 1% Pt-Al_2O_3, about 99.9%. This can be attributed to the increase in metal sites (see Table 5.1 and Figure 5.2). However, the selectivity difference between the Cu and Pt catalysts was still maintained: the selectivity for C_8 alkenes was 44.7% for the Cu catalyst. These results suggested that Pt was more active than Cu not only for the initial hydrogenation of the C_8 ketone, but also for the hydrogenation of C_8 alkenes to C_8 alkane. These results are in accordance with the fact that copper catalysts selectively hydrogenate C=O bonds and are relatively inactive for hydrogenolysis of C–C bonds [25] while platinum catalyst are very active for hydrogenating both C=O and C=C bonds [30,51].

It was also interesting to note the large amount of other products (23.7%) produced over 1% Cu-Al_2O_3 compared to the other catalysts. This was likely the result of the interplay between the chemistries on the two types of catalytic sites: metal and acidic sites. For the low loading of Cu, the hydrogenation of C_8 ketone was sufficiently slow that reactions over the acidic support could proceed, leading to products other than C_8 alkenes and C_8 alkane. When the metal chemistry was more pronounced, in the case of using Pt or increased Cu loadings, then hydrogenation of C_8 ketone took place fast enough that

other reaction pathways did not play a significant role, and the selectivities for other products dropped.

5.3.2.2 Effect of Reaction Temperature

The effect of temperature on the conversion of C_8 ketone and the distribution of major products over 20% Cu-Al_2O_3 and 1% Pt-Al_2O_3 was investigated for a temperature range of 180 °C to 260 °C. Figures 5.3a and 5.3b show the catalytic results after 1 h on stream for both catalysts using 0.5 g of the catalyst. The total flow rate of H_2 and N_2 was 85 mL/min, the flow rate of C_8 ketone was 1 mL/h, and the molar ratio of H_2/C_8 ketone was 25. Over 20% Cu-Al_2O_3, the main products were a mixture of C_8 alkenes and C_8 alkane, and the selectivity for C_8 alkane increased with increased temperatures resulting from further hydrogenation of C_8 alkenes. Over 1% Pt-Al_2O_3 however, the main product was C_8 alkane at all temperatures, although its selectivity decreased at low temperatures in favor of the C_8 alcohol.

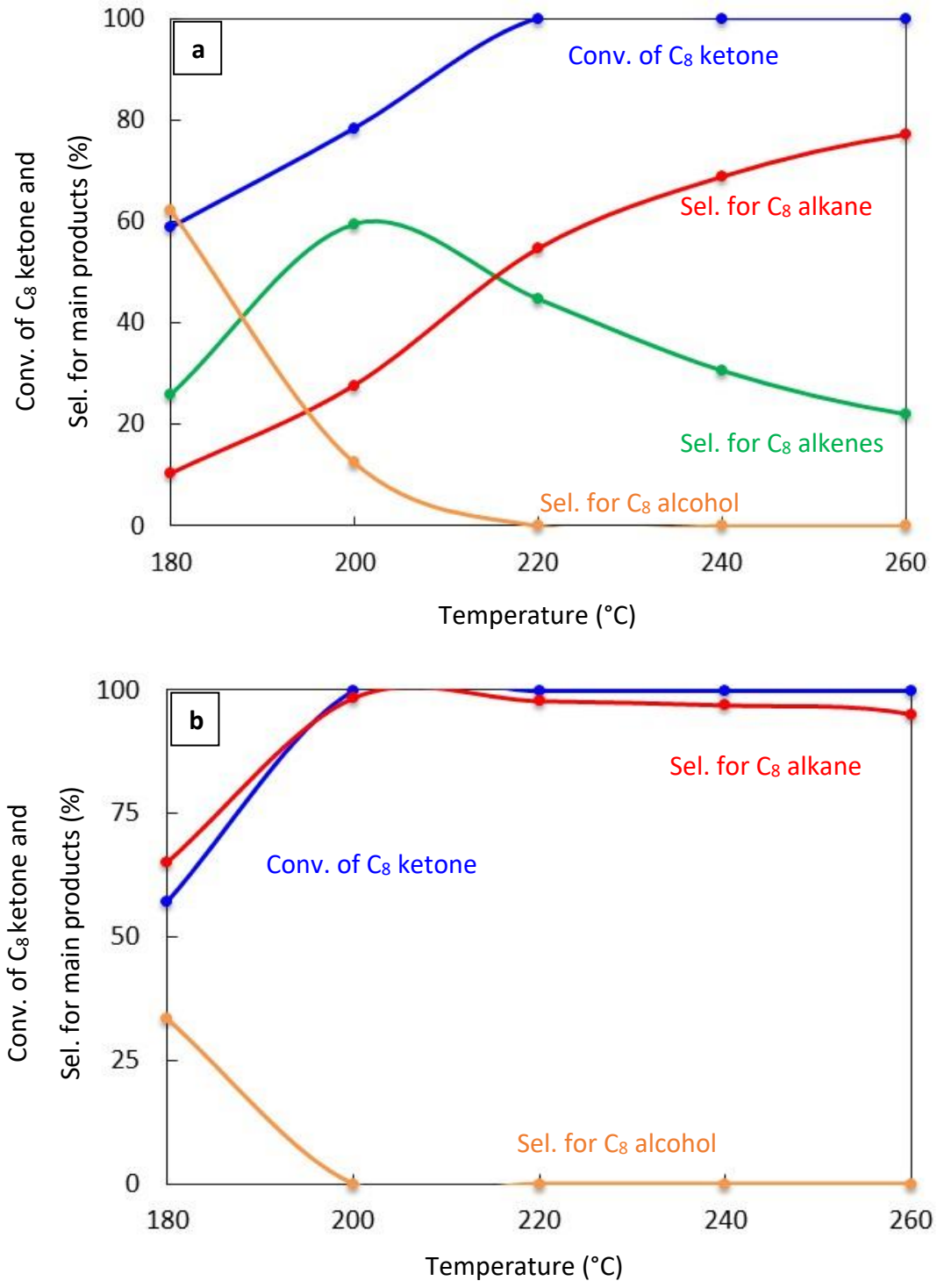

Figure 5.3. Catalytic results for the conversion of C_8 ketone to several products with different temperatures over (a) (20% Cu-Al_2O_3), (b) (1% Pt-Al_2O_3).

These results indicated that the conversion of C_8 ketone to C_8 alkane occurred by a series reaction, as summarized in Scheme 5.1. The first step in the reaction mechanism is the hydrogenation of the C_8 ketone to the C_8 alcohol, which is dehydrated to C_8 alkenes. The alkenes can further be hydrogenated to C_8 alkanes. Temperature controls the rate of all reaction pathways. At low temperatures, for both Cu-Al_2O_3 and Pt-Al_2O_3, significant amounts of C_8 alcohols were formed because subsequent reactions did not proceed at a fast enough rate. It is interesting to note that even at the lowest temperature, Pt-Al_2O_3 produced no C_8 alkenes, instead producing exclusively C_8 alkane. This suggested that Pt-Al_2O_3 was extremely active for the hydrogenation of C_8 alkenes to C_8 alkane. Higher temperatures allowed further reactions to occur, pushing the product selectivities towards C_8 alkenes and C_8 alkane.

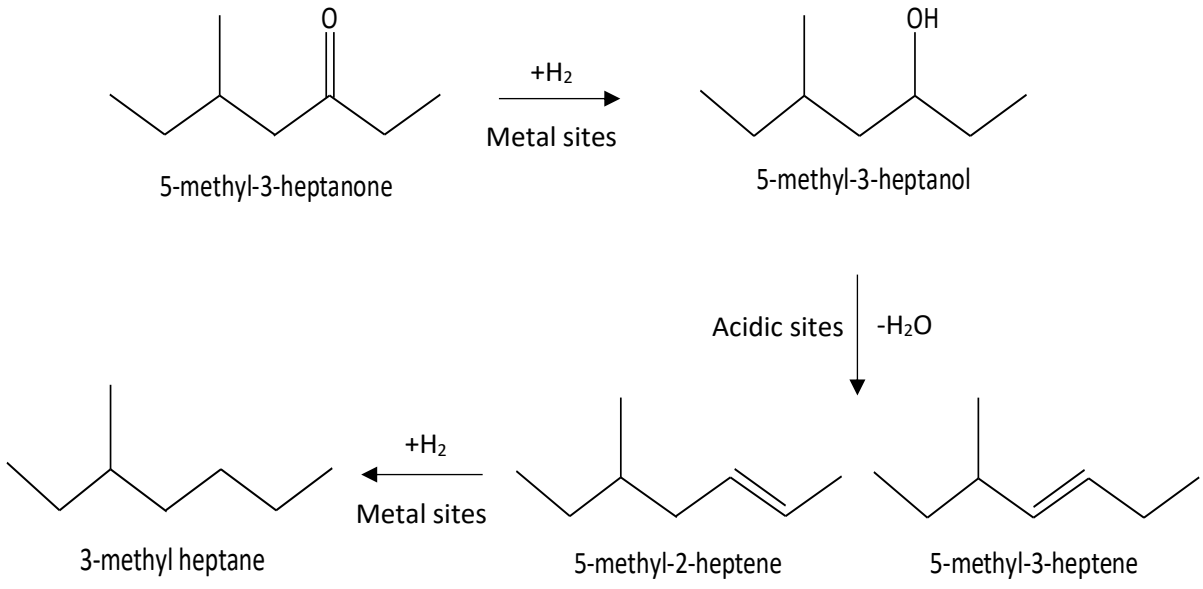

Scheme 5.1. The mechanism of conversion C_8 ketone to C_8 alkenes & C_8 alkane.

5.3.2.3 Effect of H_2/C_8 Ketone Molar Ratio

Experiments were performed to study the effect of changing the molar ratio of H_2 to C_8 ketone on the conversion of C_8 ketone and the distribution of products over both 20% Cu-Al_2O_3 and 1% Pt-Al_2O_3. Results are shown in Figures 5.4a and 5.4b for 0.5 g of the catalysts and a reaction temperature of 220 °C. The total flow rate of H_2 and N_2 was 85mL/min, the flow rate of C_8 ketone was 1 mL/h, and the molar ratio of H_2/C_8 ketone was varied from 2 to 25. The results were reported after 1 h on stream.

Figure 5.4a shows that the H_2/C_8 ketone ratio directly impacted both C_8 ketone conversion and product selectivity. Higher H_2/C_8 ketone ratio increased C_8 ketone conversion: the conversion was 100% at all ratios above 2. Also as seen from this figure, the H_2/C_8 ketone molar ratio affected the selectivity for products. With an increase in ratio from 2 to 25, the selectivity for C_8 alkenes decreased from 81.57% to 44.7%. This decrease was due to more hydrogenation of C_8 alkenes to C_8 alkane. The highest selectivity for C_8 alkenes was found at a H_2/C_8 ketone ratio of 2 with a selectivity of 81.57%.

Over 1% Pt-Al_2O_3, as shown in Figure 5.4b, the conversion of C_8 ketone increased from (43.8%) to (99.9%) when the H_2/C_8 ketone ratio increased from 2 to 25. The main product selectivity was still C_8 alkane, although the selectivity for this product decreased dramatically when the ratio was 5 or below. For those ratios, the selectivity for other products, like C_8 unsaturated ketone, butane, xylene, aromatics and condensation products, became more important.

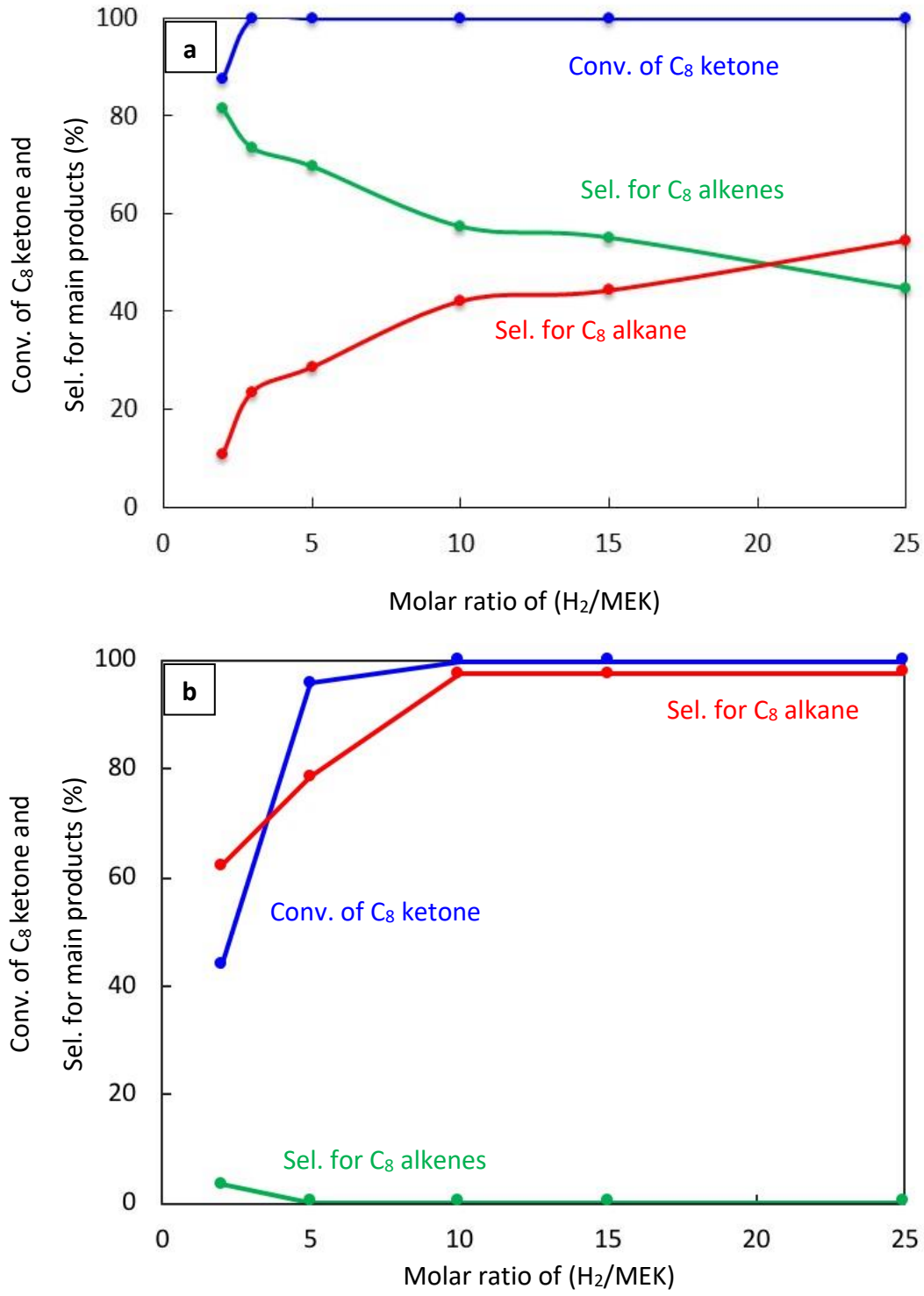

Figure 5.4. Catalytic results for the conversion of C_8 ketone to several products using different H_2/C_8 ketone molar ratio over (a) (20% Cu-Al_2O_3), (b) (1% Pt-Al_2O_3).

5.3.2.4 Effect of Space Time

The effect of space time, W/FA_0 where W is the weight of catalyst (g), and FA_0 is the molar flow rate of C_8 ketone (mol h^{-1}), was evaluated to better understand the reaction mechanism. Results for 20% Cu-Al_2O_3 and 1% Pt-Al_2O_3 at 220 °C as are shown in Figures 5.5a and 5.5b, respectively. Experiments were performed at a reaction temperature of 220 °C, a total flow rate of H_2 and N_2 of 85 mL/min, the calcination time of both catalysts was 4 h, the feed rate of C_8 ketone was 1 mL/h and the molar ratio of H_2/C_8 ketone was 5 over both 20% Cu-Al_2O_3 and 1% Pt-Al_2O_3. The results were collected after 1 h from the reaction.

As can be seen in Figure 5.5a, the conversion of C_8 ketone increased from 39.3 % to 100% when the space time increased from 15.5 to 77.3 g.mol^{-1}.h. The selectivity for C_8 alkenes decreased from 85.5% to 69.7% while the selectivity for C_8 alkane increased from 11.6% to 28.6%. In addition, a small amount of C_8 alcohol was detected at low space times.

The effect of space time on the conversion of C_8 ketone and the distribution of products over 1% Pt-Al_2O_3 is displayed in Figure 5.5b. As can be seen, the conversion of C_8 ketone increased from 30.5 % to 95.7% when the space time increased from 15.5 to 77.3 g.mol^{-1}.h, and the selectivity for C_8 alkane decreased from 87.4% to 78.5%. The drop in alkane selectivity was associated with the formation of byproducts like aromatics and condensation products. C_8 alkenes and unsaturated C_8 ketones were detected at low space times and decreased with increased space times. Unsaturated C_8 ketones were produced by dehydrogenation reactions on Pt.

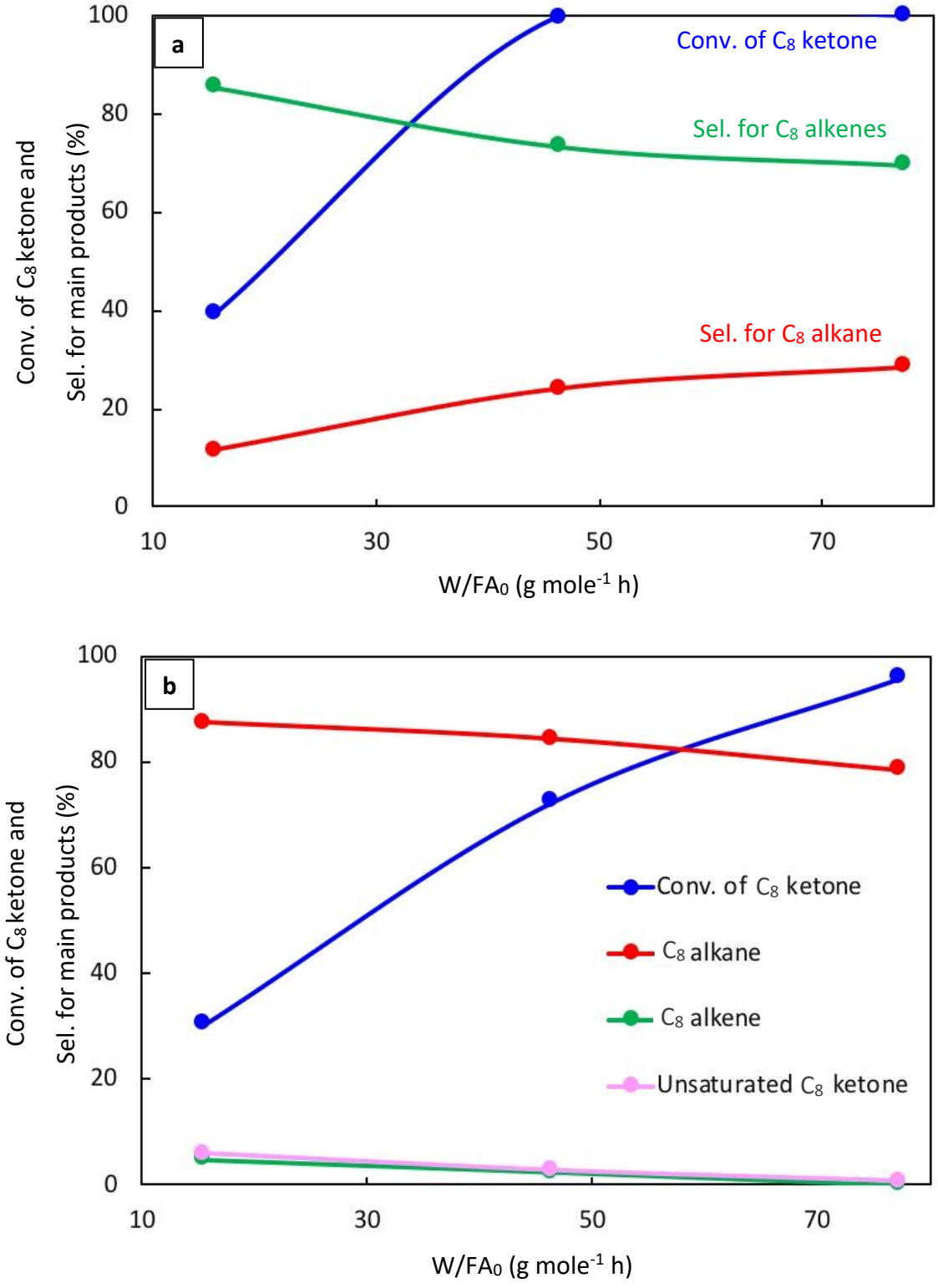

Figure 5.5. Catalytic results for the conversion of C_8 ketone to several products with different space times after 1 h of the reaction over (a) (20% Cu-Al_2O_3), (b) (1% Pt-Al_2O_3).

The results for different W/FA_0 for Cu and Pt showed a few important trends. First, it can be seen that 1% Pt-Al_2O_3 produced primarily alkanes even at the smallest space times. This indicates that the hydrogenation of alkenes to alkane was quite fast. On the other hand, this reaction was much slower on 20% Cu-Al_2O_3. The results also showed that 1% Pt-Al_2O_3 could catalyze dehydrogenation reactions under some conditions, yielding unsaturated ketones. Again, this was not noted for 20% Cu-Al_2O_3 due to its lower hydrogenation/dehydrogenation activity.

5.3.2.5 Catalyst Stability

The catalyst stability was studied for 20% Cu-Al_2O_3 with different calcination times (4 h and 8 h) and for 1% Pt-Al_2O_3 calcined for 4 h. 0.5 g of each catalyst was reduced in the reactor at 300 °C for 1 h with a flow rate of H_2 and N_2 equal to 68.5 and 16.5 mL/min, respectively, before running the reaction at 220 °C. The total flow rate of H_2 and N_2 was 85 mL/min and the flow rate of C_8 ketone was 1 mL/h. The mole ratio of H_2/C_8 ketone was 10 over both 20% Cu-Al_2O_3 catalysts with different calcination times (4 h and 8 h) and 1% Pt-Al_2O_3. Results are shown in Figures 5.6a, 5.6b, and 5.6c.

Figure 5.6a shows significant deactivation for 20% Cu-Al_2O_3 calcined for 4h. The conversion of C_8 ketone was 100% during the first 5 h but decreased to 72.77% after 10 h. C_8 alkene selectivity increased with time to reach above 75% at 6 h then decreased slightly with time to 69.7% after 10 h, which was associated with an increase in the

production of C_8 alcohol, an intermediate product. Also, the selectivity for C_8 alkanes decreased with time.

Figure 5.6b displays the conversion of C_8 ketone and the distribution of products during 12 h of reaction over 20% Cu-Al_2O_3 calcined for 8 h. As can be seen, the conversion was maintained near 100% for nearly the entire time studied, with a slight decrease to 99.5% at 12 h. The selectivity for C_8 alkenes increased with time from 68.34% at the start of the reaction to 75.77% after 12 h, while the selectivity for C_8 alkanes decreased from 26.17% to 23.3 with time. From the results in Figures 5.6a and 5.6b, it appears that longer calcination times led to more stable catalysts. This may be because the concentration of acidic sites was lower on 20% Cu-Al_2O_3 with longer calcination times than with short calcination times (see Table 5.1, NH_3 uptake results). A larger number of acidic sites would likely increase the rate of deactivation [52].

Figure 5.6c shows the conversion of C_8 ketone and the distribution of major products during 10 hours of reaction over 1% Pt-Al_2O_3. It is clear that the conversion of C_8 ketone was 99.8% during first 3 h then decreased at 4 h from 98.8% to 76.7% at 10 h. However, the selectivity for C_8 alkane as the main product was approximately constant at over 97 % and small amounts of butane were detected during the first 10 min of the reaction. Also, an experiment was conducted with a high H_2/C_8 ketone ratio (25) (not shown here). The results showed that both the conversion of C_8 ketone and the selectivity for C_8 alkane were approximately constant at over 99.8% and 97.6% respectively over 24

h. This suggests that hydrogen helps to maintain catalyst activity, most likely by preventing coke formation.

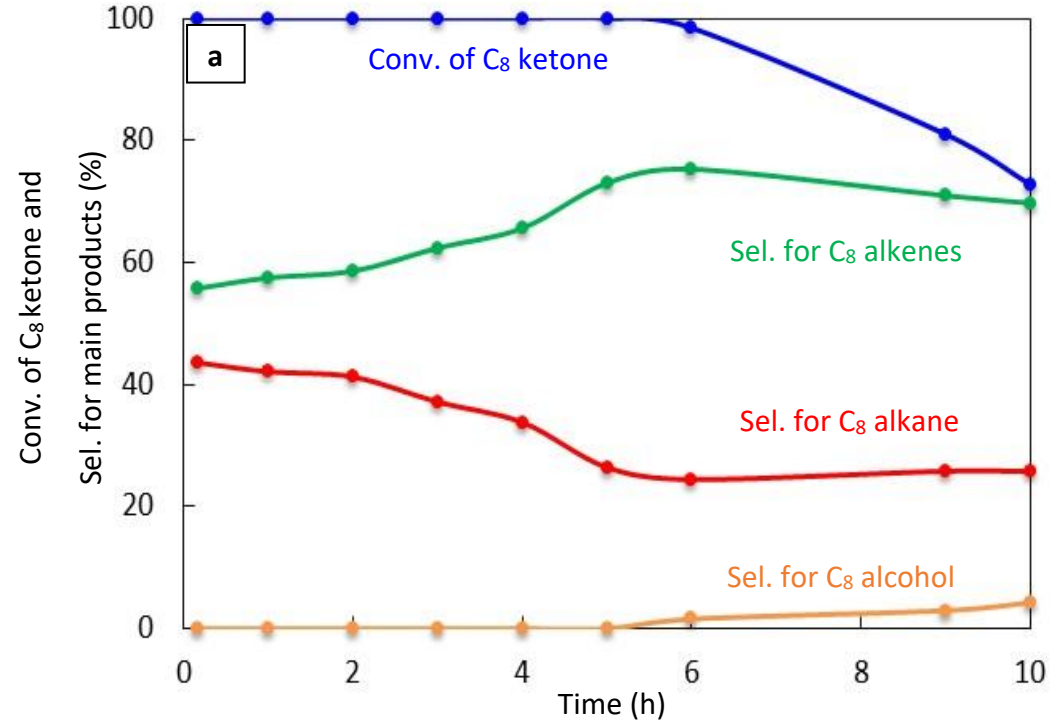

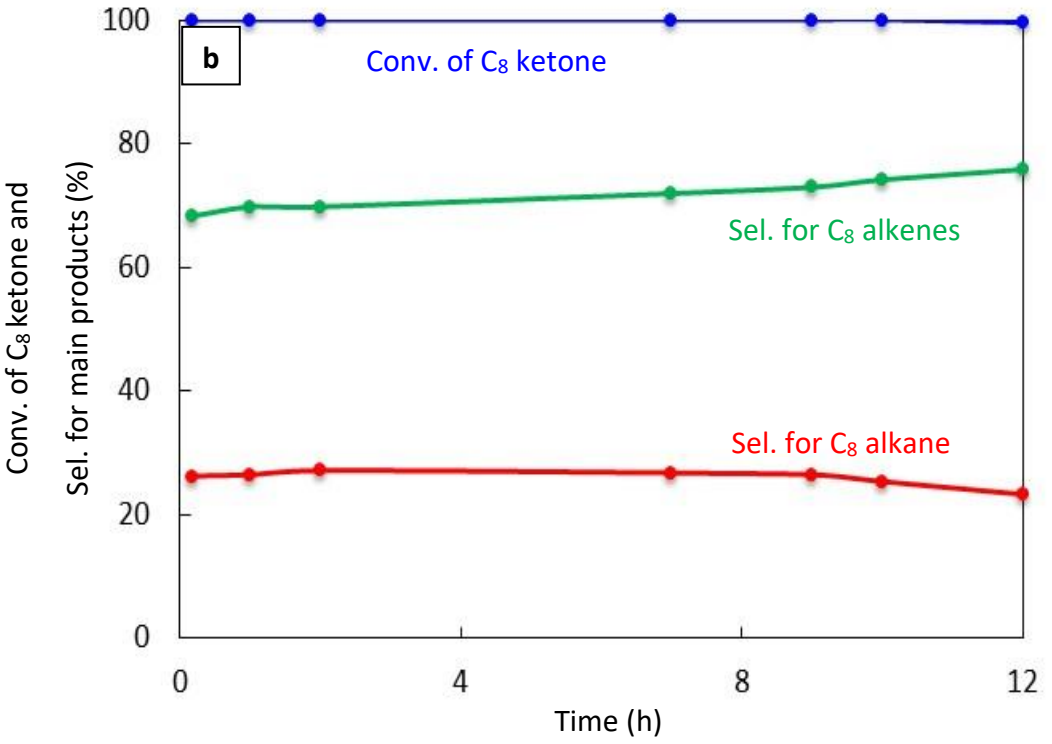

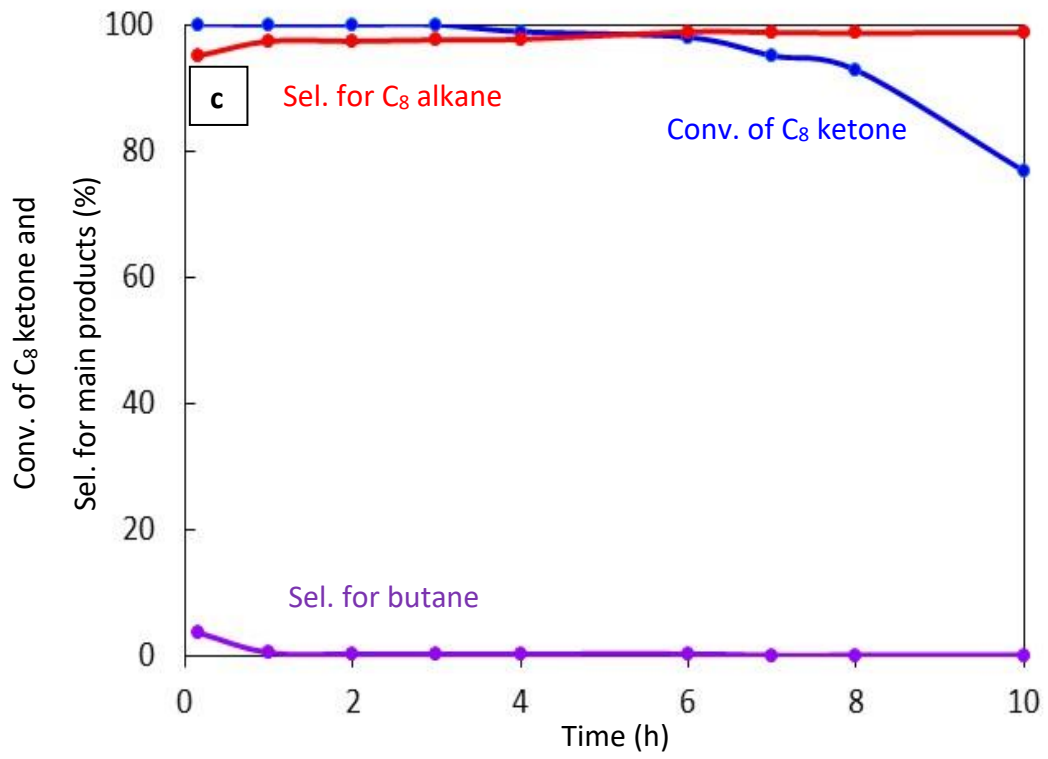

Figure 5.6. Catalytic results for the conversion of C_8 ketone to several products with time over (a) (20% Cu-Al_2O_3); calcination time (4 h), (b) (20% Cu-Al_2O_3); calcination time (8 h), (c) (1% Pt-Al_2O_3); calcination time (4 h).

5.4 Conclusion

Hydrodeoxygenation of C_8 ketone (5-methyl-3-heptanone) to C_8 alkenes (5-methyl-3-heptene and 5-methyl-2-heptene) and C_8 alkane (3-methyl heptane) was investigated using bifunctional catalysts composed of one of transition metals (Cu or Pt) loaded on Al_2O_3 to provide both hydrogenation and dehydration sites. Over 20% Cu-Al_2O_3, a mixture of C_8 alkenes and C_8 alkane was produced, while 1% Pt-Al_2O_3 produced nearly all C_8 alkane because Pt was a more active hydrogenation catalyst for the C_8 alkene. The ratio of H_2/C_8 ketone had a significant impact on catalytic chemistry. Higher ratios led to

higher production of C_8 alkane and higher C_8 ketone conversions. Higher reaction temperatures also enhanced C_8 ketone conversion and selectivity for C_8 alkane. These results are consistent with a pathway consisting of a series of reactions where C_8 ketone is hydrogenated to a C_8 alcohol on metal sites, dehydrated to C_8 alkenes on acidic sites, and further hydrogenated to C_8 alkane. Catalyst deactivation over 10 h was noted for the Cu catalyst calcined for a relatively short time and Pt catalyst, but little deactivation was noted for the Cu catalyst calcined for a longer period of time.

Acknowledgements

Higher Committee for Education Development in Iraq (HCED) is gratefully acknowledged in addition to the financial support from Navy SBIR Phase II Contr #NG8335, in collaboration with TekHolding, Inc.

References

1. Chheda, J. N.; Dumesic, J. A. An overview of dehydration, aldol-condensation and hydrogenation processes for production of liquid alkanes from biomass-derived carbohydrates. *Catal. Today* **2007**, *123*, 59–70.
2. Chheda, J. N.; Román-Leshkov, Y.; Dumesic, J. A. Production of 5-hydroxymethylfurfural and furfural by dehydration of biomass-derived mono-and poly-saccharides. *Green Chem.* **2007**, *9*, 342–350.
3. Alonso, D. M.; Bond, J. Q.; Dumesic, J. A. Catalytic conversion of biomass to biofuels. *Green Chem.* **2010**, *12*, 1493–1513.

4. Yu, E. K.; Saddler, J. N. Fed-batch approach to production of 2,3-butanediol by Klebsiella pneumoniae grown on high substrate concentrations. *Appl. Environ. Microbiol.* **1983**, *46*, 630–635.

5. Zeng, A. P.; Biebl, H.; Deckwer, W. D. Effect of pH and acetic acid on growth and 2, 3-butanediol production of Enterobacter aerogenes in continuous culture. *Appl. Microbiol. Biotechnol.* **1990**, *33*, 485–489.

6. Mas, C. De; Jansen, N. B.; Tsao, G. T. Production of optically active 2,3-butanediol by Bacillus polymyxa. *Biotechnol. Bioeng.* **1988**, *31*, 366–377.

7. Ledingham, G. A.; Neish, A. C. Fermentative Production of 2,3 butanediol. Industrial Fermentations, LA Underkofler and RJ Hickey, Eds. **1954**,2, 27–93.

8. Jansen, N. B.; Flickinger, M. C.; Tsao, G. T. Production of 2,3-butanediol from D-xylose by Klebsiella oxytoca ATCC 8724. *Biotechnol. Bioeng.* **1984**, *26*, 362–369.

9. Qureshi, N.; Cheryan, M. Effects of aeration on 2,3-butanediol production from glucose by Klebsiella oxytoca. *J. Ferment. Bioeng.* **1989**, *67*, 415–418.

10. Ji, X. J.; Huang, H.; Du, J.; Zhu, J. G.; Ren, L. J.; Hu, N.; Li, S. Enhanced 2,3-butanediol production by Klebsiella oxytoca using a two-stage agitation speed control strategy. *Bioresour. Technol.* **2009**, *100*, 3410–3414.

11. Saha, B. C.; Bothast, R. J. Production of 2,3-butanediol by newly isolated Enterobacter cloacae. *Appl. Microbiol. Biotechnol.* **1999**, *52*, 321–326.

12. Molnár, Á.; Bucsi, I.; Bartók, M. Pinacol Rearrangement on Zeolites. *Stud. Surf. Sci.*

Catal. **1988**, *41*, 203–210.

13. Multer, A.; McGraw, N.; Hohn, K.; Vadlani, P. Production of methyl ethyl ketone from biomass using a hybrid biochemical/catalytic approach. *Ind. Eng. Chem. Res.* **2012**, *52*, 56–60.

14. Emerson, R. R.; Flickinger, M. C.; Tsao, G. T. Kinetics of dehydration of aqueous 2, 3-butanediol to methyl ethyl ketone. *Ind. Eng. Chem. Prod. Res. Dev.* **1982**, *21*, 473–477.

15. Zhang, W.; Yu, D.; Ji, X.; Huang, H. Efficient dehydration of bio-based 2,3-butanediol to butanone over boric acid modified HZSM-5 zeolites. *Green Chem.* **2012**, *14*, 3441–3450.

16. Bucsi, I.; Molnár, Á.; Bartók, M.; Olah, G. A. Transformation of 1,2-diols over perfluorinated resinsulfonic acids (Nafion-H). *Tetrahedron* **1994**, *50*, 8195–8202.

17. Török, B.; Bucsi, I.; Beregszászi, T.; Kapocsi, I.; Molnár, Á. Transformation of diols in the presence of heteropoly acids under homogeneous and heterogeneous conditions. *J. Mol. Catal. A Chem.* **1996**, *107*, 305–311.

18. Nikitina, M. A.; Ivanova, I. I. Conversion of 2,3-Butanediol over Phosphate Catalysts. *ChemCatChem* **2016**, *8*, 1346–1353.

19. Lee, J.; Grutzner, J. B.; Walters, W. E.; Delgass, W. N. The conversion of 2,3-butanediol to methyl ethyl ketone over zeolites. *Stud. Surf. Sci. Catal.* **2000**, *130*, 2603–2608.

20. Kelly, G. J. Aldol condensation reaction and catalyst therefor. U.S. patent No.

6,706,928. **2004**.

21. Zheng, Q.; Wales, M. D.; Heidlage, M. G.; Rezac, M.; Wang, H.; Bossmann, S. H.; Hohn, K. L. Conversion of 2,3-butanediol to butenes over bifunctional catalysts in a single reactor. *J. Catal.* **2015**, *330*, 222–237.

22. Zheng, Q.; Grossardt, J.; Almkhelfe, H.; Xu, J.; Grady, B. P.; Douglas, J. T.; Amama, P. B.; Hohn, K. L. Study of mesoporous catalysts for conversion of 2,3-butanediol to butenes. *J. Catal.* **2017**, *354*, 182–196.

23. Al-Auda, Z.; Al-Atabi, H.; Li, X.; Zheng, Q.; Hohn, K. L. Conversion of Methyl Ethyl Ketone to Butenes over Bifunctional Catalysts. *Appl. Catal. A Gen* (in press) **2018**.

24. Al-Auda, Z.; Al-Atabi, H.; Hohn, K. L. Copper Catalyst for the Aldol Condensation of Methyl Ethyl Ketone to Higher Ketone. *Catalysts* (under review) **2018**.

25. Brands, D. S.; Poels, E. K.; Bliek, A. Ester hydrogenolysis over promoted Cu/SiO_2 catalysts. *Appl. Catal. A Gen.* **1999**, *184*, 279–289.

26. Fan, X.; Liu, S.; Yan, X.; Du, X.; Chen, L. A continuous process for the production of 2,2,6,6-tetramethylpiperidin-4-ol catalyzed by Cu–Cr/γ-Al_2O_3. *Catal. Commun.* **2010**, *11*, 960–963.

27. Saadi, A.; Rassoul, Z.; Bettahar, M. M. Gas phase hydrogenation of benzaldehyde over supported copper catalysts. *J. Mol. Catal. A Chem.* **2000**, *164*, 205–216.

28. Nagaraja, B. M.; Kumar, V. S.; Shasikala, V.; Padmasri, A. H.; Sreedhar, B.; Raju, B. D.; Rao, K. S. R. A highly efficient Cu/MgO catalyst for vapour phase hydrogenation of furfural to furfuryl alcohol. *Catal. Commun.* **2003**, *4*, 287–293.

29. Chambers, A.; Jackson, S. D.; Stirling, D.; Webb, G. Selective hydrogenation of cinnamaldehyde over supported copper catalysts. *J. Catal.* **1997**, *168*, 301–314.

30. Poondi, D.; Vannice, M. A. The influence of MSI (metal-support interactions) on phenylacetaldehyde hydrogenation over Pt catalysts. *J. Mol. Catal. A Chem.* **1997**, *124*, 79–89.

31. Vannice, M. A.; Sen, B. Metal-support effects on the intramolecular selectivity of crotonaldehyde hydrogenation over platinum. *J. Catal.* **1989**, *115*, 65–78.

32. Vannice, M. A.; Poondi, D. The effect of metal-support interactions on the hydrogenation of benzaldehyde and benzyl alcohol. *J. Catal.* **1997**, *169*, 166–175.

33. Kijeński, J.; Winiarek, P.; Paryjczak, T.; Lewicki, A.; Mikołajska, A. Platinum deposited on monolayer supports in selective hydrogenation of furfural to furfuryl alcohol. *Appl. Catal. A Gen.* **2002**, *233*, 171–182.

34. Knözinger, H.; Köhne, R. The dehydration of alcohols over alumina: I. The reaction scheme. *J. Catal.* **1966**, *5*, 264–270.

35. Knözinger, H.; Scheglila, A. The dehydration of alcohols on alumina: XII. Kinetic isotope effects in the olefin formation from butanols. *J. Catal.* **1970**, *17*, 252–263.

36. Knözinger, H.; Bühl, H.; Kochloefl, K. The dehydration of alcohols on alumina: XIV. Reactivity and mechanism. *J. Catal.* **1972**, *24*, 57–68.

37. Bondt, N.; Deiman, J. R.; Van Troostwyk, P.; Lauwerenburg, A. In: Shi, B.; Davis, B. Alcohol dehydration: mechanism of ether formation using an alumina catalyst. *J. Catal.* **1995**, *157,* 359-367.

38. Kostestkyy, P.; Yu, J.; Gorte, R. J.; Mpourmpakis, G. Structure–activity relationships on metal-oxides: alcohol dehydration. *Catal. Sci. Technol.* **2014**, *4*, 3861–3869.

39. Nakagawa, Y.; Liu, S.; Tamura, M.; Tomishige, K. Catalytic total hydrodeoxygenation of biomass-derived polyfunctionalized substrates to alkanes. *ChemSusChem.* **2015**, *8*, 1114–1132.

40. Ma, J.; Liu, S.; Kong, X.; Fan, X.; Yan, X.; Chen, L. A continuous process for the reductive deoxygenation of aromatic ketones over $Cu_{30}Cr_{10}$/γ-Al_2O_3. *Res. Chem. Intermed.* **2012**, *38*, 1341–1349.

41. Kong, X.; Lai, W.; Tian, J.; Li, Y.; Yan, X.; Chen, L. Efficient Hydrodeoxygenation of Aliphatic Ketones over an Alkali-Treated Ni/HZSM-5 Catalyst. *ChemCatChem.* **2013**, *5*, 2009–2014.

42. Yang, J.; Li, N.; Li, G.; Wang, W.; Wang, A.; Wang, X.; Cong, Y.; Zhang, T. Synthesis of renewable high-density fuels using cyclopentanone derived from lignocellulose. *Chem. Commun.* **2014**, *50*, 2572–2574.

43. Hronec, M.; Fulajtarová, K. Selective transformation of furfural to cyclopentanone. *Catal. Commun.* **2012**, *24*, 100–104.

44. Hronec, M.; Fulajtarová, K.; Liptaj, T. Effect of catalyst and solvent on the furan ring rearrangement to cyclopentanone. *Appl. Catal. A Gen.* **2012**, *437*, 104–111.

45. Zhou, M.; Zhu, H.; Niu, L.; Xiao, G.; Xiao, R. Catalytic hydroprocessing of furfural to cyclopentanol over Ni/CNTs catalysts: model reaction for upgrading of bio-oil. *Catal. Letters.* **2014**, *144*, 235–241.

46. Li, X. L.; Deng, J.; Shi, J.; Pan, T.; Yu, C. G.; Xu, H. J.; Fu, Y. Selective conversion of furfural to cyclopentanone or cyclopentanol using different preparation methods of Cu–Co catalysts. *Green Chem.* **2015**, *17*, 1038–1046.

47. Guo, J.; Xu, G.; Han, Z.; Zhang, Y.; Fu, Y.; Guo, Q. Selective conversion of furfural to cyclopentanone with CuZnAl catalysts. *ACS Sustain. Chem. Eng.* **2014**, *2*, 2259–2266.

48. Augustine, R. L. Heterogeneous catalysis for the synthetic chemist; CRC Press, **1995**; ISBN 0824790219.

49. Chary, K. V. R.; Sagar, G. V.; Srikanth, C. S.; Rao, V. V. Characterization and catalytic functionalities of copper oxide catalysts supported on zirconia. *J. Phys. Chem. B.* **2007**, *111*, 543–550.

50. Sagar, G. V.; Rao, P. V. R.; Srikanth, C. S.; Chary, K. V. R. Dispersion and Reactivity of Copper Catalysts Supported on Al_2O_3− ZrO_2. *J. Phys. Chem. B.* **2006**, *110*, 13881–13888.

51. Alotaibi, M. A.; Kozhevnikova, E. F.; Kozhevnikov, I. V Efficient hydrodeoxygenation of biomass-derived ketones over bifunctional Pt-polyoxometalate catalyst. *Chem. Commun.* **2012**, *48*, 7194–7196.

52. Bartholomew, C. H. Mechanisms of catalyst deactivation. *Appl. Catal. A Gen.* **2001**, *212*, 17–60.

Chapter 6 - Conclusions and Future Work

From the outlined studies, one can conclude that MEK is an attractive feedstock which can be derived from renewable resources, for example by dehydrating 2,3 butanediol, produced in high yields from biomass-derived sugars. This thesis describes the conversion MEK to different useful chemicals in a single step via heterogeneous catalysis using bifunctional and multifunctional catalysts.

Biomass-derived MEK can be converted to butene directly with high selectivity (over 97%) over 20% Cu-ZYNa. Cu-ZYNa acts as a bifunctional catalyst with hydrogenation and dehydration properties. MEK was first hydrogenated to 2-butanol over metal sites and then dehydrated to butene over acidic sites.

It was also shown that MEK can be converted to higher ketones (C_8 ketone) by creating C-C bonds between molecules of MEK using a multifunctional catalyst having aldol condensation (aldolization and dehydration) and hydrogenation properties. The main product was 5-methyl-3-heptanone, an important intermediate for producing higher aliphatic alcohols (5-methyl-3-heptanol) or C_8 alkenes and C_8 alkane for use as a potential gasoline blending agents. The results showed that using a variety of metals (Cu, Ni, Pt and Pd) supported on ZrO_2 can produce high conversions of MEK and selectivites for C_8 ketone. The highest conversion was over 1% Ni-ZrO_2 (82%) and 1% Cu-ZrO_2 (78%), giving a selectivity for C_8 ketone above 63% at a temperature of 180 °C and a molar ratio of H_2/MEK of 2.

Finally, the conversion of C_8 ketone was investigated over Cu-Al_2O_3 and Pt-Al_2O_3 to produce a mixture of C_8 alkenes and C_8 alkane via hydrogenation-dehydration reactions in a one-reactor catalytic process. Experimental results demonstrated that the main product over Cu-Al_2O_3 was a mixture of C_8 alkenes and C_8 alkanes with different percentages depending on the operating conditions. However, using Pt-Al_2O_3 the major product was C_8 alkane (3-methyl heptane) with a high selectivity above 97% and conversions up to 100%.

6.1 Future Work

For future work, there are a couple of trends noted in this thesis that could be studied further. First, as noted in Chapter 5, the calcination time affected the rate at which the Cu catalyst was deactivated. One extension of this work would be to study the effect of calcination temperature on the conversion of C_8 ketone and the distribution of major products. Another challenge noted in the thesis was the relatively fast deactivation noted for most catalysts. Future work could look into how to decrease the rate of deactivation by changing the catalyst preparation procedure and reaction conditions.

A final idea for future work inspired by this thesis is to explore the potential production of aromatic components such as xylene, which is an important chemical, from MEK. First, the catalysts used to make butene and butane from MEK could be modified to promote dehydrocyclodimerization reactions. Another approach is to start from C_8 alkenes or C_8 alkane (see Chapter 5) and use dehydrocyclization reactions on an appropriate bifunctional catalyst to make xylene. This could be acheived by in-depth

research on the catalyst properties necessary for dimerization and dehydrocylization for butene as a reactant or dehydrocylization for C_8 alkene as a reactant. The rest of this chapter includes some information about the importance of xylene, its types, uses and a brief literature review in addition to a brief discription of the routes to obtain it from MEK derived from biomass.

6.1.1 Types and Uses of Xylenes

Xylene (C_8H_{10}) is an important platform chemical in the petrochemical industry. It consists of three isomers: *para*-xylene, *ortho*-xylene and *meta*-xylene, which differ in the positions of the two methyl groups on the benzene ring. The molecular structures of these isomers are shown in scheme 6.1.

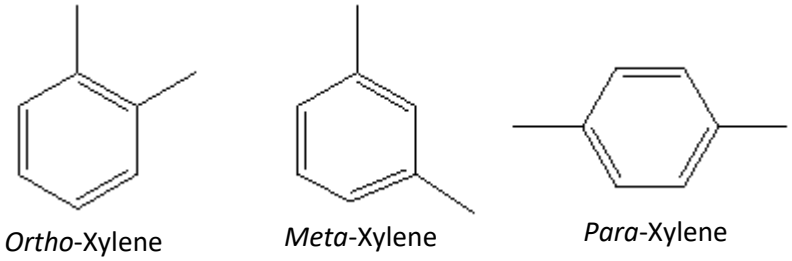

Scheme 6.1. Isomers of xylene.

Among those isomers, *para*-xylene is the most valuable xylene isomer, and it is used to produce terephthalic acid and dimethyl terephthalate, which are useful in producing polyethylene terephthalate fibers, resins, and films. *Ortho*-xylene can be converted into phthalic anhydride. This component is the base for many other chemicals such as plasticizers used in flexible polyvinyl chloride (PVC) resins, polyester resins used

in glass-reinforced plastics, and alkyd resins used for surface coatings. *Ortho*-xylene can also be used to produce phthalonitrile and converted to copper phthalocyanine, a pigment. Most *meta*-xylene is isomerized to *para*-xylene and *ortho*-xylene, but it can also be used to produce isophthalic acid and isophthalonitrile. Isophthalic acid is the starting material for unsaturated polyester resins which possess good corrosion resistance, and its strength and modulus are greater than resins derived from phthalic anhydride. Also, isophthalonitrile is a basic building block for the fungicide tetrachloroisophthalonitrile [1].

6.1.2 Production of Renewable Xylene

Butene and butane, which can be produced from biomass-derived MEK, can be converted to xylene via a dehydrocyclodimerization reaction to produce xylene and H_2 through two subsequent reaction steps: a dimerization reaction followed by a dehydrocylization reaction over a dehydrogenation catalyst. Dehydrocyclodimerization reactions can be conducted above 260 °C over bifunctional catalysts possessing acidic and dehydrogenation properties [2].

Generally, the dehydrocyclodimerization of olefins is faster than paraffins. Csicsery [3] studied the dehydrocyclodimerization of *trans*-butene and butane over platinum-alumina. He found that the conversion of *trans*-butene to aromatics is approximately one and one half times as high as that of butane. In addition to that, the amount of C_5-C_8 olefins and naphthenes produced was considerable at shorter residence times, while for longer contact times the product contained more aromatics and less naphthenes. These results demonstrated that the aromatization of butenes goes through

C_6-C_8 olefinic and naphthenic intermediates. Also, Csicsery investigated the reaction of olefins over free metal silica-alumina and acidic alumina under dehydrocyclodimerization conditions, and the results showed that 13% of the butenes were converted to aromatics**.** The fraction of C_5-C_8 olefins and naphthenes formed over alumina and silica-alumina was greater than over catalysts having dehydrogenation properties, emphasizing the ability of the dehydrogenation catalyst to convert C_6-C_8 aliphatics and naphthene intermediates to aromatics [4]. Mathew *et. al.* [5] studied the conversion of bio *iso*-butanol to xylene. After obtaining *iso*-butanol via fermentation of glucose using a modified bacterial biocatalyst (GEVO 1780), *iso*-butanol was then dehydrated to *iso*-butene over γ-Al_2O_3 at 325 °C and atmospheric pressure with a selectivity of 95% and a conversion of 99.8%. Then using ZSM-5, *iso*-butene was dimerized and oligomerized to *iso*-octane, trimers and tetramers at 175 °C and 750 psig. Finally, *iso*-octane was dehydrocyclized over a commercial chromium-oxide catalyst to produce p-xylene at 550 °C and 1 atm with a selectivity greater than 80%.

Through the selection of suitable reaction conditions, like reaction temperature, and the appropriate catalysts containing acidic and dehydrogenation properties, dimerization and dehydrocyclization reactions can occur at the same time, and C_4 alkenes can be converted directly to p-xylene in a single reaction step, or through a rapid series of steps where the C_4 alkene is converted into an intermediate like C_8 alkene, which is then rapidly converted to p-xylene [5].

Xylene can also be produced from C_8 alkenes and C_8 alkane via dehydrocylization reactions (dehydrogenation-cyclization) through the elimination of five moles of hydrogen, starting from the alkane or three moles starting from the alkene. US. Pat. No. 3,428,702 disclosed the dehydrocyclization of 2,5-dimethylhexene using a chromia-alumina catalyst in the presence of H_2S. The conversion of 2,5-dimethylhexene to *para*-xylene was 30-40% [6].

In conclusion, two different routes to convert MEK to xylene are possible. One of them is hydrogenation MEK to 2-butanol, dehydration of the alcohol to give butene, and finally dehydrocyclodimerization (dimerization-dehydrocylization) of butene to produce xylene. The other path goes through a multi-step mechanism with the direct condensation of MEK (aldol reaction), dehydration of the aldol products to obtain unsaturated C_8 ketone, hydrogenation of unsaturated ketone to C_8 ketone, further hydrogenation of ketone to produce C_8 alcohol, dehydration of the alcohol to produce C_8 alkenes, and finally dehydrocylization reaction to convert the alkenes to xylene.

References

1. Cannella, W. J. Xylenes and ethylbenzene. *Kirk-Othmer Encycl. Chem. Technol.* **2007**.

2. Chao, T.H. Phosphorus containing alumina catalyst for the production of aromatics. U.S. Patent No. 4,654,455. **1987**.

3. Csicsery, S. M. Dehydrocyclodimerization: IV. The reactions of butenes. *J. Catal.*

1970, *17*, 323–330.

4. Csicsery, S. Dehydrocyclodimerization. *Ind. Eng. Chem. Process Des. Dev.* **1979**, *18*, 191–197.

5. Peters, M. W.; Taylor, J. D.; Jenni, M.; Manzer, L. E.; Henton, D. E. Integrated process to selectively convert renewable isobutanol to p-xylene. U.S. Patent Application No. 12/899,285. **2011**.

6. Downs, R. O.; Franz, R. A. Dehydrocyclization of 2,5-dimethyl-hexene to para-xylene. U.S. Patent No. 3,428,702. **1969**.